INDUCTION OF ANGIOGENESIS IN MICROFLUIDICS BY USING PROLYL HYDROXYLASE INHIBITOR AND SPHINGOSINE 1-PHOSPHATE

LIM SEI HIEN

(B. Eng. Chemical and Biomolecular Engineering, Nanyang Technologial University)

A THESIS SUBMITTED FOR THE DEGREE OF DOCTOR OF PHILOSOPHY

DEPARTMENT OF BIOENGINEERING

NATIONAL UNIVERSITY OF SINGAPORE

2013

DECLARATION

I hereby declare that this thesis is my original work and it has been written by me in its entirety. I have duly acknowledged all the sources of information which have been used in the thesis.

This thesis has also not been submitted for any degree in any university previously.

Lim Sei Hien

21st April 2014

ACKNOWLEDGEMENTS

I would like to take this opportunity to express my sincere gratitude to my advisors, Professor Roger Kamm and Associate Professor Michael Raghunath. I could not have finished my thesis and the learning journey of PhD without their supports. Professor Kamm is patience, supportive, caring and incredibly dedicated to the field of science. He has always been a great mentor who not only shares his immense knowledge with me but he also inspires and encourages me to continue pursuing my research direction. I would like to thank Professor Kamm for his great efforts in maintaining a stimulating and inspiring research atmosphere within the group and I also appreciate the freedom of research that has been entrusted by him. Just as importantly, I want to thank Associate Professor Raghunath for his pragmatic inputs and comments on my research direction that help tremendously in improving the quality of my work. Without his guidance, my PhD studies would have been much more difficult. I am grateful to have the privilege to work with them in this exciting interdisciplinary research project.

I appreciate the chance to work with a group of supportive and enthusiastic lab mates in both Biosym and TML labs who make the life in the laboratory much more enjoyable. Their friendships have helped me get through the many ups and downs in the long winding path of PhD studies. I am especially grateful to have Dr. Amir Aref and Dr. Choong Kim as my mentors. They have spent great efforts in teaching me the microfluidic techniques to ensure I could utilize the microfluidics for my studies. Without their helps, I would have spent much more time in learning the sophisticated microfluidic techniques. I want to thank Dr. Clarice Chen for teaching me the cell culture techniques and also the basics in conducting biological research which are very important in my PhD studies especially in the early phase when I was a novice in this field. There are many other names to list but I want to express my gratitude to O,TY, Levi, Soheila, Evan and Zhiyong, who have been helping

me in one way or another. I would also like to thank Dr. Narayanan Balasubramanian, Shu Jing, Wendy and Chee Keong for their supports and great work in maintaining the lab. During my PhD studies, I spent 6 months at MIT working in Professor Kamm's lab. It was a great experience for my learning and I enjoyed every moment that I spent there especially the stimulating discussions with Yannis and Jordy.

I would also like to thank my parents, family and friends for their continual supports that give me the strength to face the many challenges in my PhD studies. I would like to share the joy in finishing this thesis with them.

TABLE OF CONTENT

SUMMARY

Angiogenesis, an essential process in wound healing and tumor growth, also represents a therapeutic target for tissue repair. Its inherently complex nature requires participation of multiple chemokines and also the crosstalk between endothelial cells (EC) and other cell types. This process was studied in a microfluidic platform that allows endothelial cells (EC) to migrate out from a monolayer then invade into a collagen gel up a gradient of factors secreted by a pool of encapsulated fibroblasts. Prolyl hydroxylase inhibitor (PHi) that can prevent the degradation of hypoxia inducible factor-1α (HIF-1α) primarily in fibroblasts induced sprouts formation in EC, but the most complex vascular networks with true lumina were achieved after pairing PHi with the signaling sphingolipid, sphingosine 1-phosphate (S1P). I have demonstrated that a cross gradient of mutually stimulating factors was generated as each cell type responded differently to the compounds, especially to the PHi. EC showed increased secretion of placental growth factor, endothelin-1, epidermal growth factor and interleukin-8 while fibroblasts showed upregulated secretion of hepatocyte growth factor, insulin-like growth factor-binding protein 2, urokinase plasminogen activator and most importantly, vascular endothelial growth factor (VEGF). I also showed that S1P induced migration was S1P receptor 1 (S1P1) dependent and more importantly the expression of S1P1 on EC could be modulated by both PHi and S1P. The downregulation of either VEGF or S1P1 showed attenuated capillary sprouting and also change of sprouting morphologies. The proangiogenic monocyte chemotactic protein (MCP)-1 was mainly secreted by fibroblasts, but only in the presence of EC-conditioned medium (CM). Antibody interference with MCP-1 also reduced the sprouting response. The EC-fibroblast interactions could be replaced by neither fibroblast CM nor EC-lung carcinoma crosstalk. These observations not only confirm the importance of EC-fibroblast crosstalk in angiogenesis but also suggest that the combination of PHi and S1P enhances this effect and thus might be of therapeutic value for tissue repair and regeneration.

LIST OF FIGURES

LIST OF TABLES

LIST OF ABBREVIATIONS

Abbreviation	Full name
2OG	2-oxoglutarate
ANG	Angiopoietin
bFGF	basic fibroblast growth factor
BMC	Bone marrow cell
CCR7	C-C chemokine receptor 7
CLS	Capillary like structure
CM	Conditioned medium
CPH	Collagen prolyl hydroxylase
CPX	Ciclopirox olamine
CSC	Cardiac stem cell
CXCR	C-X-C chemokine receptor
DMSO	Dimethyl sulfoxide
EC	Endothelial cell
ECM	Extracellular matrix
EGF	Epidermal growth factor
ELISA	Enzyme-linked immunosorbent assay
EPC	Endothelial progenitor cell
ET-1	Endothelin-1
ETT	Exercise tolerance test
FIH	Factor inhibiting HIF
GPCR	G protein coupled receptor
HDZ	Hydralazine hydrochloride
HGF	Hepatocyte growth factor
HIF	Hypoxia inducible factor
HMVEC	Human adult dermal microvascular endothelial cell
HRE	Hypoxia responsive element
HUVEC	Human umbilical vein endothelial cell
IGFBP	Insulin-like growth factor binding protein
IL	Interleukin
MAPK	Mitogen-activate protein kinase
MCP-1	Monocyte chemotactic protein

MMP	Matrix metalloproteinase
MSC	Mesenchymal stem cell
OEC	Outgrowth endothelial cell
PAI	Plasminogen activator inhibitor
PAR-1	Protease activated receptor -1
PDCA	2,4-pyridine-dicarboxylic acid
PDGF	Platelet derived growth factor
PDL	Poly-D-lysine
PDMS	Polydimethylsiloxane
PEDF	Pigment epithelium derived factor
PHD	Prolyl hydroxylase domain
PHi	Prolyl hydroxylase inhibitor
PlGF	Placental growth factor
PTX3	Pentraxin-3
pVHL	von Hippel-Lindau tumor suppressor protein
S1P	Sphingosine 1-phosphate
SDF	Stromal derived factor
SMC	Smooth muscle cell
SPECT	Single-photon emission computed tomography
SphK	Sphingosine kinase
SPL	S1P lyase
TGF	Transforming growth factor
TIMP	Tissue inhibitor of metalloproteinase
TNF	Tissue necrosis factor
Txr-Dex	Texas red-conjugated dextran
uPA	Urokinase plasminogen activator
VEGF	Vascular endothelial growth factor

CHAPTER 1. INTRODUCTION

1.1 Problem Statement

Angiogenesis has been implicated in more than 70 disorders affecting more than one billion people worldwide [1, 2]. The consequences of either too much or too little angiogenesis are reflected in various world leading causes of deaths including cancer and ischemic heart disease. Consequently, there has been search of ways to control angiogenesis for decades but none is successful so far. This depicts the fact that vascularization is a much more complex process than expected and this is the reason why conventional therapies that deal with either one or few angiogenic factors fail. The strategies for promoting vascularization are not only significant for therapeutic angiogenesis but they also lay ground for discovering effective approaches against unregulated vascularization such as the vascularization in tumor growth. Furthermore, insufficient vascularization has always been a key limitation in tissue engineering which leads to its unavoidable failure [3]. Therefore, the need to promote angiogenesis through a multifactorial approach arises.

1.2 Motivation

Prolyl hydroxylase inhibitors (PHis) possess both angiogenic and antifibrotic effects and this fortunate combination has been demonstrated in human cell cultures and transgenic zebrafish [4]. Inhibition of prolyl hydroxylase results in stabilization of hypoxia inducible factor-1α (HIF-1α) and promoting transcription of over 70 target genes, including VEGF and its receptor, VEGFR1, hence, an angiogenic cascade will be triggered [5]. Similarly, sphingosine 1-phosphate (S1P) has been shown to modulate angiogenesis in various aspects including cell proliferation, cell migration and vasculature permeability [6, 7]. It has also been shown that HIF and S1P could each affect

the other but the exact mechanism and their causal relationship still remain unclear [8]. Therefore, I hypothesize that the combination of these two compounds might indeed be effective in inducing angiogenesis through their multiple actions.

The importance to include a second cell type such as fibroblasts to enhance angiogenesis has been well documented and previously I have also shown that PHis exert greater effect in stabilizing HIF-1α expression in fibroblasts as compared to endothelia [4]. However, the current *in vitro* human cell culture represents a 2D system which is not an ideal platform for studying angiogenesis especially when I need to include a second cell type in the studies. Consequently, microfluidic devices that can accommodate multiple cell type at ease are used as they can offer great control over solute concentration gradients and can allow the growth of capillary sprouts from an endothelial monolayer into 3D collagen gel scaffold.

1.3 Objectives

The main goal of this project is to study the combinatorial effects of PHi and S1P induced angiogenesis in the presence of fibroblasts as mediating cells by using a microfluidic platform.

1.4 Dissertation overview

PHis and S1P have been shown to promote angiogenesis independently but their combined effects have yet to be tested. The beneficial effects of fibroblasts in maintaining capillary sprouts and the advantages of using microfluidic platform to study angiogenesis have been discussed previously in literature [9]. Nonetheless, this is the first study that combines PHis and S1P to induce angiogenesis in a fibroblast populated microfluidic platform. I not only look into the morphological development brought by PHis and S1P but also try to find out their effects on endothelia and fibroblasts. With the help

of microfluidics, I could also appreciate the importance of endothelia-fibroblast interactions, especially in the presence of PHis and S1P. I set off to discover new strategies for therapeutic angiogenesis while the knowledge that I have contributed also help to understand the effects of hypoxia or S1P in a wound healing context.

In the following chapters I will discuss:

- the detailed features of the microfluidic platform that I used and also the validation of such platform in studying angiogenesis

- the selection of PHis based on their potency in inducing angiogenesis. Ciclopirox olamine (CPX) was selected and combined with S1P and in combination, these compounds could induce a complex vascular network with lumen in a 3D collagen matrix

- the effects of CPX in enhancing the secretion of differential and complementary angiogenic proteins from both endothelia and fibroblasts. I have also demonstrated that VEGF secreted by fibroblasts can be further enhanced by CPX. The interference of VEGF not only attenuates the capillary formation but also changes the morphologies of sprouts

- the pro-migratory effects of S1P on endothelial cells is mediated through the $S1P_1$ receptor. Expression of $S1P_1$ could be affected by both CPX and S1P. Inhibition of $S1P_1$ leads to reduced capillary sprouts and also affects the diameter and tip cell formation of sprouts

- the indispensable effects of endothelia-fibroblast crosstalk where endothelia could communicate with fibroblasts and lead to upregulation of proangiogenic cytokine, monocyte chemotactic protein (MCP)-1. The neutralization of MCP-1 also reduces sprout formation. The importance of the crosstalk was further demonstrated

through conditioned medium (CM) experiment and also by substituting fibroblasts with another cell type

Combined, this thesis has contributed to the first application of PHi and S1P in inducing angiogenesis. This thesis has also demonstrated the importance of fibroblasts in mediating angiogenesis in an *in vitro* microfluidic platform for studying angiogenesis.

CHAPTER 2. BACKGROUND & LITERATURE REVIEW

2.1 Basis of angiogenesis

Angiogenesis is the growth of new blood vessel from a pre-existing one [10]. This growing process is usually quiescent in adult and will only be activated during wound healing, reproductive cycling or ocular maturation [11]. Angiogenesis is initiated by local increase of angiogenic stimuli, including vascular endothelial growth factor (VEGF), which would bind to specific receptors on endothelial cells (EC) of nearby pre-existing vessels thus activating EC to secrete various molecules and increase endothelial proliferation while also decrease cell-cell adhesion at the same time. Subsequently, the activated EC would lead to vasodilation and increase permeability of the pre-existing vessels in response to nitric oxide synthase and VEGF [11]. Following that, the basement membrane surrounding pre-existing vessels would be either remodeled or degraded through the activation of matrix metalloproteinase (MMP)2, MMP3 and MMP9 and suppression of tissue inhibitor of metalloproteinase (TIMP)1 and TIMP2 [12, 13]. The disturbed extracellular matrix (ECM) allows the activated EC to sprout forward easily. Sprouting angiogenesis is always led by a pioneer cell called tip cell which is responsible for the directional migration whereas stalk cells align and form a lumen behind tip cells [14]. The sprouts anastomose to connect with neighboring vessels and form a functional network that can circulate blood [10, 11].

However, the sprouts formed at this stage are less stable and require the recruitment of mural cells and generation of ECM to stabilize them. In physiological conditions, functional and stable vessels are always covered by several smooth muscle cells (SMC) in the proximal part of larger vessels or

pericytes in smaller vessels to help regulate the proliferation and survival of EC [1, 15]. During the wound healing process, mural cells are recruited through several pathways: platelet derived growth factor (PDGF) B – PDGF receptor; Sphingosine-1-phosphate (S1P) – endothelial differentiation sphingolipid G-protein-coupled receptor-1 (EDG1 or $S1P_1$); Angiopoietin (ANG)1 – Tie 2; and transforming growth factor (TGF)-β –TGF-β receptor II [11, 16-19]. Once mural cells are recruited to the site of sprouts, they would start depositing extracellular matrix such as laminin and fibronectin followed by collagen I to allow attachment and adhesion of endothelium [20].

Stromal cells around the capillaries such as fibroblasts are important for mediating angiogenesis where fibroblasts have been shown to control the capillary morphogenesis through complex spatiotemporal regulation of multiple angiogenic proteins including VEGF, Ang1, hepatocyte growth factor (HGF), fibronectin and MMP production and also through matrix remodeling [21-24]. Besides, angiogenesis also relies on cell-cell interactions such as endothelia-fibroblast interplays that depend on endothelin-1 secretion from endothelia [25]. Fibroblast-cardiomyocyte interplays also affect the secretion level of interleukin (IL)-6 and tumor necrosis factor-α (TNF-α) [26]. Inflammatory response is a concomitant mechanism to spur neoangiogenesis [27]. The increase of vascular permeability and EC activation is the first step in angiogenesis and this process is usually triggered by inflammation [28]. Various types of immune cells including neutrophils, T-cells, monocytes/macrophages, mast cells and dendritic cells have been shown to be able to secrete VEGF and other inflammatory cytokines such as IL-8 during a wound healing process [28, 29]. In particular, monocytes/macrophages have been shown to participate in angiogenesis actively through several pathways including the secretion of MMPs for vessel guidance, the activation of VEGFR3 on EC and also the recruitment of EC progenitor cell to the sprouting site [28]. From these studies, I can clearly see that angiogenesis is a highly complex biological event that requires the efforts and communications from multiple cell types to ensure that it is well regulated.

2.2 Angiogenesis implicated diseases

In 2005, a comprehensive study on angiogenesis implicated disorders has been published by Fischer et al and the list that they compiled shows that at least 70 diseases affecting different organs such as cancers, psoriaris, diabetic retinopathy, arthritis and synovitis, inflammatory bowel disease and the world number one killer, coronary heart diseases are directly related to either excessive or insufficient angiogenesis [1]. In 2011, another list of disorders characterized by angiogenesis was compiled by Bhadada et al. Both studies are quite similar except that Bhadada et el. pointed out that certain kidney diseases are related to excessive angiogenesis such as end-stage renal disease, autosomal dominant polycystic kidney disease and chronic kidney disease which were missed out in previous study [30]. From the long list of diseases that are associated with angiogenesis, I could appreciate the importance of angiogenesis in various biological processes. Among the disorders that are mentioned in the two compiled list, ischemic conditions with insufficient angiogenesis in different parts of human body; and cancer with excessive angiogenesis in various organs are the two major diseases that draw the greatest attention and potential therapeutic approaches have been proposed. In this thesis, I focus primarily on the factors that are proangiogenic.

2.3 Therapeutic angiogenesis

2.3.1 Protein therapy

Therapeutic angiogenesis that targets ischemic tissue or chronic wound with insufficient angiogenesis has been widely studied. Generally, they can be divided into three major methods to enhance angiogenesis: protein therapy, gene therapy and cellular therapy [10]. Protein therapy, also known as growth factor therapy, is the most traditional method of therapeutic

angiogenesis. It uses purified growth factors such as VEGF or basic fibroblast growth factor (bFGF) to promote angiogenesis through different administration routes [31]. However, none of the protein therapy approaches have been approved by the FDA for treatment of any ischemic disorders. This is because phase II clinical trials based on recombinant human (rh)VEGF and bFGF did not show significant improvement in ischemic patients in terms of exercise tolerance test (ETT) and single-photon emission computed tomography (SPECT) [32, 33]. Over nearly a decade, no further clinical trial has been planned for protein based therapeutic angiogenesis due to the disappointing clinical trials mentioned above. The major reason contributing to the failure of protein therapy is the ineffective route of administration which leads to insufficient exposure time and concentration to the target tissue hence limiting its effectiveness [34].

2.3.2 Gene therapy

Gene therapy is another approach to therapeutic angiogenesis. There are two gene delivery techniques which are commonly used: plasmid or adenoviral vectors. The main benefit of using gene delivery over conventional protein therapy is the sustained release of therapeutic agents at target areas hence repetitive administration of therapeutic proteins is no longer required. Based on the compiled data from Zachary et al, gene therapies that focus on single VEGF gene activation have failed thus far [34]. Most recently, a phase II clinical trial on percutaneous intramyocardial transfer of bicistronic VEGF165/bFGF plasmid failed to show improvement on SPECT and only marginal improvement on ETT was observed [35]. Similarly, TAMARIS phase III clinical trial was carried out by Sanofi-Aventis where naked FGF-1 plasmid or also known as XRP0038/NV1FGF was tested in patients with critical limb ischemia but it was not found to reduce the rate of amputation as compared to the placebo control [36]. Nevertheless, there are still two ongoing phase I and phase III clinical trials that use VEGF-D and FGF-4 as their target genes, respectively. KAT301 is a phase I clinical trial that evaluates the possible

application of catheter mediated endocardial adenovirus VEGF-D gene in patients with myocardial infarction. AWARE, is another ongoing clinical trial that aims to reduce the time to onset myocardial ischemia in women with stable angina through the infusion of Ad4FGF-4 [34]. The major reason that impedes the efficacy of current gene therapy is the low transduction efficiency. The transduction efficiency is estimated to be around 5 -10 % by using the most effective vectors available to human [37].

2.3.3 Cellular therapy

Cell-based therapies open up another possibility in the search of the solutions for therapeutic angiogenesis. Various cell types such as endothelial progenitor cells (EPCs), bone marrow-derived cell (BMCs), mesenchymal stem cells (MSCs), cardiac stem cells (CSCs), skeletal myoblasts, hematopoietic progenitors, cord blood cells, adipose cells, cardiomyocytes and embryonic stem cells (ESCs) have been studied for the feasibility to be infused into the recipients to promote angiogenesis. However, the translation of cell-based therapies from bench top to bed side has encountered various challenging issues and the results among different research groups are sometimes contradictory [38, 39]. The two main reasons that cause the variations between groups are: different processing methods in cell purification and unclear functions of various cell types in the process of angiogenesis. For example, EPCs that are cultured differently could lead to two distinct putative EPC populations: early EPCs and outgrowth endothelial cells (OECs). These two cell types show distinctive behaviors in terms of proliferation rate, cell surface antigens expression and morphology [40]. The differences in the cellular behaviors would affect the roles that they play during angiogenesis such as the early EPCs would secrete higher amounts of angiogenic peptides that contribute to paracrine effects while the donor OECs with higher proliferation rate might differentiate actively to form vessel lining in recipients [41]. In short, cellular based therapeutic angiogenesis remains attractive and numerous clinical trials that focus on BMCs, MSCs, CSCs and

EPCs are ongoing despite of the limited success of previous studies and various challenges such as the threat of forming tumors lay ahead.

The conventional protein or gene therapies for therapeutic angiogenesis have been focusing on single protein administration or induction while these methods have so far been proven to be less effective in enhancing angiogenesis [32, 34]. Besides, angiogenesis is a complex process that involves accurate orchestration of various cytokines and molecules as discussed earlier hence the need for careful manipulation of various angiogenic factors arises. Prolyl hydroxylase domain (PHD) inhibitors or also known as prolyl hydroxylase inhibitors (PHis) could serve as a solution to current unmet clinical needs as PHis stabilize the master switch of hypoxia, HIF-1α. This results in the simultaneous up-regulation of various angiogenic genes in a way similar to angiogenesis under hypoxic stress. To further strengthen the angiogenic effects, S1P that complements the actions of PHis through modulating multiple angiogenic processes such as endothelial migration, cell proliferation, mural cell recruitment and barrier protection can be combined with PHis to maximize their angiogenic potential [6].

2.4 Hypoxia inducible factors (HIF)-1

HIFs are heterodimeric transcription factors comprised of α and β subunits [42]. The α-subunit is degraded rapidly under normoxic conditions in an oxygen dependent manner while the β-subunit, HIF-1β (also known as aryl hydrocarbon receptor nuclear translocator, ARNT) is oxygen insensitive and constitutively expressed [42]. There are three different α-isoforms in mammalian cells: HIF-1α, HIF-2α and HIF-3α [43]. Although HIF-1α and HIF-2α share structural similarities, they have distinct spatiotemporal expression patterns and cellular functions and are regulated differently [44]. HIF-1α is believed to be the main regulator of vascular formation instead of HIF-2α, which is mainly responsible for regulation of renal Epo synthesis [44]. Conversely, HIF-3α that lacks the C-terminal transactivation domain has been

reported to play a negative role in regulating HIF signaling and also angiogenesis [45, 46]. The expression of HIF-3α is cell type specific [47]. Endothelial cells express multiple splice variants of HIF-3α but only the expression of HIF-3α2 elevates during hypoxia [47]. Interestingly, another splice variant HIF-3α4 has also been shown to suppress angiogenesis in a brain tumor model [46]. Nonetheless, HIF-1α that is ubiquitously expressed still plays a dominant role in activating the downstream angiogenic cascade during hypoxia hence it will be the primary isoform that I focus on.

Under normoxic conditions, the expression of HIF-1α is suppressed by prolyl hydroxylase domains (PHDs) and factor inhibiting HIF (FIH). Similar to α subunit of HIF, there are three PHD isoforms as well: PHD1, PHD2 and PHD3 each having different regulatory functions to the α subunit of HIF-1. PHDs require oxygen to hydroxylate HIF-1α and their Michaelis-Menten constant, K_m for oxygen is higher than the physiological oxygen concentration in tissue hence PHDs are highly sensitive to the change of oxygen concentration [44]. The proline residues at 402 and/or 564 of HIF-1α would be hydroxylated by PHDs into hydroxyproline in the presence of ferrous iron, ascorbic acid and 2-oxoglutarate (2-OG) as co-factors or co-substrate when oxygen is available (normoxic conditions) [43]. The hydroxylated HIF-1α would then be recognized by von Hippel-Lindau tumor suppressor protein (pVHL) hence leads to the ubiquitination of HIF-1α followed by proteosomal degradation of it. This process is rapid as accumulated HIF-1α under hypoxic conditions can be degraded rapidly with a half-life of less than 5 minutes on reoxygenetion *in vitro* [48].

By using PHis, the activity of PHDs will be attenuated even under normoxic conditions. Therefore, the hydroxylation of proline residues at 402 and 564 can be prevented so that HIF-1α can escape from the proteosomal degradation pathway. The stabilized HIF-1α is then dimerized with the HIF-1β and translocate into nuclei to activate the transcriptions of downstream target genes. In short, PHis can be used to stabilize HIF-1α and to activate angiogenesis cascade under normoxic conditions.

On the other hand, FIH uses oxygen to hydroxylate HIF-1α under normoxic conditions too. Its K_m is 3 three time lower than that for the PHD family and the hydroxylation site for FIH is asparagine residue, Asn 851 in HIF-1α or another similar Asn residue in HIF-2α. Once hydroxylated by FIH, HIF-1α would be prevented from interacting with p300/CBP, a transcriptional activator at the HRE [43]. Consequently, the hydroxylation of HIF-1α by FIH could severely reduce the transcriptional activity of HIF-1 and this mechanism is different from the destabilization effects of PHD family on the α subunit of HIFs. A schematic drawing of oxygen dependent-HIF regulation under either normoxic or hypoxic conditions is shown in Figure 2-1, adapted from Mole et al. [49]. There are several oxygen-independent controls of HIF signaling such as phosphoinositide-3 kinase (PI-3K), mitogen-activated protein kinase (MAPK), mammalian target of rapamycin (mTOR), nitric oxide (NO) and carbon monoxide (CO) but they are beyond the scope of this work hence will not be discussed further [49, 50].

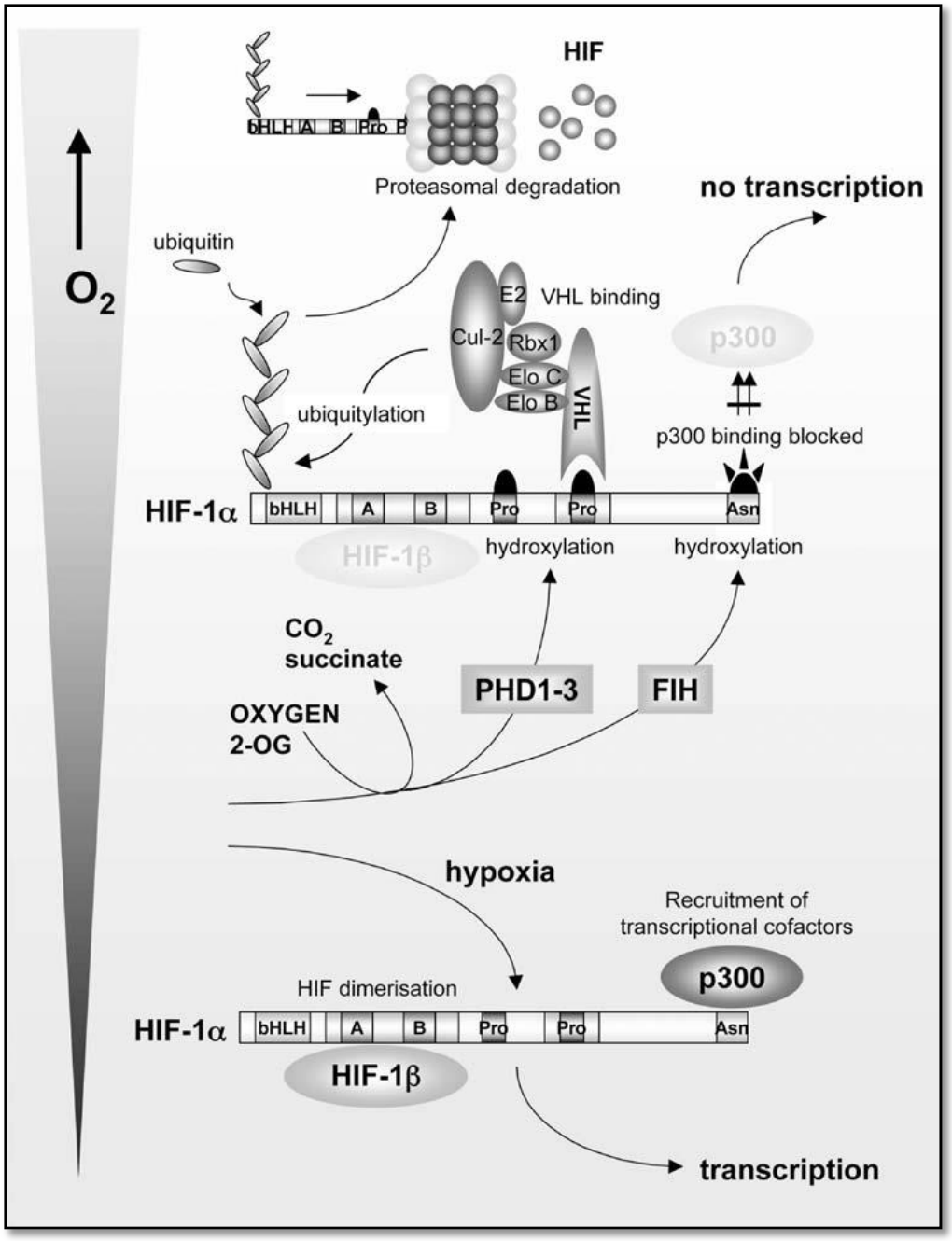

Figure 2-1 Oxygen dependent regulation of HIF signalling adapted from Mole et al. [49]. Under normoxic conditions, PHD family hydroxylate Pro402 and Pro564 residue in HIF-1α which leads to the recognition by pVHL and followed by the ubiquitin-ligase binding and it will finally be degraded through proteosomal destruction. FIH also hydroxylate Asn 851 in HIF-1α and causes the reduced transcriptional activity through inhibition of binding of transcriptional cofactors p300/CBP binding. When oxygen concentration goes lower, the PHD and FIH activity would be inhibited hence HIF-1α dimerize with HIF-1β and bind to HRE of target genes which leads to activation of various HIF target genes.

2.5 Multiple genes are regulated by HIF-1

As hypoxia regulates not only angiogenesis but also other functions such as glycolysis and cell proliferation, the target genes regulated by HIF are anticipated to be numerous. According to the gene profiling study that was done by Semenza group [5], whereby arterial endothelial cells were transfected with AdCA5 that encoded a constitutively-active form of HIF-1α. They have found that 245 gene probes show at least 1.5 fold increase under hypoxic conditions or being transfected with AdCA5 while 325 gene probes show at least 1.5 fold decrease in the same conditions [5]. As I am interested in the proangiogenic genes, a summary only of proangiogenic proteins regulated by hypoxia is provided in Table 1 [43].

Table 1 Hypoxia induced angiogenesis related proteins

Protein	Hypoxia Response	References
Angiopoietin-1	Increase/Decrease	[51, 52]
Angiopoietin-2	Increase/Decrease	[51, 52]
basic Fibroblast Growth Factor (bFGF)	Increase	[53]
C-X-C chemokine receptor type 4 (CXCR-4)	Increase	[5]
Endothelin-1 (ET-1)	Increase	[5]
Epidermal growth factor (EGF)	Increase	[54]
Flt-1 (VEGFR-1)	Increase	[55]
Hepatocyte growth factor (HGF)	Increase	[56]
Insulin-like growth factor binding protein 2 (IGFBP-2)	Increase	[57]
Insulin-like growth factor binding protein 3 (IGFBP-3)	Increase	[5]
Interleukin 8 (IL-8)	Increase	[58]
Platelet-derived growth factor (PDGF-B)	Increase	[5]
Placenta growth factor (PlGF)	Increase	[5]
Stromal cell-derived factor 1 (SDF-1)	Increase	[59]
Urokinase plasminogen activator (uPA)	Increase	[60]
Vascular endothelial growth factor (VEGF)	Increase	[5]

"Increase/Decrease" refers to conflicting data resulting from different studies.
"Increase" refers to upregulation of protein expression/secretion under hypoxia

2.6 Current Research Status of PHis

PHis are proposed to be used as angiogenesis induction agents because PHis can effectively inhibit the activity of PHDs hence stabilize the HIFs and cause the up-regulation of HIF target genes under normoxic conditions. Various PHis have been studied and some of them are initially being used as inhibitors for collagen prolyl hydroxylase (CPH) to counter fibrosis. Hydralazine hydrochloride (HDZ), ciclopirox olamine (CPX) and 2,4-pyridine-dicarboxylic acid (PDCA) are just a few examples [4, 61, 62]. The uses of PHis

for ischemic and inflammatory disease have recently been reviewed by Fraisl et al. and are summarized in Table 2, adapted from Fraisl et al. [63].

Table 2 Selected list of inhibitors of PHD, adapted and modified from Fraisl et al. [63]

PHi	**Principle of action**	**Physiological effects**
Dimethyloxalylglycine (DMOG) [64, 65]	Mimics 2-OG	Promotes angiogenesis, confers hypoxia tolerance, ischaemic preconditioning
Desferrioxamine (DFX) [66, 67]	Chelates Fe^{2+}	Confers hypoxia tolerance, ischaemic preconditioning
L-Mimosine [68, 69]	Blocks active site, chelates Fe^{2+}	Promotes angiogenesis, anti-fibrotic
Metal ions (i.e. Co^{2+})[70]	Substitution for Fe^{2+} interferes with cofactor	Promotes secretion of VEGF
FG-0041[71]	Blocks active site, chelates Fe^{2+}	Confers hypoxia tolerance
FG-2229 (ciclopirox olamine, CPX) [71]	Blocks active site, chelates Fe^{2+}	Promotes angiogenesis, antimycotic
FG-4497[72]	Blocks active site	Confers hypoxia tolerance, suppresses inflammation
2,4-pyridine-dicarboxylic acid (PDCA) [4]	Mimics 2-OG	Reduces collagen deposition, promotes angiogenesis,
GSK360A [73]	Mimics 2-OG	Improves ventricular remodeling and vascularization
Hydralazine (HDZ) [4, 62, 74]	Chelates Fe^{2+}	Promotes angiogenesis, ischaemic preconditioning
TM 6008 [75]	Blocks active site, chelates Fe^{2+}	Promotes angiogenesis, neutoprotective
TM 6089 [75]	Blocks active site	Promotes angiogenesis
Dealanylalahocin analogues [76]	Block active site	Not determined
8-Hydroxyquinolines [77]	Block active site	Not determined
Pyrazolopyridines [78]	Block active site	Not determined

*2-OG: 2-oxoglutarate

This list shows most of the PHis that are being actively investigated for applications in therapeutic angiogenesis. Among these, dimethyloxalglycine

(DMOG), desferrioxamine (DFX) and L-Mimosine (L-mim) are the three most widely studied PHis [68, 79, 80]. Their angiogenic properties have been shown in different models such as the mice femur fracture model and diabetic mice model [80, 81]. PDCA has been around as potent CPH inhibitor and has been shown to be effective in inducing in *in vivo* transgenic zebra fish model [4, 49, 82]. Interestingly, PDCA has been reported to be able to affect the epigenetic profile through disruption on 2-OG dependent JMJD2 subfamily of histone demethylases [83]. Besides, GlaxoSmithKline (GSK, King of Prussia, PA) has developed GSK360A that competes with the 2-OG for the binding site on PHD family. The rat model shows that GSK360A could help improve ventricular performance, remodeling and vascularization, but the response is limited after myocardial infarction. That was the first animal model that studied the benefits of PHi post-myocardial infarction which is more clinically relevant in terms of treatment for myocardial infarction [73]. Of particular note are the PHis, TM6008 and TM6089, as they represent a novel class of PHis that have been identified through docking simulations to bind to PHD2 specifically [75]. Among these, TM6008 also acts as iron chelator hence its angiogenic potential and protective effects on cerebral ischemic injury (observed in a gerbil model) are much greater than TM6089 but the latter still holds great potential as it has specificity towards PHD but not other co-substrates or co-factors, hence lower cytotoxicity is expected. Besides, pyrazolopyridines and 8-hydroxyquinolines are synthesized through structure-based design with the intention of increasing specificity to PHD2 [77, 78]. Novel compounds with high specificity towards PHD2 are potential therapeutic agents with fewer unwanted side effects as compared to the conventional iron chelators or 2-OG analogs. Nevertheless, the properties of pyrazolopyridines and 8-hydroxyquinolines are not well characterized and more evidence needs to be gathered to prove their efficacy.

Other than therapeutic angiogenesis, PHis have been studied as alternatives for treatment of chronic kidney disease and anemia. The AKB-6548 designed by Akebia Inc is a PHi that could stabilize HIF-2α hence increase natural

production of Epo in anemia patients. AKB-5448 is currently in a clinical phase II trial. On the other hand, Fibrogen Inc is the leading company in discovering novel PHis for different therapeutic purposes such as for anemia, myocardial infarction and fibrotic disease. FG4592 is one of the most successful PHis that could treat CKD anemia and is currently under clinical trial phase II [44].

Several 2-OG analogs have been patented by Schofield et al. and they showed that those 2-OG analogs can effectively modulate the activity of HIF prolyl hydroxylase [84]. Besides, researchers from the same group also patented those 2-OG analogs for the application in treating β thalassemia and sickle cell disease as those 2-OG analogs could increase the fetal hemoglobin production [85]. Gene therapies that target HIF pathway have also been patented by Semenza et al. and Arbeit et al. for the applications in therapeutic angiogenesis including enhancing wound healing and reducing the risk of ischemia-related tissue damage [86, 87]. However, the efficacy of gene therapies is limited by current technology as mentioned earlier [37].

2.7 Sphingosine 1-phosphate

S1P is formed through the phosphorylation of sphingosine by sphingosine kinase 1 and 2 (SphK1 and SphK2). The physiological balance of S1P is maintained by SphK1 and SphK2 and S1P-targeted enzymes such as S1P lyase (SPL) and S1P phosphatase [88]. Predominantly, S1P governs multiple biological processes including immune response, cell proliferation and angiogenesis mainly through engaging specific cell surface G-protein coupled receptors (GPCRs), $S1P_{1-5}$ [89, 90]. The receptors are ubiquitously expressed but they have different expression profiles in different cells which allow S1P to modulate multiple physiological processes [91]. For example, $S1P_1$ plays an important role in trafficking of immune cells where CCR7 deficient T cells egress from lymphoid organs more rapidly when treated with FTY720, an agonist that causes internalization of $S1P_1$ [92]. $S1P_4$ has also been shown to

play a role in neutrophil trafficking and inflammation in an S1P lyase-deficient mouse model where S1P is prevalent [93]. $S1P_5$ is another receptor that has been associated with the egress of natural killer cells from lymph nodes and bone marrow [94].

S1P and S1P receptor interactions are also particularly important in vascular tone and angiogenesis. In particular, $S1P_1$, $S1P_2$ and $S1P_3$ are three major receptors in blood vessels where loss of function of $S1P_1$, $S1P_2$ and $S1P_3$ causes embryonic lethality due to vascular abnormalities [95]. $S1P_1$ and $S1P_3$ have been suggested to mediate S1P induced endothelia proliferation and migration in a p38 MAP kinase dependent manner [96, 97]. Moreover, $S1P_1$ and $S1P_3$ activation would also lead to Rho-dependent integrin activation which favors the endothelial migration [98]. $S1P_1$ is the main receptor that mediates angiogenesis [99]. Its ligand S1P reduces endothelial permeability through activation of protease activated receptor -1 (PAR-1) thus increasing endothelial barrier integrity [100]. In addition, a $S1P_1$ specific antagonist was demonstrated to abrogate VEGF-induced angiogenesis in a cornea model [101]. In contrast, the functions of $S1P_2$ in angiogenesis remain unclear as conflicting studies indicate both pro-angiogenic and anti-angiogenic effects of $S1P_2$ [102, 103]. $S1P_3$ also mediates endothelial nitric oxide synthase (eNOS) and nitric oxide production in endothelia which leads to vasodilation [104].

It has long been speculated that S1P not only exerts its effects through extracellular receptor signaling but it also serves as an intracellular messenger. Not until recently though, has it been elucidated that S1P and sphingosine are present in nuclei and the S1P produced in nucleus also affects the balance of histone acetylation through inhibition of histone deacetylase (HDAC) 1 and HDAC2 [105]. Its other functions as intracellular messenger such as regulating mitochondrial assembly together with its extracellular signaling roles make S1P a powerful signaling molecule that has implications in multiple diseases including Alzheimer's disease, atherosclerosis, myocardial infarction and multiple sclerosis (reviewed in [88]). In particular, the research of S1P on multiple sclerosis has been most

successful and FTY720 that causes internalization of $S1P_1$ has been approved by the FDA as a first line treatment for relapsing multiple sclerosis [106]. Besides, LX2931, a S1P lyase inhibitor, is currently in a phase II clinical trial for treatment of active rheumatoid arthritis. These show the potential of modulating S1P in affecting pathological conditions including angiogenesis related diseases.

S1P and lysophosphatidic acid (LPA) have been patented for the applications in implantable medical devices by Astafieva et al. and Trollsas et al. [107, 108]. As claimed in these patents, S1P and LPA can be used to coat the implantable medical devices including stents and act as chemo-attractants for endothelial cells to help improve healing effects. In addition, Elbert et al. have patented the use of S1P and sphingosine kinase in biomaterials such as polyethylene glycol (PEG) hydrogel to improve the recruitment of endothelial cells to the wound site [109]. Furthermore, S1P has also been patented for the use in bio-interface membrane , between biosensor and tissue, to help forming vascularization around an analyte sensor system such as blood glucose sensor for more accurate measurement of the analytes [110].

As mentioned earlier, S1P is a multi-function signaling molecule which also plays a role in HIF-1 activity. Interestingly, SphK1 that is responsible for the production of S1P is also found to be upregulated during hypoxia. However, the mechanism of this is still unclear as Ader et al. suggested SphK1 is an upstream regulator to HIF-α and it could stabilize HIF-α through the pVHL pathway while Anelli et al. suggested the opposite, showing that SphK1 is the downstream target of HIF [111, 112]. This opens up a new territory in cancer research where strategies that inhibit S1P or SphK1 could also interrupt HIF-1 activity. For example, FTY720 has been shown to inhibit S1P and VEGF induced angiogenesis and also tumor cell proliferation and apoptosis [113]. Nonetheless, the combined effects of HIF-1 activity and S1P signaling for therapeutic angiogenesis are yet to be explored.

2.8 Angiogenesis in Microfluidic Systems

Recently, the study of angiogenesis has been extended into microfluidic platforms where control of flow, 3D cell culture environment, solute concentration gradients and real time observation of sprout formation could be realized. All these beneficial features of microfluidic devices are not readily available in conventional 2D cell culture or in animal models. For example, a way to determine the angiogenic potential of PHis is through its induction of capillary like structures (CLS) in endothelial cell-fibroblast co-culture. In this case, endothelial cells are seeded on top of fibroblasts where elongated structures of endothelial cells on 2D are referred as CLS [4]. However, CLS is not an optimum way to study angiogenesis as this does not occur *in vivo* during angiogenesis. Microfluidic devices serve as an alternative *in vitro* system with added benefits to help understand angiogenesis and possibly help screen potential angiogenic agents before application in animal models. Besides, microfluidic devices could also provide other unmatched advantages such as the real time observation of sprout formation and greater control over solute concentration gradients. Consequently, microfluidics is adopted as a platform to study PHis and S1P induced angiogenesis in the present study.

Vickerman et al. utilized microfluidic devices with two channels and a 3D collagen gel scaffold, for the study of sprouting angiogenesis in human adult dermal microvascular endothelial cells (HMVECs) under the effect of shear stress, and interstitial flow. They showed that HMVEC first migrated in 2D collectively and then formed tube-like structures in 3D collagen scaffold [114]. Chung et al. also utilized microfluidic devices with three independent channels and showed that HMVEC could response differently by co-culturing with different cancer cell types. They also studied the effects of different collagen gel stiffness on HMVEC sprouting angiogenesis and found that stiffer matrices would inhibit the migration of HMVEC but also simultaneously helped the formation of thicker tube-like structures [115]. These previous studies revealed that HMVEC usually migrate collectively in 2D prior to the

formation of sprouts, hence Chung et al. further improved the microfluidic cell culture technique by application of PDL surface coating before the filling of collagen (Figure 2-2). This allows the formation of sprouts in 3D from a pre-formed endothelial cell monolayer which highly resembles the *in vivo* conditions [116].

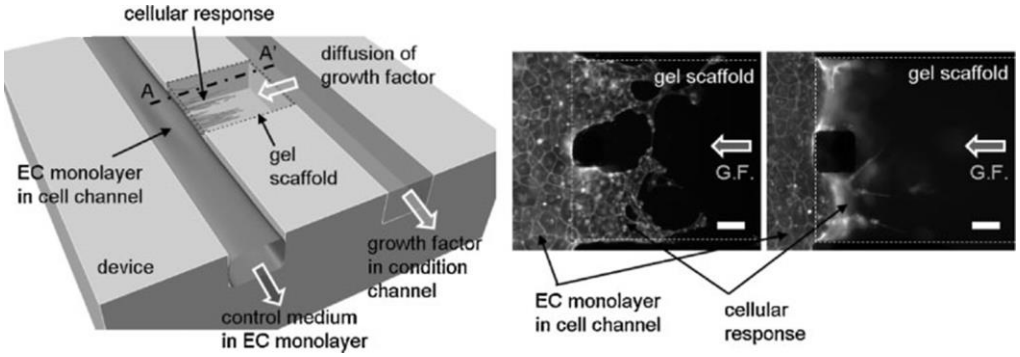

Figure 2-2 Schematic drawings of microfluidic device adapted from Chung et al.[116] The growth factor in condition channel induces HMVEC invasion into the 3D gel scaffold in a two-channel microfluidic platform. PDL pre-treatment solves the issue of collective cell migration in the microfluidics.

Sudo et al. demonstrated that microfluidic devices could be used as a platform to study the interactions between primary rat hepatocytes and endothelial cells. They successfully grew hepatocytes into a tissue-like structure through the manipulation of interstitial flow and they also showed that rat endothelial cells were greatly induced by hepotocytes thus forming stable sprouts across the 3D collagen gel [117]. Shin et al. subsequently showed that orchestration of ANG-1 and VEGF gradients spatiotemporally could help prevent the regression of sprouts as compared to the induction by VEGF gradients alone. As a result, the number of tip cells that remain attached on stalk cells increased with the stabilization effect provided by 50 ng/ml of ANG-1 [118]. Most recently, Kim et al. demonstrated the angiogenic potential of fibroblasts encapsulated in alginate beads for co-culture with HUVEC in microfluidics. They showed that VEGF production is dependent on cell encapsulation density which then affects the capillary sprouting [9].

Other than the above-mentioned microfluidic devices that were developed using a similar 3D collagen gel concept, several other strategies have been explored to study angiogenesis in 3D. Cardiac fibroblasts have been proven to be inhibitory to angiogenesis through contact-dependent mechanism in fibrin gel assays performed by Nehls et al. They coated endothelial cells and fibroblasts onto microcarrier beads before embedding them into fibrin gel and the angiogenesis process was observed in 3D subsequently [119]. The microcarrier bead technology is incorporated into a microfluidic device by Shamloo et al. by pre-coating endothelial cells onto microcarrier beads and then embedding the beads into 3D collagen matrix inside a microfluidic device with source and sink channels. Consequently, the concentration gradient of VEGF could be well established in the devices and they also confirmed that higher matrix density could increase the stability of lumen formation under the induction of a VEGF gradient [120]. In a similar setting, the authors further demonstrated that VEGF gradient induced-endothelial pathfinding in capillary sprouting is extracellular matrix-dependent [121].

Nguyen et al. developed a microfluidic platform that could accommodate a collagen type I matrix with two cylindrical voids inside the matrix [122]. They cultured endothelia in one void and applied angiogenic cocktails in another void. The cocktails consist of selections of angiogenic compounds from basic fibroblast growth factor (bFGF), hepatocyte growth factor (HGF), VEGF monocyte chemotactic protein-1 (MCP-1), sphingosine-1-phosphate (S1P), and phorbol 12-myristate 13-acetate (PMA). These angiogenic cocktails could elicit capillary sprouting that travelled across the 3D collagen gel with lumina structures. In another study, Kim et al. utilized microfluidic platform that allows co-culture of endothelia and fibroblasts to study angiogenesis and vasculogenesis in a collagen I enriched fibrin matrix. With these setups, they were able to form perfusable vascular network that allows studies of flow induced responses and also stromal cell interactions with vasculature *in vitro* [123]. This was the first report on formation of perfusable networks in *in vitro* system through angiogenesis and vasculogenesis which were different from

previously reported perfusable networks that were formed through endothelial lining on structural supports [124, 125].

There are other interesting microfluidic designs that help to elucidate the endothelial cells behaviors. Barkefors et al. designed a microfluidic chemotaxis chamber (MCC) with three independent inlets that are connected at the downstream hence steady concentration gradients could be achieved. By using this design, they showed that endothelial cells migrate up VEGF concentration gradients and they also proposed that endothelial cells would turn into a non-migratory phenotype at the high end of the gradient [126].

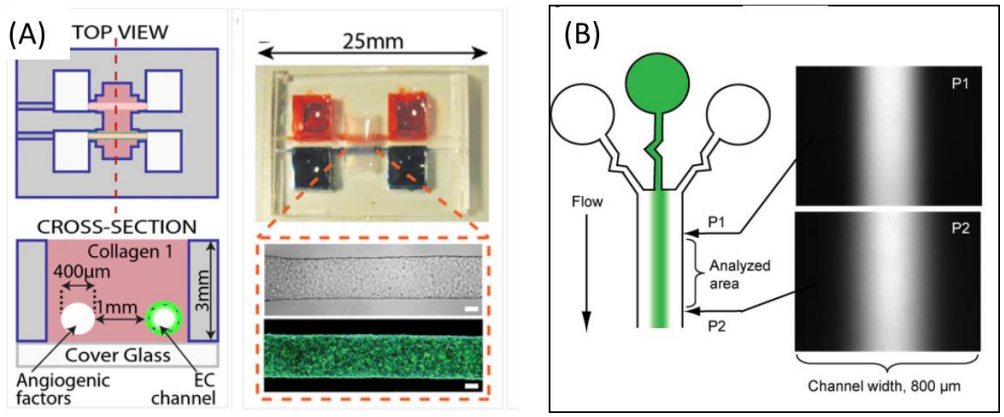

Figure 2-3 Schematic drawings of microfluidic devices, adapted from Nguyen et al. and Barkefors et al. [122, 126]. (A) Microfluidic device with two cylindrical voids inside a collagen gel matrix for growing capillary sprouting from one void to the other [122]. (B) Three-inlet design used to study the VEGF chemotaxis in endothelial cell migration [126].

Certainly, there are unmet clinical needs in therapeutic angiogenesis especially in critical limb ischemia, myocardial infarction, stroke and diabetic ulcers. From the relatively unsuccessful translation of protein therapy and gene therapy to clinical applications, I learn that the manipulation of one growth factor is insufficient to activate the complex angiogenesis cascade [127]. Consequently, PHis that can regulate multiple angiogenic genes through the stabilization of HIF-1α can be coupled with multi-action signaling lysophospholipid, S1P as a new strategy for therapeutic angiogenesis. As

angiogenesis requires an interplay between different cell types such as endothelial- fibroblast crosstalk, the need to study PHis + S1P induced angiogenesis in a co-culture platform arises. In order to accommodate multiple cell types while maintaining the ability to visualize capillary sprouting under the induction of PHis+S1P, I choose a microfluidic platform that creates a more *in vivo*-like 3D environment for my studies.

CHAPTER 3. METHODS

3.1 Cell Cultures

Human umbilical vein endothelial cells (HUVEC), isolated from umbilical cord (kindly provided by Dr. Jerry Chan, National University of Singapore, Singapore), were plated in cell culture flasks that had been coated with 50 µg/ml rat tail collagen I solution (BD, Bedford, MA) in 0.02 M acetic acid (VWR, PA) for 30 min, and maintained in EGM-2mv (Lonza, Walkersville, MD) until they were 80 % to 90 % confluent. IMR-90 human lung fibroblasts and A549 human lung carcinoma epithelial cell line were obtained from ATCC (Manassas, VA) and maintained in culture medium, DMEM (Gibco, NY) supplemented with 10 % fetal bovine serum (Gibco, NY) and 1 % Penstrep (Gibco, NY). All experiments were carried out with HUVEC at passages 5 to 6 and IMR-90/ lung carcinomas at passages 16 to 18. Cultures were kept at 37 °C in a humidified incubator with 5% CO_2. As previously reported, the amounts of VEGF secreted by fibroblasts correlate directly with the concentration of encapsulated fibroblasts [9]. In this study, solutions containing 25 million fibroblasts / lung carcinomas per ml were used.

3.2 Preparation of PDMS Microfluidic Device

Microfluidic devices are fabricated from polydimethylsiloxane (PDMS) comprised of two gel regions and three cell seeding channels with two bead traps to contain alginate beads (Figure 3-1). The microfluidic devices were fabricated using standard soft lithography as described earlier [9]. In short, PDMS was poured onto an SU-8 master mold and cured for 4 h at 70 °C before peeling, trimming and punching holes into features as shown inFigure 3-1. PDMS devices were autoclaved to ensure sterility and then bonded to cover slips (VWR, PA) after plasma treatment for 90 s (Femto Science, Korea) to render the hydrophobic surface hydrophilic and facilitate adhesion.

Microfluidic devices were immediately treated with 1 mg/ml Poly-D-lysine (PDL) solution (Sigma, St Louis, MO) for at least 4 h to enhance cell attachment as well as to prevent leakage of collagen gel during the gel filling step. The PDL treated microfluidic devices were then washed twice with filtered DI water and then kept in an oven (72 °C) for 48 h to return the PDMS devices to their hydrophobic nature and to evaporate any remaining water.

Prior to cell seeding, collagen type I was injected into the devices through the collagen filling port (Figure 3-1). Once polymerized (1 h at 37 °C), collagen type I served as 3D scaffold for endothelial cells to grow into a capillary-like network. The devices are ready for cell culture after rehydration with culture medium in the channels.

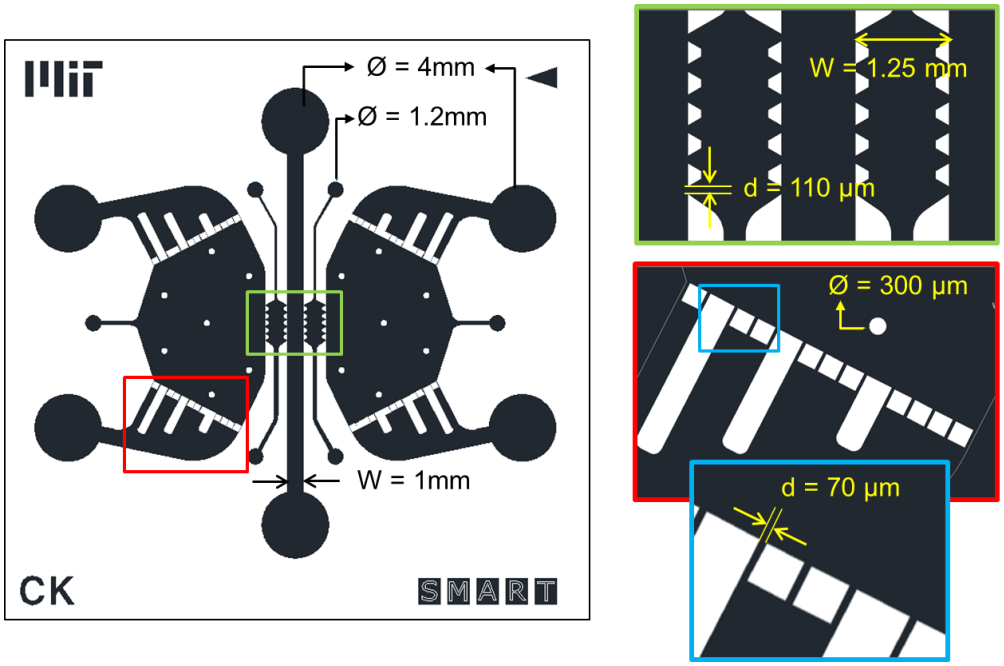

Figure 3-1 Detailed design of microfluidic device. The device comprises three culture media channels that allow culturing of multiple cell types, and two independent collagen gel regions intercalate between the three media channels. The width of the central channel is 1.2 mm and it is connected to two opening ports with 4 mm diameter. The side channels each have two rows of square posts with 70 µm spacing that act as bead trap regions to retain cells encapsulated or empty alginate beads in the channel. There are 7 cylindrical posts in the side channel with 300 µm diameter act as supportive pillars to prevent the channel from collapsing due to larger area of side channels. The collagen gel region is divided into 6 observation regions by trapezoidal posts that are spaced 110 µm apart and the width of gel region is 1.25 mm. The height of the channels and collagen gel regions is 120 µm throughout.

3.3 Cell Seeding

HUVECs were trypsinized and centrifuged at 200 g for 5 min and then resuspended in EGM-2mv at 2.5 M cells/ml. Media ports were then emptied, and 60 µl of HUVEC cells suspension was added into the center channel. Media were changed after 4 h to remove unattached cells from the channel. Microfluidic devices were incubated overnight at 37 °C to allow the formation of HUVEC monolayer that covered the collagen gel region. Subsequent cell cultures in microfluidic devices were static.

3.4 Cell Encapsulation

Fibroblasts were encapsulated in alginate beads as described earlier [128]. Briefly, 1% (w/v) alginate solution was made by dissolving 1 g of sodium alginate (Sigma, St Louis, MO) in 10 ml of culture medium. Fibroblasts were suspended in 1% alginate solution at 25 M cells/ml and then the suspension was passed through a two-phase microencapsulation device where alginate was calcified by calcium enriched oleic acid thus forming alginate beads containing fibroblasts. The beads were then injected into the right channel of endothelial cell-seeded microfluidic devices through the bead-inlet by micropipette. Injection through bead-inlet was necessary to contain beads within the bead trap region of the microfluidic devices. Similar procedures were used to encapsulate A549 lung carcinoma epithelial cells.

3.5 Preparation of Conditioned Medium (CM)

CM of endothelial cells was prepared by conditioning EGM-2mv with 83 k cells/ml (comparable to the cell concentration in the microfluidic device) HUVEC in 6-well plate over 24 h and the collected medium was centrifuged to remove cells and then used to culture fibroblasts in 6-well plates without further concentration or dilution.

CM of fibroblasts was prepared by conditioning EGM-2mv (Lonza, Walkersville, MD) with 100 k cells/ml IMR-90 in a 6 well plate over 24 h and then the CM was concentrated through dialysing with a 3 kDa filter (Millipore, MA). The concentrated CM was then diluted with EGM-2mv to reconstitute into concentration comparable to concentration in microfluidic devices.

3.6 Selection of PHis

Previously, works have been done on PDCA, HDZ and CPX and these three will remain the main study agents as PDCA shows promising angiogenic effects in *in vivo* model. Besides, both HDZ and CPX are FDA approved drug and are used as vasodilator and anti-mycotic agent respectively.

3.7 Preparation of Prolyl Hydroxylase Inhibitors, S1P and VEGF

Since angiogenesis is a highly complex biological process that requires participation of multiple angiogenic proteins, PHis that could upregulate various angiogenic cytokines through HIF-1α stabilization are of great interest for therapeutic angiogenesis [127]. Previously, our group demonstrated that ciclopirox olamine (CPX), hydrochloride hydralazine (HDZ) and 2,4-pyridinedicarboxylic acid (PDCA) were able to induce angiogenesis either in 2D cell culture or zebrafish models [4]. Therefore, these three PHis were selected to test for their angiogenic potencies in microfluidics. The working concentrations of these three PHis were determined through previously reported values from our group [4].

Ciclopirox olamine, CPX (Sigma, St. Louis, MO) stock solution was made in to 0. 5M by dissolving 67 mg of CPX in 500 µl of methanol. Stock solution was further diluted into 500 µl of culture medium to make yield 1 mM. CPX was used at 8 µM to stimulate angiogenesis. Hydralazine hydrochloride, HDZ (Sigma, St. Louis, MO) stock solution was made by dissolving 19.7 mg of HDZ

into one ml of filtered DI water at room temperature to yield 100 mM. 2,4-pyridine-dicarboxylic acid, PDCA (Sigma, St. Louis, MO) powder (110 mg) was dissolved in 2 ml ultrapure water together with 120 mg of sodium bicarbonate (Sigma, St. Louis, MO) to form 300 mM solution of 2,4-pyridine-dicarboxylate through acid-base reaction. For simplicity, 2,4-pyridine-dicarboxylic and 2,4-pyridine-dicarboxylate will be used synonymously as PDCA throughout the report.

S1P powder (Sigma, St. Louis, MO) was added in methanol:water (95:5) to 0.5 mg/ml, then sonicated at 45 °C until S1P was suspended in the solution. The solvent was removed by using a stream of dry nitrogen until a thin film of S1P formed and then stored at -20 °C as stock. Fatty acid-free BSA (Sigma, St. Louis, MO) with a minimum concentration of 4 mg/ml was used as the S1P carrier to make 125 µM solution. The final concentration of S1P in culture media was 250 nM. Recombinant human $VEGF_{165}$ (R&D, MN) was reconstituted at 100 µg/ml in sterile PBS containing 0.1 % BSA (Sigma, St. Louis, MO).

3.8 Preparation of Avastin, Gefitinib, W146 and MCP-1 neutralizing antibody

A 25 mg/ml stock solution of Avastin (Roche, Switzerland) was diluted with media into 0.1 mg/ml. human IgG (GenScript, NJ) was dissolved in recipient (240 mg of α,α-trehalose dehydrate (Sigma, St. Louis, MO), 23.2 mg of monobasic, monohydrate sodium phosphate (Sigma, St. Louis, MO), 4.8 mg of dibasic, anhydrous sodium phosphate (Sigma, St. Louis, MO), and 1.6 mg of polysorbate 20 (Sigma, St. Louis, MO) in 4ml of sterile water) to yield 25 mg/ml and then diluted with media into 0.1 mg/ml as an appropriate control.

To yield 10 mM primary stock, 50 mg of gefitinib (Eurasian chemicals, India) was dissolved in 11.2 ml of DMSO (VWR, PA). The working concentration of gefitinib was 10 µM.

To yield 0.15 mg/ml (0.329 mM) of primary stock, 1 mg of W146 (Cayman chemical, MI) was dissolved in 6.67 ml of ethanol (VWR, PA). The stock solution was diluted with culture media to final concentration of 10 µM or 1µM.

Human MCP-1 neutralizing antibody, AF-279-NA and normal goat IgG (R&D Systems, MN) were reconstituted at 0.2 mg/ml in sterile PBS.

3.9 Immunohistochemistry

HUVEC and IMR-90 cells were fixed in microfluidic devices with 4 % paraformaldehyde (Sigma, St. Louis, MO) for 15 min at room temperature followed by PBS washing, twice. Cells were permeabilized by 0.1 % Triton X-100 (Sigma, St. Louis, MO) for 10 min at room temperature and washed with PBS once, then blocked with 0.5 % BSA (Sigma, St. Louis, MO) blocking solution for 2 h at room temperature. VE-cadherin primary antibody (Enzo Life Sciences) was diluted to 1:100 and incubated with cells overnight at 4 °C . Microfluidic devices were washed with washing buffer (0.1% BSA in PBS) 3 times, each with 5 minutes incubation time and then incubated with Alexa Fluor-conjugated goat anti rabbit-secondary antibody (Molecular Probes, Eugene, OR) at a dilution of 1:100 for 4 h at room temperature. Microfluidic devices were again washed with buffer 3 times, each with 5 min incubation time. Cells were then counterstained with 10 µg/ml Hoechst (Molecular Probes, Eugene, OR) and 100 times diluted 300 U Phalloidin rhodamine (Molecular Probes, Eugene, OR) for 30 min at room temperature. Fluorescence was detected using a confocal microscope (OLYMPUS, FluoView FV1000).

3.10 Dextran concentration gradient assay

HUVECs were seeded in the middle channel one day before the assays were run to form monolayer of HUVECs in the channel. Subsequently, 2 µM of 40

kDa (which resembled VEGF with molecular weight of 45kDa) Texas Red-conjugated dextran (Molecular Probes, Eugene, OR) was infused into the right media channel while the middle/left channel was kept as EGM-2mv to allow formation of dextran concentration gradient across the collagen gel. Images were analyzed with Metamorph and Image J.

3.11 Proteomic analysis

In order to collect cultured media for proteomic analysis, 83 k cells HUVEC and 200 k cells IMR-90 were seeded in 6-well plates and subjected to the following conditions in culture media (EGM-2mv): 8 µM CPX and 250 nM S1P, 8 µM CPX only, 250 nM S1P only and medium only. In a parallel experiment, endothelial CM (see above) was applied to IMR-90 in 6-well plates to study communication between endothelial cells and fibroblasts. The supernatant of each condition was collected and then centrifuged at 200 G for 5 min at room temperature to remove cells and kept at -20 °C in aliquots before proteomic analysis.

Proteome profiler, human angiogenesis array kit (R&D Systems, MN) was used to detect the presence of angiogenesis-related proteins in the cell culture supernatant as per the manufacturer's instruction. Briefly, 700 µl of cell culture supernatant were incubated with a primary biotinylated antibody mixture at room temperature for 1 h and then incubated with array membranes at 4°C overnight. Bound antibodies were detected and visualized with streptavidin-HRP chemiluminescent substrate using a chemiluminescent imaging system (Syngene, G:Box, UK), and the intensity was quantified through Image J software (http://rsbweb.nih.gov/ij/).

ELISA assays (R&D Systems, MN) were run to quantitatively measure the protein concentration of VEGF, MCP-1 and PlGF as per the manufacturer's protocol. Colorimetric enzyme reaction was performed as per manufacturer's protocol and analysed in a microplate reader (Tecan, Sunrise Magellan, Switzerland) at 450 nm. The data obtained were processed using Prism

(GraphPad Software, CA) that is capable of generating a four parameter logistic (4-PL) curve fit.

3.12 Western Blot

Cell lysate was prepared from endothelial culture in 24-well culture plate where endothelia were subjected to 4 different pharmacological inductions as mentioned above. The protein concentration in each cell lysate was then determined by Bradford assay against the BSA standard curve. Subsequently, 8 % resolving and 5 % stacking polyacrylamide gels were casted in house. Then, 10 µg of total protein from each sample was loaded and then the gels were run for electrophoresis together with ladder control and the proteins were then transferred to PVDF (Biorad, CA) membrane through electroblotting. Membranes were incubated with primary antibody against $S1P_1$ (Cayman Chemical, MI) in a 1:200 dilution in 5% BSA-0.05% tween-PBS buffer overnight at 4 °C with gentle shaking. The membranes were washed 3 times in 0.05% tween-PBS, 10 min incubation each. The membranes were then incubated with HRP-conjugated secondary antibody (Santa Cruz, TX) in 1:2000 dilution for 1.5 h at room temperature followed by washing steps as mentioned. The membrane was exposed to x-ray film (Konica Minolta, Japan) for at least 10 s and developed using KD-90 developer and KF fixer (Konica Minolta, Japan). α-tubulin was used as a loading control and detected using primary antibody (Santa Cruz, CA) and HRP-conjugated secondary antibody (Santa Cruz, CA) both in 1:5000 dilution. The film was then scanned and analyzed using Image J (http://rsbweb.nih.gov/ij/) plugin, “Gels” that allows comparing the area under the curve (AUC) between bands.

3.13 Quantification of sprouts in microfluidic devices

The cell number is quantified by using the inbuilt Image J function, 3D objects counter, to measure the Hoechst stained nuclei across different depths from confocal images. The maximum sprout length of each gel region was determined by drawing a line from the edge of the collagen gel to the tip of the furthest grown sprout, using Image J software (http://rsbweb.nih.gov/ij/). In order to measure the skeletal length of the sprouts, 3D confocal fluorescence images of VE-cadherin staining were projected onto a 2D plane and processed in the following order: enhancing contrast, reducing noise through despeckling, smoothening through Gaussian blur, converting to binary image through auto threshold, and finally skeletonizing with the Image J plugin, AnalyzeSkeleton (see Figure 3-2) [129]. These manipulations were written into a macro that batch-processed the images automatically to avoid bias. Area of capillary sprouting was determined by accessing the VE-cadherin positive areas from the projected stacked image after automatic threshold. Estimated diameter was obtained by dividing area of capillary sprouting by skeletal length. Migration distance of migrating cells was measured by the shortest distance between nuclei position and the edge of collagen gel where the endothelial monolayer was.

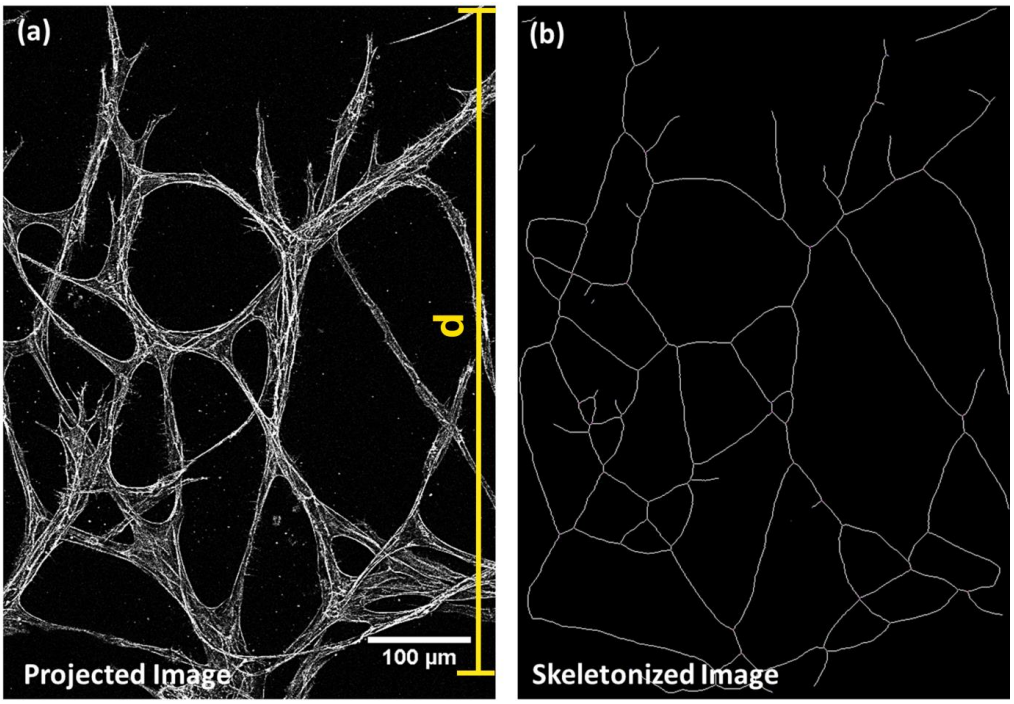

Figure 3-2 Skeletal length measurement is made through skeletonizing confocal images.(a) Projected 2D image of VE-cadherin stained capillary network from 3D confocal stack images. The vertical yellow line represents the maximum sprout length, d that measures the distance of the furthest grown sprout from the edge of collagen gel. (b) Skeletonized image of (a) by using Image J plugin, AnalyzeSkeleton. Skeletal length is the total length of the skeletonized network. Scale bar = 100 µm.

3.14 COMSOL Simulation

The model was built based on a 2D transport of diluted species model by using COMSOL Multiphysics simulation software. The diffusion coefficients of 40 kDa Texas red-conjugated dextran, VEGF and PlGF in cell culture media, collagen gel and alginate beads were estimated based on a 40 kDa inert molecule from Stokes-Einstein equation and also adapted based on previous findings [130-132]. The values of diffusion coefficient for VEGF and PlGF are identical based on Stokes-Einstein estimation because their molecular weights are both in the range of 40k Da [133, 134]. The secretion and consumption rates of VEGF and PlGF were calculated based on the ELISA results that I obtained previously and normalized against cell number in microfluidics. The initial concentration of 40 kDa dextran was set as $2x10^{-3}$ mol/m^3 in the right channel and 0 in every other region based on the

concentration of 40 kDa that has been added into the microfluidic. The initial concentration of VEGF and PlGF was set as 3.2x10-8 mol/m^3 and 0 respectively based on the concentration of these two proteins in culture media as determined through ELISA. The parameters are summarized in Table 3 .

Table 3 Parameters for COMSOL simulation

	Dextran	VEGF	PlGF
Diffusion coefficient in media, D_{media} ($\times 10^{-11}$ m^2/s)	5.9	6.0	6.0
Diffusion coefficient in media, D_{beads} ($\times 10^{-11}$ m^2/s)	N.A.	5.5	5.5
Diffusion coefficient in media, D_{gel} ($\times 10^{-11}$ m^2/s)	4.9	4.9	4.9
Reaction rate in EC, R_{EC} ($\times 10^{-13}$ mol/s.m^3)	N.A.	-3.04	2.84
Reaction rate in IMR-90, R_{IMR-90} ($\times 10^{-13}$ mol/s.m^3)	N.A.	7.81	0
Initial concentration,C_0 ($\times 10^{-8}$ mol/m^3)	200000	3.20	0

3.15 Statistical Analysis

Numerical values were expressed as the means ± SE (standard errors) of at least three independent experiments. One way analysis of variance (ANOVA) with Newman-Keuls post-test was used to determine statistical significance when comparing multiple means. Student's *t*-tests were conducted, when applicable, to compare means between two groups. Statements of significance were based on P-values < 0.05, 0.01 and 0.001.

CHAPTER 4. MICROFLUIDIC DEVICES FOR ANGIOGENESIS RESEARCH

Recent advances in microfluidic technologies have brought angiogenesis research to a new level and have provided insights on angiogenesis that conventional angiogenesis assays could not. The advantages of microfluidic platforms include the abilities to

- observe the formation of capillary sprouting within a physiologically relevant 3D collagen gel matrix
- form a endothelial monolayer that resembles that in a pre-existing blood vessels prior to angiogenesis
- allow interactions of multiple cell types in a single device
- establish control over solute concentration gradients

These advantages are important in the study as the ability to form capillary sprouting with true lumen in a 3D matrix that can anastomose is the first step in pursuing solutions for therapeutic angiogenesis. This feature can be achieved by using microfluidics with loaded collagen gel as a scaffold. Moreover, the formation of endothelial monolayer prior to the capillary sprouting differentiates the angiogenesis process from vasculogenesis. As angiogenesis requires the interplay between endothelia and other cell types such as fibroblasts [22], the ability to culture multiple cell types in a single device makes microfluidic device an attractive platform to study angiogenesis. Angiogenesis is a highly regulated process that requires participation of numerous cytokines especially ones that can induce directed chemotaxis on endothelia [118, 126]. Therefore, microfluidics offer direct control over solute concentration gradients that can affect how the endothelia respond to

the cytokines, either added exogenously or secreted spontaneously from a nearby cell source. Microfluidic devices are powerful tools that can provide new insight to enrich the knowledge of current field but these advantages also come with certain price. The fabrication of microfluidic devices takes at least 3 days (discussed in details in Chapter 3: Materials and Methods) before they are ready for experiment. In addition, the sprouting experiment usually takes 4 days for more developed vascular network to be formed while the commercially available Matrigel and transwell assays usually do not last more than 24 h [135]. The long preparation process and experiment time frame for microfluidic assays restrict the potential to obtain large amount of data within limited time. The small operating volume is a double-edged sword in a microfluidic assay. The small operating volume saves reagents and the tiny microenvironment within a microfluidic device also offers greater control over solutes distribution [114]. However, general biochemistry assay such as ELISA will require higher amount of working volume than a typical microfluidic device can yield [136]. In addition, the retrievable number of cell from a single microfluidic device is usually too low for further quantifications such as western blot or PCR analysis. Therefore, culture media or cells have to be pooled from multiple devices for accurate analysis. Nevertheless, the advantages that microfluidic platform can offer outweigh its disadvantages for the studies on angiogenesis; therefore I have adopted it as a functional assay in my studies. Based on different designs of microfluidics, various treatments that are usually not applicable to conventional cell culture are made possible such as the application of shear and interstitial flows and mechanical stretching. Song et al. showed that sheared stress inhibited the VEGF-induced sprouting through nitric oxide signalling in a microfluidic angiogenesis assay [137]. In addition, they also showed that interstitial flow can increase the EC invasion into the collagen through a Rho-A dependent pathway and similar results were obtained by Vickerman et al. where they showed the interstitial flow not only improved cell migration but also vascular formation in another microfluidic assay [114, 137, 138]. The shear stress inhibition of angiogenesis ensures that the mature vessels with flow

can maintain a non-sprouting phenotype while vessels with low flow are prone to angiogenesis [137]. Meanwhile, the interstitial fluid pressure of solid tumours is usually higher than surrounding tissue which leads to the generation of interstitial flow that triggers the angiogenesis cascade [139]. Although those treatments are beyond the scope of this thesis they demonstrate the new dimension and perspective that microfluidic technology has brought to angiogenesis research.

Design of the microfluidic device that I use consists of several main regions: a central channel where the endothelial cells were seeded flanked on each side by a chamber that contains a 3D matrix (collagen type 1 in this case), then two larger side channels with bead trap region for empty alginate beads or cell-containing alginate beads (see Figure 3-1). The trapezoidal posts at the two sides of gel region serve to contain the gel solution due to surface tension during filling, and stabilize the gel against mechanical disruption. The collagen gel regions contained between the trapezoidal posts serve as observing regions for the growth of vascular network (Figure 3-1). The alginate beads with the size of around 100 µm can be injected into the bead trap region through a bead inlet and they are contained by rows of square posts spaced 70 µm apart (Figure 3-1).

With those features mentioned, endothelial cells in the middle channel form a monolayer 2 days post seeding which serves as a pre-existing blood vessel that is adjacent to 3D collagen matrix for studying angiogenesis (Figure 4-1). Based on Figure 4-1, I have observed that endothelial cells formed a continuous monolayer in the microfluidic channel that covered the flank side of collagen gel and also the glass bottom and PDMS top surfaces. Although the cross-section of the channel is rectangular, the continuous EC monolayer preferred a cylindrical tubular structure and Zheng et al. showed a similar EC curvature in a PDMS microfluidic channel [125]. Barreto-Ortiz et al. also showed that the circumferential alignment of EC deposited-collagen IV, fibronectin and laminin; that are important in helping vessel to withstand the circumferential stress, can only be maintained on a curved surface but not on

2D flat surface [140]. The growth of new sprouts took place from this curved EC monolayer and extended into the collagen regions. Blood vessels are usually surrounded by layers of extracellular matrix including collagen type I, IV, XVIII, laminin and proteoglycans [141]. Therefore, I cannot rule out that the possibility that PDMS top and glass bottom would affect the angiogenic behaviour in the system even though the region of interest is the collagen scaffold with growing sprouts. Nevertheless, Mammoto et al demonstrated that EC grown on stiffer fibronectin-coated polyacrylamide gel (4000 Pa) showed higher expression of VEGFR2 but the receptor expression levels were significantly lower in EC grown on rigid glass coated with fibronectin [142]. In addition, Lopez-Garcia also showed that the stiffness of 2.5 mg/ml (the concentration that I used) of collagen type I at physiologically relevant displacement rate was near the range of 4000 Pa [143]. Therefore, the EC that adhered to the flank side of collagen might be more responsive to VEGF induction due to higher expression of VEGFR2.

As fibroblasts are usually more abundant than endothelial cells *in vivo* i.e. 27 % of cells in the heart are comprised of fibroblasts but only 7 % are endothelial cells, I have to accommodate about 4 times more fibroblasts than endothelia in the devices to address this difference [144]. In addition, as the cell size of fibroblasts is generally larger than endothelial cells, the common equal-channel width design shown in Figure 4-2 that I previously used could not accommodate a sufficient number of fibroblasts to support the growth of new vessels. In fact, the ratio of endothelia to fibroblasts in the equal-channel width design is 3:1. Fibroblasts favour collagen gel and they invade into collagen matrix readily which would obstruct the observation of sprout formation in the 3D collagen gel and might even cause gel contraction in some cases. In order to address both cell number and fibroblast invasion issues, cell encapsulation by using alginate beads was chosen, thus the need for including bead trap regions in the enlarged side channels in the microfluidic devices.

Alginate bead encapsulation can prevent most of the fibroblasts from entering the collagen gel matrix and only some of the encapsulated fibroblasts would break free from alginate beads and invade into collagen gel in the later part of experiment .The number of fibroblasts in the beads can be controlled by adjusting the concentration of fibroblast in suspension during encapsulation [9]. As the diameter of alginate beads fall in the range of 70 to 100 µm, they are trapped within bead trap region by the square posts during injection. Consequently, fibroblasts in the side channel only communicate with endothelial cells through paracrine signalling.

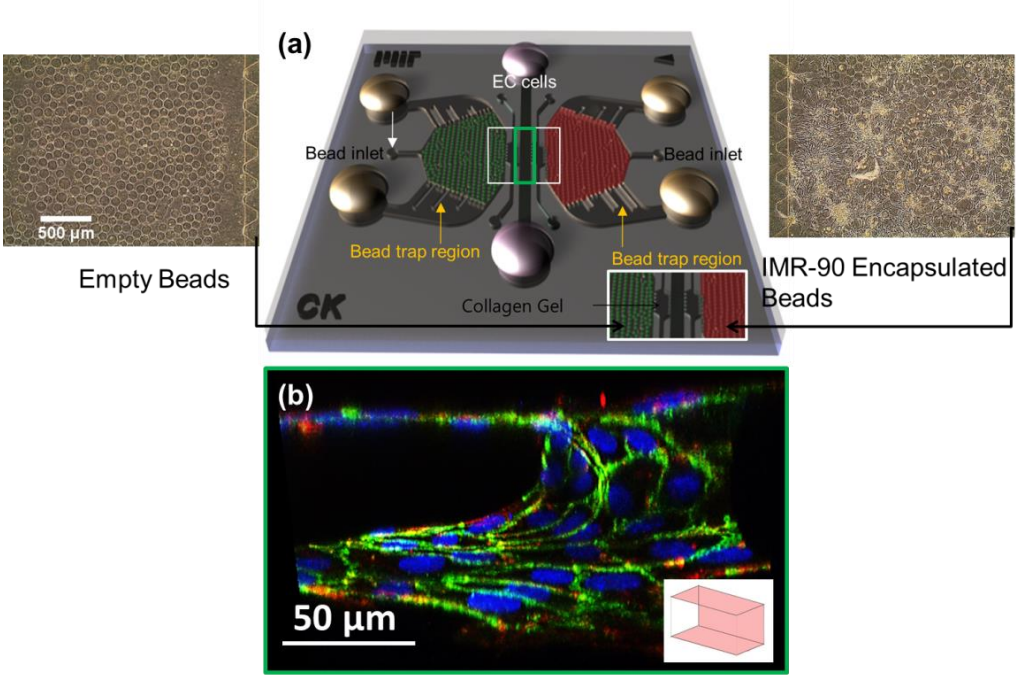

Figure 4-1 Schematic diagram of microfluidic devices and experimental setup. (a) Endothelial cells were seeded in the middle channel and cultured for one day to form a monolayer that represented a pre-existing vessel for studying angiogenesis. Red spheres denote fibroblast-encapsulated alginate beads while green spheres denote empty alginate beads. Alginate beads were introduced via the bead inlet and contained in the bead trap regions of side channels by square posts with 70 µm spaces. (b) Confocal image of endothelial cells with Hoechst stained nuclei (blue), rhodamine phalloidin stained actin (red) and Alexa fluor 488 immunostained VE-cadherin (green), formed a monolayer lining the medium channel. The monolayer is adjacent to the collagen gel region that allows growth of new sprouts in 3D

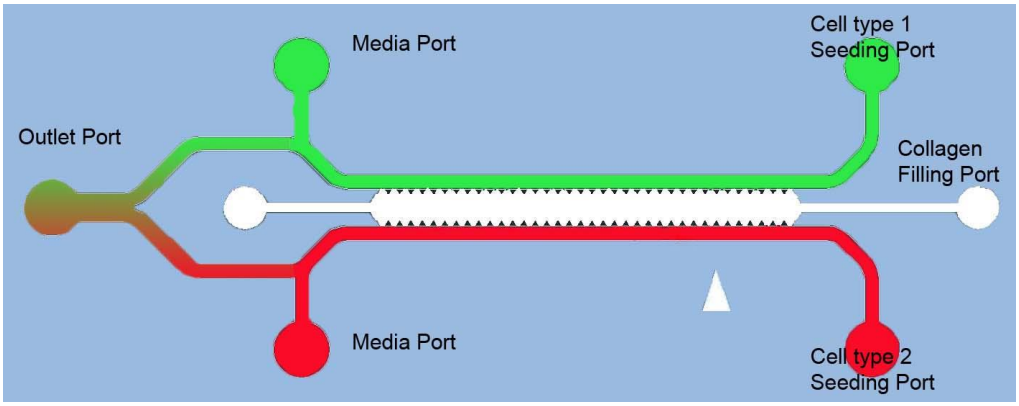

Figure 4-2 Schematic diagram of microfluidic device with equal channel width. This microfluidic device consists of two media channels with 500 µm width which are separated by a matrix region and are reconnected downstream at the outlet port. The trapezoidal pillars at the matrix region provide sufficient surface tension to contain the collagen gel during gel filling.

As paracrine signalling is expected to affect the endothelial sprouting behaviour, I then validated the system by running dextran diffusion assay to determine the diffusion and concentration gradient profiles in the microfluidic devices. Texas Red-conjugated dextran (Txr-Dex) with a molecular weight of 40 kDa was diluted in media to yield 2 µM solution. The solution was injected into the right channel where fibroblasts were seeded to simulate the diffusion profile of fibroblasts secreted VEGF (45 kDa) across the collagen gel region. From Figure 4-3, I determine that Txr-Dex diffused through the collagen gel attaining a steady concentration gradient profile at 24 h. I also observed that Txr-Dex reached a plateau near the right edge of collagen where endothelial cells formed a monolayer. This is due to the diffusive barrier that is created by endothelial monolayer and this also shows that the integrity of endothelial monolayer was not compromised in the experiments. With these results, I confirmed that proteins secreted from fibroblasts could form steady concentration gradients across the collagen gel and reach the endothelial cells.

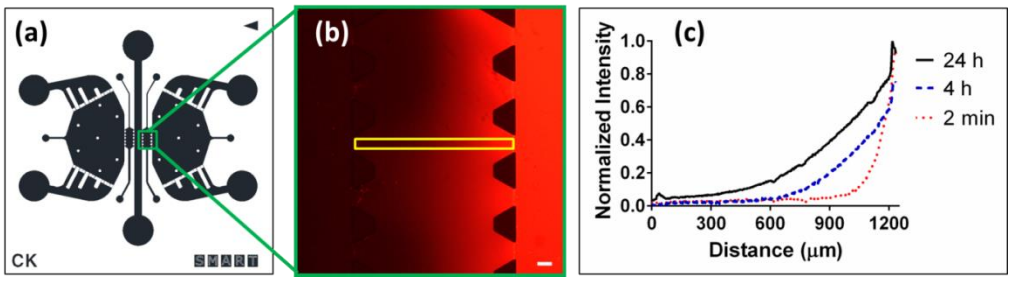

Figure 4-3 Concentration gradient assays in microfluidic device. (a) Schematic drawing of microfluidic device and the arrow head denotes the direction of diffusion. (b) 4x epifluorescent image of microfluidic device with 2 μM of TxR-Dex injected into right channel at 24 h time point. The middle channel was seeded with HUVECs that formed a monolayer whereas the right channel was filled with alginate-encapsulated fibroblasts. The yellow rectangular box denotes the region taken for quantitative measurement of fluorescent intensity across the gel region. (c) Quantitative plots of fluorescent intensity versus distance across the gel region. Distance 0 denotes the edge between the middle channel and the collagen gel. The plots show that the concentration gradients reached a plateau near the right edge of collagen gel at 24 h. Scale bar = 100 μm.

In order to further validate this device for studying angiogenesis, I employed VEGF, a well-known potent angiogenic factor to induce angiogenesis in the microfluidics. Therefore, 20 ng/ml of VEGF was added to the right and left channels that contained fibroblasts encapsulated alginate beads (right channel) and empty alginate beads (left channel) respectively but not in middle channel to create VEGF concentration gradients in both collagen gels. From the phase contrast images of Figure 4-4, I can see that VEGF could induce capillary sprouting after 4 days of culture. Based on the images, I could confirm that the sprouts formed in the collagen contained lumina and that they also formed in 3D. The sprouts that grew in 3D could anastomose in a later stage once they extended further into the collagen gel region which is yet another key feature in a functional vessel network. Hence, I successfully demonstrate that microfluidic devices as exceptional functional platforms for studying angiogenesis in a 3D context with applied chemokine gradient in a co-culture condition.

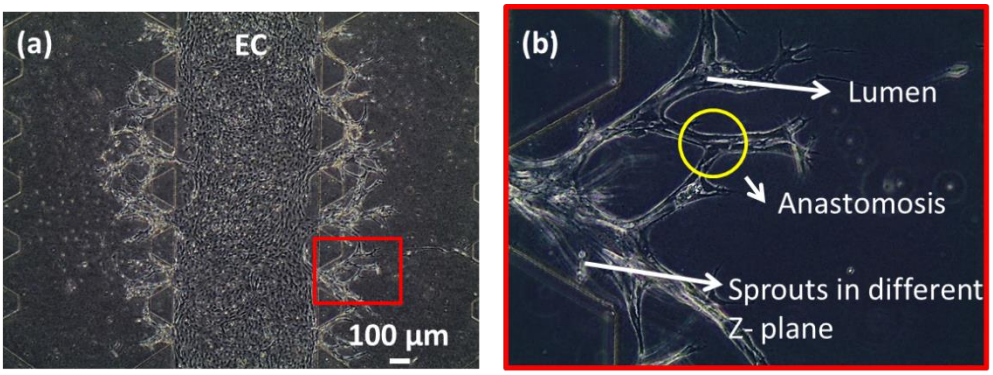

Figure 4-4 VEGF-induced capillary sprouting in 3D collagen gel. (a) 4x Phase contrast image of VEGF-induced capillary sprouting in 3D collagen gel. (b) Magnified image of specified area in (a) that shows the sprouts with lumen grew in collagen gel across different depth and also shows the anastomosis of two nearby sprouts. Scale bar = 100 µm.

As fibroblasts have been shown to stabilize the formation PHi induced capillary-like structure [4], I then carried out systematic quantifications to confirm the stabilizing effects of fibroblasts on immature sprouts. Fibroblasts are able to induce and maintain capillary sprouting even in the absence of any exogenous angiogenic stimulus as they could secrete various angiogenic chemokines including VEGF naturally [145]. In microfluidic assay, some immature sprouts could form during the early stage of the experiments. However, those immature sprouts could not be maintained and would either regress or detach from the endothelial monolayer if they were growing towards empty alginate beads on day 4. Conversely, the capillary sprouts that grew towards fibroblasts were stabilized as reflected by the skeletal length, cell number and maximum length of the sprouts. The skeletal length and maximum length of sprouts growing towards fibroblasts encapsulated beads were about 2x more than the sprouts growing towards empty beads while the cell number in the sprouts was about 3x more. These results confirm the importance of fibroblasts in inducing and stabilizing capillary sprouting in microfluidics and the experimental results that I show in following chapters are always with fibroblasts encapsulated alginate beads in right channel while empty alginate beads in left channel serve as control unless otherwise specified.

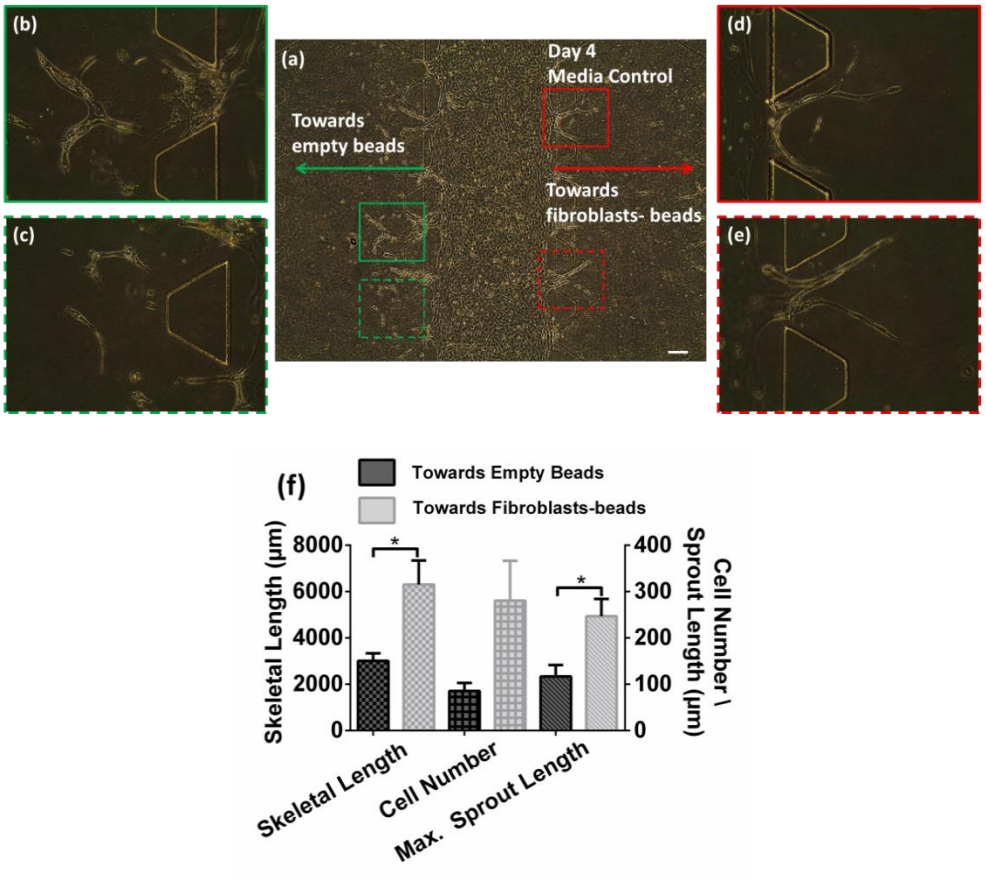

Figure 4-5 Fibroblasts induce and stabilize endothelial sprouting in collagen gel. (a) 4x phase contrast image of endothelial cell sprouting assay in cell culture media on day 4. (b) and (c) 20x phase contrast images of detached sprouts and endothelial cells from the EC monolayer that were growing towards empty alginate beads. (d) and (e) 20X phase contrast images of sprouts growing towards alginate-encapsulated fibroblasts . (f) Quantification of skeletal length, cell number and maximum sprout length for sprouts growing towards empty beads and towards fibroblast-encapsulated beads in cell culture media. Without the support of fibroblasts, sprouts would regress or detach from EC monolayer on day 4. Scale = 100 µm. * $p < 0.05$

Barkefors et al. have shown that VEGF and FGF gradients are important in inducing the endothelial migration in a microfluidic platform while Gerhardt et al. also demonstrated that VEGF distribution is important in guiding tip cell migration and disruption of the VEGF gradients would lead to misguidance of tip cell filopodia in a mice retinal angiogenesis model [126, 146]. The dextran assay proved that concentration gradients can be maintained across the

collagen gel, which is an absolute advantage of using microfluidics in studying angiogenesis *in vitro*. Formation of functional vascular networks involves multiple processes including cell proliferation, guided migration, formation of lumen, branching of neo-vessel, anastomosis of vessels and vessel pruning [147]. With a single microfluidic assay, I could observe all the above-mentioned processes and the morphologies of vascular networks in great detail.

The importance of mural cells in vascular development has been highlighted in the literature over the years and among those assisting cell types, I am particularly interested in employing fibroblasts as mediating cells in thesystems as it has been shown that fibroblasts could regulate angiogenesis through growth factor secretion such as VEGF, ANG-1 and HGF and also through matrix remodelling by secreting MMPs or depositing collagen and fibronectin [21, 22]. Most importantly, our group has previously shown that fibroblasts could response more aggressively to the stimulation of PHi and leads to HIF-1a stabilization which then promotes angiogenesis [4]. I have demonstrated the ability of incorporating fibroblasts encapsulated alginate beads in the devices that can promote angiogenesis even in the absence of exogenously added angiogenic proteins.

Various in vitro angiogenesis models that can study different stages of the angiogenesis processes such as matrix degradation, migration, proliferation and morphogenesis were summarized by Goodwin [148]. Among various models that are available, only limited in vitro models are able to capture the whole event of angiogenesis and this microfluidic assay is one of the few. The commonly used Matrigel assay or Transwell assays only provide information on endothelial cell morphogenesis and migration respectively [148]. Endothelial cells can form capillary-like structures (CLS) spontaneously when they are cultured on Matrigel. Often time, the CLS on Matrigel grow in 2D but tubular structures may be observed too [149]. Nonetheless, the matrix degradation and branching events that can be observed in a microfluidic assay are not able to be shown in a Matrigel assay. In addition, the

application of concentration gradient of angiogenic stimuli in a Matrigel assay is usually very difficult. Commercially available Transwell assay can be used to study the endothelial migration towards a higher concentration of chemoattractant but endothelial cells will not form capillary or tubular structure in this assay [148]. Other more developed assay such as microbead assay allows the observations of sprouting events from endothelial cell coated microbeads that are embedded in a matrix [150]. This assay can essentially capture all stages of angiogenesis but the quantification might be challenging as the vessels grow in radial direction.

In short, the microfluidic device that I use have been validated through the studies of its diffusion profile, its ability to allow formation of sprouts with lumina and also its versatility in accommodating a second cell type together with endothelia. With these features, the microfluidic device serves as an excellent platform for studying angiogenesis *in vitro*.

CHAPTER 5. RESULTS

5.1 Comparisons between PHis

Among the three PHis tested, CPX showed the greatest angiogenic potential while PDCA could induce little to no sprout formation. When these three PHis were introduced individually into microfluidics, 8 µM CPX could help promote angiogenesis in collagen on the right side that was adjacent to fibroblast-encapsulated beads within 4 days while 10 mM PDCA induced the least sprout formation and 100 µM HDZ showed angiogenic potential that was greater than PDCA but obviously weaker than CPX (Figure 5-1 (a)-(c)).

Similarly, S1P that can affect angiogenesis through multiple pathways (as mentioned in Introduction) also holds great promise for therapeutic angiogenesis [89]. While the angiogenic effects of PHIs and S1P have been shown individually, it has remained unclear if they would further promote angiogenesis as a combination. I then tested if the angiogenic potentials of PHis could be further boosted by combining them with S1P. Interestingly, I did not observe any increase of capillary sprouting in the preliminary experiments when PDCA was coupled with S1P but I could clearly observe that both HDZ and CPX responded well with the addition of S1P and showed increased sprout formation (see, e.g., Figure 5-1 (d)-(e)). In addition, the sprouts induced by CPX + S1P extended more than 800 µm into collagen gel within 4 days as compared to 400 µm with the HDZ + S1P combination and less than 150 µm with PDCA + S1P. CPX + S1P induced capillary sprouting also showed complex vascular structure indicating sprout anastomosis, hence this combination held the promise to be used to develop fully functional networks. Since CPX showed the greatest angiogenic potential among the PHis tested, I focused on CPX and its combination with S1P in inducing angiogenesis in *in vitro* microfluidic assays.

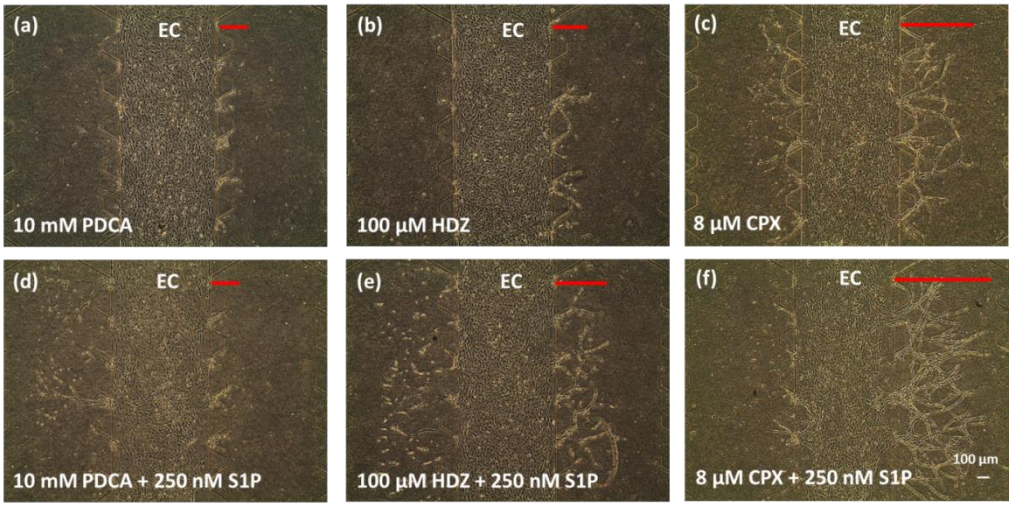

Figure 5-1 Different PHis show differential angiogenic potentials. (a) – (c) Phase contrast images of 10 mM PDCA, 100 µM HDZ and 8 µM CPX induced angiogenesis in collagen that is adjacent to the fibroblasts encapsulated alginate beads in right channel. (d) – (e) Phase contrast images of endothelial sprouting under the induction of different PHis combined with S1P. CPX outperformed HDZ and PDCA in inducing angiogenesis in *in vitro* microfluidic assay, regardless of being applied individually or in combination with S1P. Red bars denote approximate length of sprouts. Scale bar = 100 µm.

5.2 In combination, CPX and S1P induce an extensive vascular network with true lumina

I then proceeded to study the pro-angiogenic effects of CPX and S1P in microfluidics in the presence of fibroblasts as mediating cells. In order to increase fibroblast density while preventing direct contact with endothelial cells, fibroblasts were encapsulated in microbeads as described previously. I tested four conditions in microfluidic devices containing encapsulated fibroblasts: EGM-2mv as control, 8 µM CPX in EGM-2mv, 250 nM S1P in EGM-2mv and 8 µM CPX + 250 nM S1P in EGM-2mv. The concentrations of CPX and S1P were adapted from previous reported assays that could effectively induce angiogenesis *in vitro* [4, 151].

Endothelial cells showed some spontaneous sprouting into collagen gel before the application of the mentioned conditions but those sprouts persisted only if growing towards fibroblasts and these results were

consistent with previously shown data that indicated stabilization by fibroblasts of endothelial sprouting (Figure 4-5). With fibroblasts only, I observed relatively fewer longer sprouts, which did not anastomose. When CPX or S1P were introduced an increase of sprout length ensued with the formation of a basal network and formation of anastomoses. However, when CPX and S1P were combined, the resulting sprouts almost traversed the entire collagen gel width and extended as long as 0.8 mm in 4 days (Figure 5-2 (a)-(d) and Figure 5-3). This was comparable to the previous reported growth speed of capillaries in a rabbit corneal model of 0.2 mm/day [152].

I assessed skeletal length, maximum sprout length and the number of cells forming sprouts to compare the effectiveness of CPX and S1P in inducing angiogenesis. Skeletal length was calculated as the sum total of all sprout lengths, and used to document sprout density and complexity. CPX + S1P induced dense sprouting networks with 20800 ± 2790 µm skeletal length while S1P, CPX and media control produced 12900 ± 2220 µm, 9450 ± 195 µm and 6310 ± 1550 µm, respectively. Maximum length was determined from the longest sprouts to assess sprouting distance covered. The CPX + S1P combination again induced capillary sprouting that extended furthest into the collagen gel, 525 ± 69 µm as compared to S1P, CPX and media control that had maximum lengths of 372 ± 58.1, 297 ± 46.6 and 232 ± 52.6, respectively. The cell number of sprouts was an indicator of maturity in terms of endothelial participation in building sprouts where CPX + S1P increased the number of cells in sprouts to 678 ± 80.9 cells as compared to S1P, CPX and media control which had only 398 ± 67.0, 301 ± 76.7 and 241 ± 47.8 cells in the sprouts, respectively. All three metrics demonstrated that the CPX + S1P outperformed the monosubstance treatment with statistical significance (Figure 5-2 (e)-(g)). Confocal imaging demonstrated that the sprouts formed in the presence of CPX/S1P developed into a complex vascular network structure with clear evidence for lumina which can be clearly seen in the confocal images of the vascular network (Figure 5-4). The diameter of the capillary sprouting ranged between 10 and 30 µm where sprouts near the

endothelial monolayer were typically wider and comprised more cells because they were more mature as compared to the sprout tips that extended deeper into the collagen gel. VE-cadherin staining of the vascular network also confirmed that the integrity of the intercellular junctions was maintained during angiogenesis.

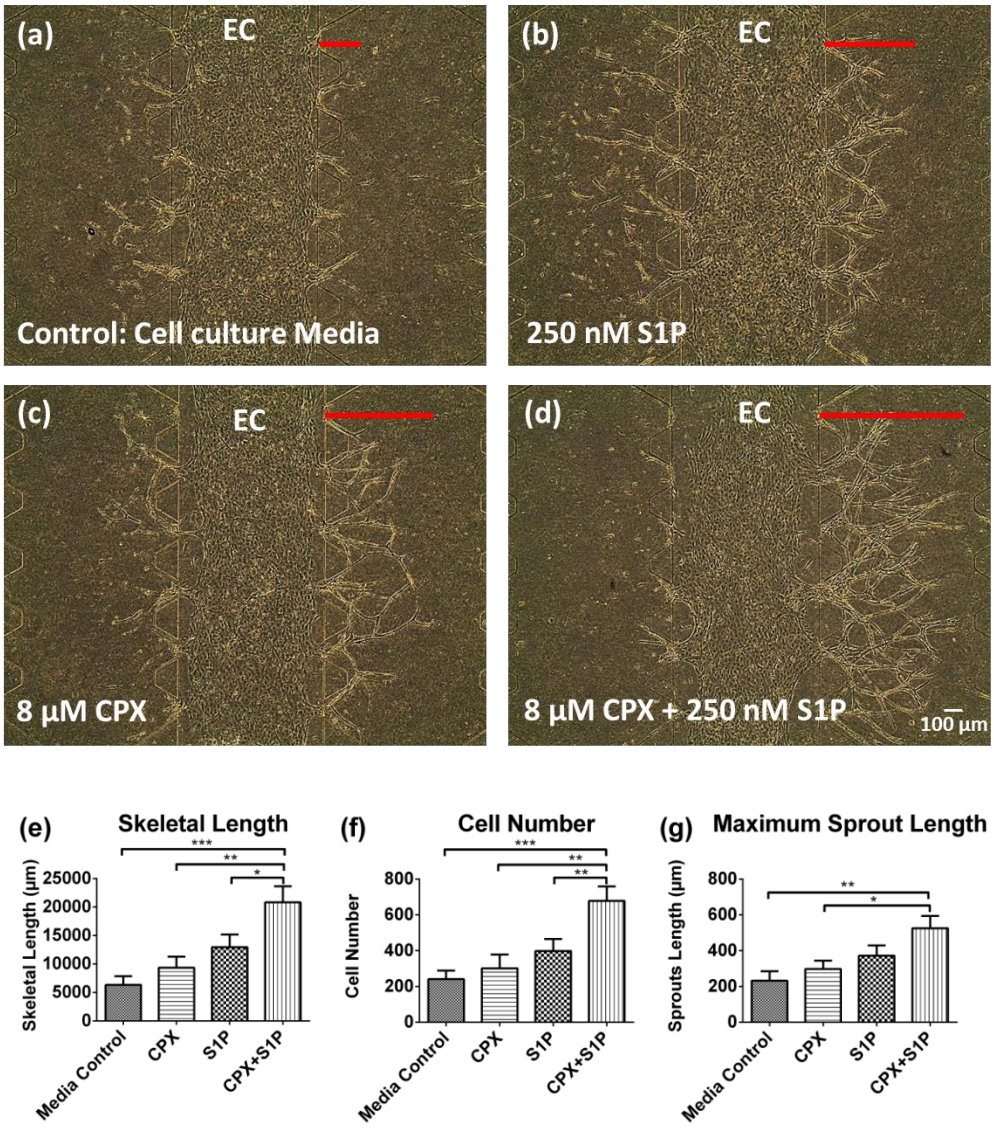

Figure 5-2 CPX and S1P together induce an extended vascular network in the presence of fibroblasts. (a) – (d) 4x phase contrast images of endothelial cells sprouting into collagen gels under different pharmacological conditions. Sprouts on the right side of the channel grow toward encapsulated IMR-90 fibroblasts. Red bars denote approximate length of sprouts. (e) – (g) Quantifications of skeletal length, cell number and maximum sprout length. CPX and S1P induce a more complex vascular network structure that is longer and contains more cells. Scale bar = 100 µm. Error bars denote standard error. * $p \leq 0.05$, ** $p \leq 0.01$, *** $p \leq 0.001$

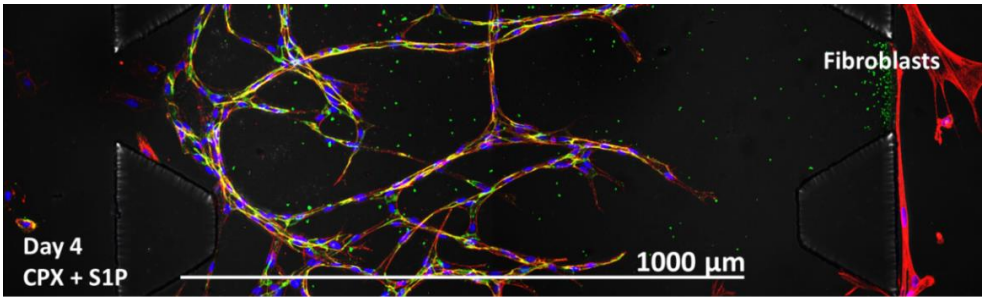

Figure 5-3 Sprouts that extend three quarters of the way across the collagen region under the induction of CPX + S1P . Stitched 20 X confocal images with Hoechst stained nuclei (blue), rhodamine phalloidin stained actin (red) and Alexa fluor 488 immunostained VE-cadherin (green) show that sprouts grew and extended around 800 µm into collagen gel in 4 days under the influence of CPX and S1P. Scale bar = 1000 µm.

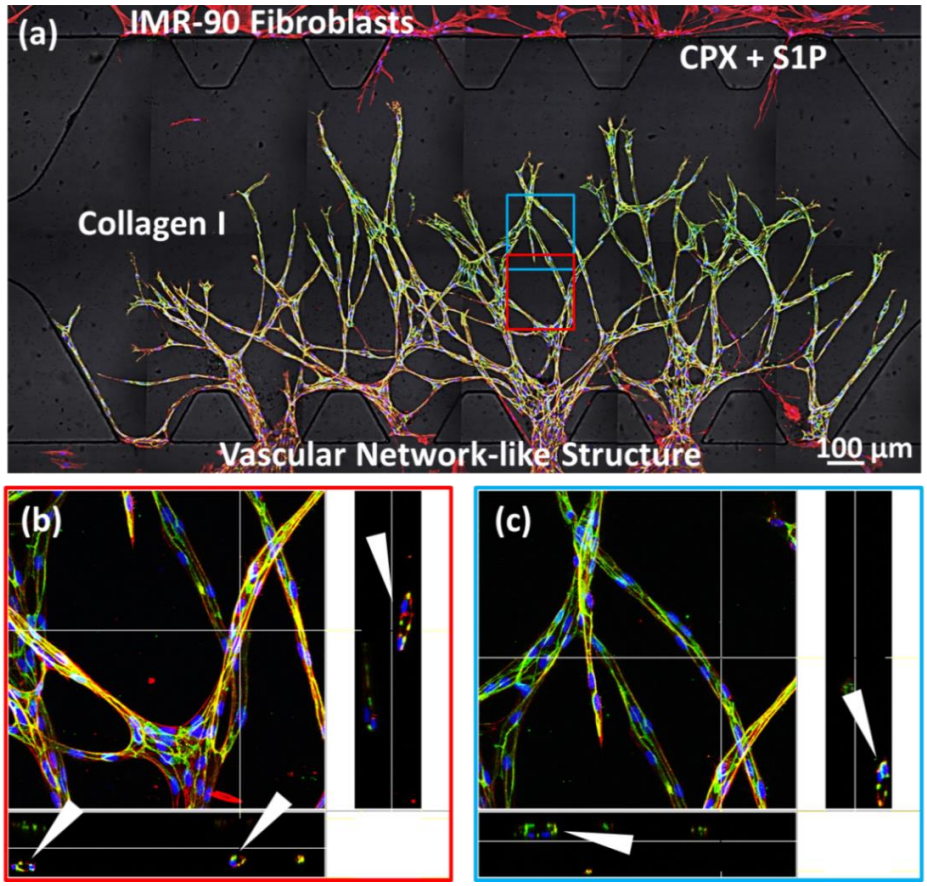

Figure 5-4 In combination, CPX and S1P induces formation of vascular network structure with defined lumina. (a) Stitched; (b) and (c) sectioned 20x confocal images of Hoechst stained nuclei (blue), rhodamine phalloidin stained actin (red) and Alexa fluor 488 immunostained VE-cadherin (green) show sprouts that anastomose under

8 µM CPX and 250 nM S1P induction. White arrows indicate lumina of endothelial sprouts with diameters around 20 µm. Scale bar = 100 µm

5.3 CPX induces secretion of complementary angiogenic proteins from both fibroblasts and endothelial cells

As endothelia and fibroblasts were separated by a collagen gel matrix in two adjacent channels, I hypothesized that soluble factors that can diffuse through collagen gel were responsible for the CPX + S1P induced angiogenesis. Therefore, I assessed the secretion of angiogenic factors by fibroblasts and endothelial cells in the presence of CPX and S1P, respectively. Proteome profiler data showed increased secretion of 4 proteins including PlGF (4.9 fold), IL-8 (3.7 fold), EGF (4.7 fold) and endothelin-1 (1.8 fold) by CPX + S1P treated endothelial cells among 55 angiogenesis related proteins that the proteome profiler can detect (Figure 5-5 (a)-(d)). Highly comparable increases were found in the presence of CPX alone with the exception of EGF secretion where CPX + S1P combination further boosted its secretion level by another 45 % as compared to CPX alone. No significant increase in proteomic secretions was observed with S1P only. The secretions of these factors were tested in fibroblast culture but fibroblasts did not express PlGF, EGF and endothelin-1 and the expression level of IL-8 was not altered by the treatment of CPX + S1P.

In fibroblasts, CPX + S1P increased the expression of HGF (1.6 fold), IGFBP-2 (2.2 fold), uPA (1.9 fold) and VEGF (11 fold) (see Figure 5-5 (f)-(i)). Similar to proteomic secretion by EC, highly comparable increases were found in the presence of CPX alone, and none were observed with S1P only. Based on proteomic profiling results, other angiogenesis related proteins including amphiregulin, IGFBP-3 and pigment epithelium-derived factor (PEDF) were detected in fibroblast cultures while endostatin/collagen XVIII, pentraxin 3 (PTX3), plasminogen activator inhibitor (PAI)-1, tissue inhibitor of

metalloproteinases (TIMP)-1 and thrombospondin-1 were detected in both cultures but their expression levels were not affected by neither CPX nor CPX + S1P combination.

I validated these data for PlGF and VEGF through ELISA. I found that CPX + S1P can increase the PlGF secretion rate in endothelia from 765 ± 37.1 (± SE) to 3300 ± 631 pg/ml-Million cell-day while S1P did not show any significant effect; these results were similar to those I have obtained through proteomic profiling. In fibroblasts I confirmed an increase of VEGF secretion from 280 ± 59.6 to 2080 ± 60.3 pg/ml-Million cell-day when fibroblasts were subjected to induction by CPX + S1P as compared to basal control. Again, while CPX alone induced comparable increase of VEGF production, S1P alone did not elicit measurable effects (see summary in Table 4).

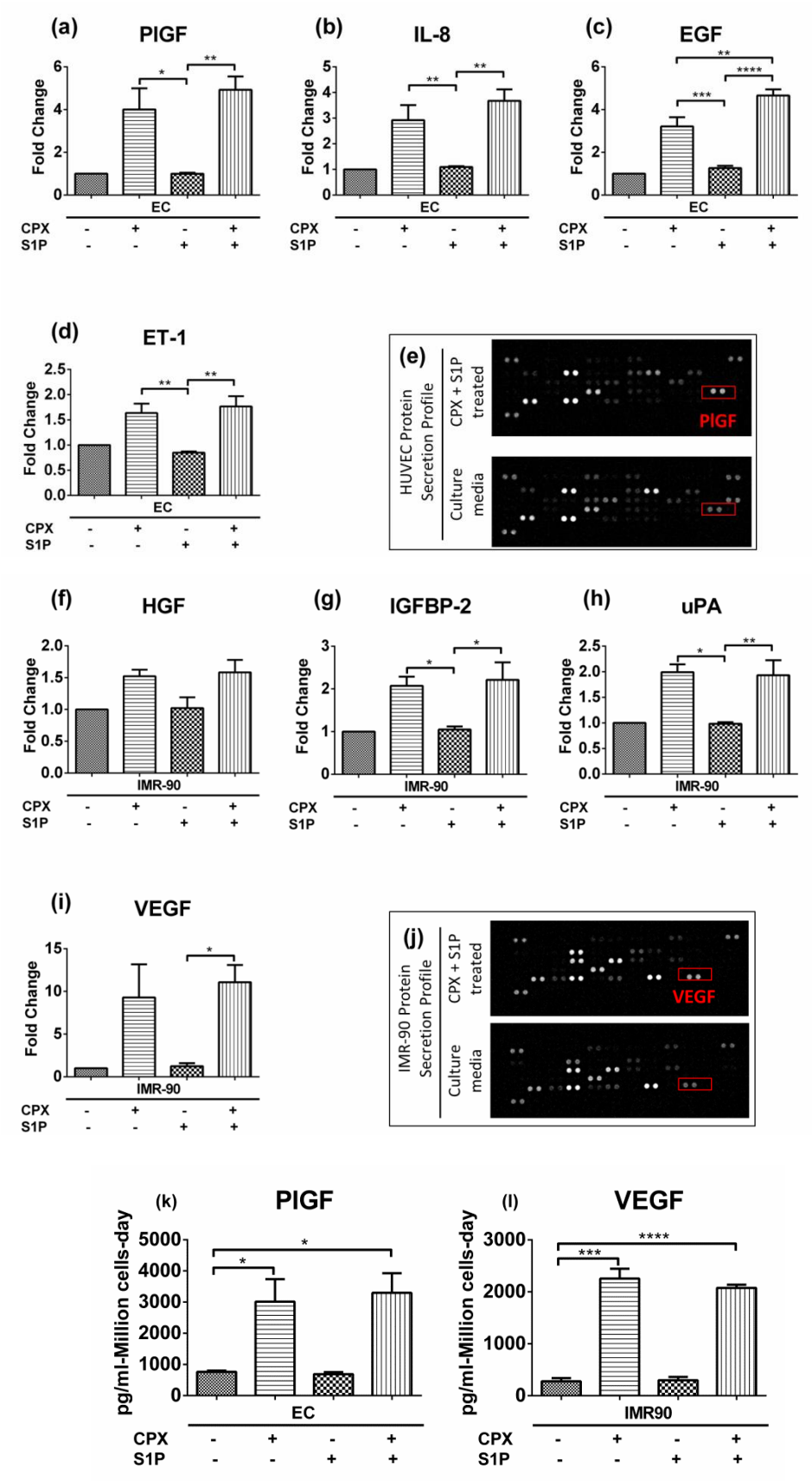

Figure 5-5 CPX induces secretion of different angiogenic proteins by endothelial cells and fibroblasts. (a-d): proteomic analysis plots of proteins upregulated in HUVEC

treated with CPX + S1P. The upregulated proteins are PlGF (4.9x), IL-8 (3.7x), EGF (4.7x) and endothelin-1 (1.8x). CPX and S1P combination further increased EGF expression by 45 % as compared to CPX only. (f-i): proteomic analysis plots of proteins upregulated in IMR-90 fibroblasts treated with CPX + S1P. The upregulated proteins include HGF (1.6x), IGFBP-2 (2.2x), uPA (1.9x) and VEGF (11x). CPX appears to be the main compound causing the observed upregulation. (e) and (j): representative images of 3 proteomic profiler membranes showing differences in protein secretion between CPX and S1P treated group and non-treated group (culture media control). (k) and (l): ELISA quantitation of PlGF and VEGF corroborating semi-quantitative results shown in (a) and (i) where PlGF secretion was increased from 765 ± 37.1 (± SE) to 3300 ± 631 pg/ml-Million cell-day while VEGF was upregulated from 280 ± 59.6 to 2080 ± 60.3 pg/ml-Million cell-day. Fibroblasts were cultured in VEGF free media for ELISA quantification to obtain true secretion rate of VEGF by fibroblasts. Error bars denote SE. * $p \leq 0.05$, ** $p \leq 0.01$, *** $p \leq 0.001$, **** $p \leq 0.0001$

Table 4 Angiogenic proteins secreted by EC and fibroblasts under the effects of CPX + S1P

Proteins	**Fibroblasts**	**HUVEC**	**Changed by**
HGF	+ →++	-	CPX
IGFBP-2	+ →++	-	CPX
uPA	+ →++	-	CPX
VEGF	+ →++	-	CPX
Endothelin-1	-	+ →++	CPX
PlGF	-	+ →++	CPX
EGF	-	+ →++	CPX
IL-8	+ →+	+ →++	CPX
MCP-1	+ →+	++ →+	CPX/S1P
	+ →++	N/A	Endothelial CM

"+→++" denotes upregulation of protein secretion; "-" denotes no protein secretion spontaneously; "++ →+" denotes downregulation of protein secretion

5.4 Effects of VEGF on CPX + S1P induced Angiogenesis

Among the proteins that were detected in fibroblast culture, VEGF was one of the most potent pro-angiogenic chemokines. I have confirmed that CPX and its combination with S1P could induce upregulation of VEGF in fibroblasts through proteomic profiling membrane and ELISA. Besides, the dextran assay shown earlier also confirmed that solutes in the side channel could diffuse through the collagen gel and reach EC in the middle channel. Therefore, I hypothesized that VEGF secreted by fibroblasts played a significant role in CPX + S1P induced angiogenesis in the *in vitro* microfluidic assay. In order to test the angiogenic potential of VEGF in these settings, Avastin (also known as bevacizumab) that could bind to and inhibit VEGF was employed. Avastin was used at a concentration of 0.1 mg/ml based on previous *in vitro* testing in tube formation assays and also its recommended dosage for clinical cancer treatment [153]. As shown in Figure 5-6 (a)-(d), 0.1 mg/ml of Avastin could reduce the CPX + S1P induced capillary sprouting back to background levels in the right collagen gel which was comparable to EGM-2mv cell culture media control. Meanwhile, 0.1 mg/ml of human IgG did not show inhibitory effects on CPX + S1P induced angiogenesis. Although endothelia that invaded into left collagen gel (towards empty alginate beads) could not be maintained and many had detached from monolayer and turned into migrating cells, I could observe that Avastin also greatly hindered cell migration as compared to IgG control or CPX + S1P positive control. I then quantified the results by measuring the skeletal length, cell number and maximum sprout length of the sprouts. The inhibitory effects of Avastin were clearly seen in all three metrics that I tested where skeletal length was reduced from 12300 ± 2170 to 4210 ± 402 µm, cell number was decreased from 303 ± 96.0 to 108 ± 28.5 and maximum sprout length was also shortened from 394 ± 51.6 to 144 ± 33.3 µm as compared to IgG control. With the confirmation from these quantification results, the importance of VEGF in CPX + S1P induced angiogenesis in microfluidics is verified.

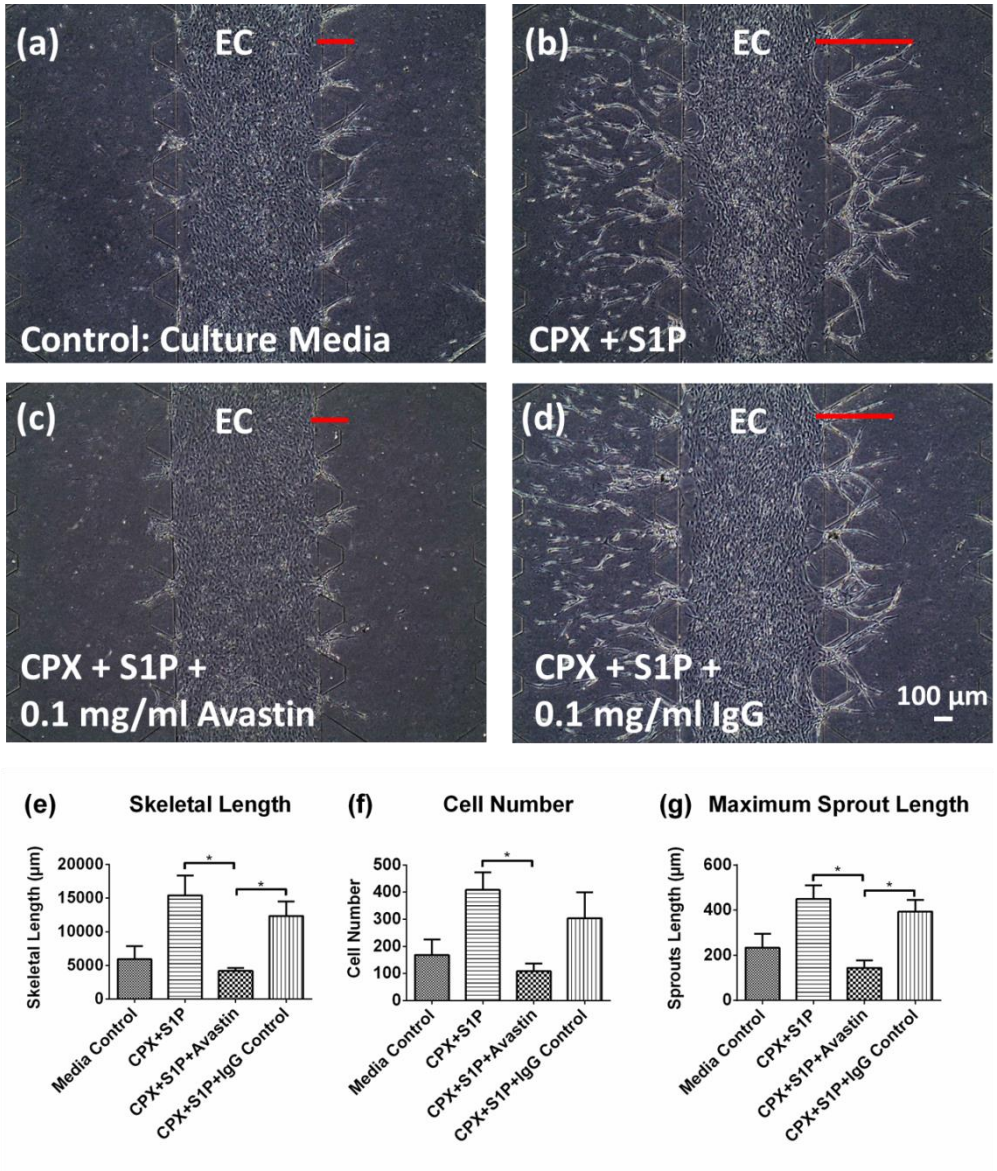

Figure 5-6 Avastin inhibits CPX + S1P induced angiogenesis. (a) – (d) 4x phase contrast images of CPX+ S1P induced capillary sprouting in collagen gel in the presence of fibroblasts encapsulated alginate beads. With 0.1 mg/ml of Avastin, CPX + S1P induced angiogenesis was reduced to basal level similar to culture media control. Red bars denote approximate length of sprouts. (e) – (g) Quantifications of skeletal length, cell number and maximum sprout length. Avastin reduced capillary sprouting density in microfluidics that led to shorter skeletal and maximum sprout length and fewer cells. Scale bar = 100 µm. Error bars denote standard error. * $p < 0.05$

I also observed that Avastin not only reduced the density of capillary sprouting but also changed the morphologies of the sprouts formed. As illustrated in Figure 5-7, Avastin resulted in sprouts with larger diameters as

compared to the other three conditions. The diameter of sprouts increased from 16.4 ± 0.9 to 21.8 ± 1.6 µm or 33 % increment as compared to IgG control. The confocal images also confirmed that lumen formation in capillary sprouts was independent of the presence of Avastin but I observed a clear increase in lumina diameter when Avastin was introduced.

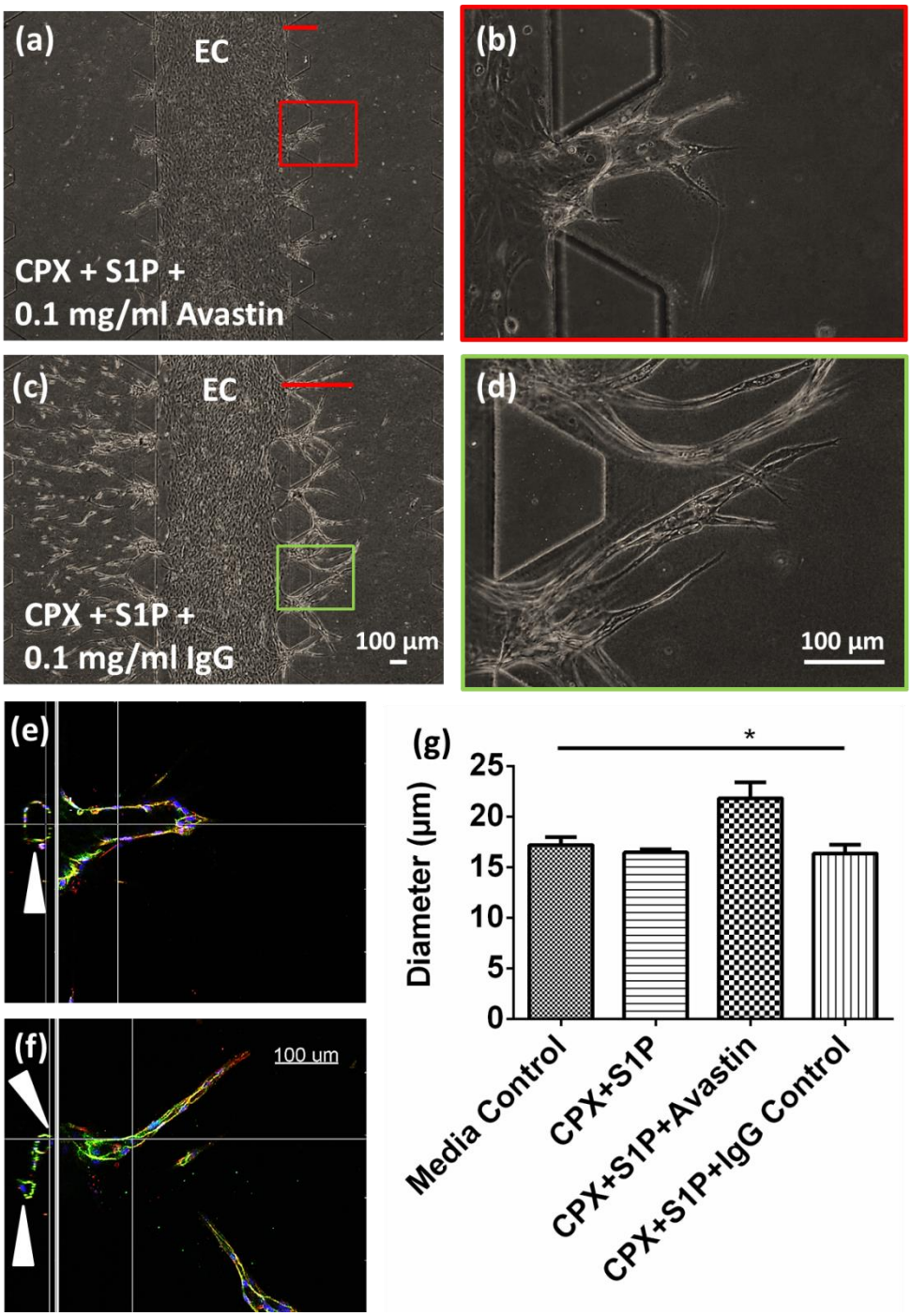

Figure 5-7 Avastin increases diameter of sprouts. (a) 4x phase contrast images of CPX + S1P induced capillary sprouting in microfluidics with 0.1 mg/ml Avastin or (c) 0.1 mg/ml IgG. (b) and (d) Magnified images of specified areas (marked by red and

green rectangles) in (a) and (c), respectively that show detailed morphologies of sprouts in collagen gel. (e) and (f) sectioned 20x confocal images of Hoechst stained nuclei (blue), rhodamine phalloidin stained actin (red) and Alexa fluor 488 immunostained VE-cadherin (green) show that sprouts formed lumina under 8 µM CPX and 250 nM S1P induction with (e) Avastin or (f) IgG control. White arrows indicate lumina of endothelial sprouts. (g) Quantifications of diameter of sprouts under the effects of culture media, CPX + S1P, CPX + S1P + Avastin and CPX + S1P + IgG. The diameter of sprouts was increased by 33 % in the presence of Avastin as compared to IgG control but the diameters of sprouts between non-Avastin treated groups were not significantly different. Scale bar = 100 µm. Error bars denote standard error. * $p < 0.05$

5.5 Effects of EGF on CPX + S1P induced Angiogenesis

As demonstrated earlier, VEGF that played an important role in CPX + S1P induced angiogenesis was prominently upregulated by CPX in fibroblast culture. I also showed that CPX could upregulate multiple proangiogenic proteins in endothelial culture including PlGF, IL-8, EGF and ET-1. Since EGF secretion was further increased by CPX + S1P by another 45 % as compared to CPX alone, I hypothesized that EGF was also important in CPX + S1P induced angiogenesis in microfluidics. In order to test this hypothesis, I utilized a tyrosine kinase inhibitor, Gefitinib, which targeted the tyrosine kinase domain of EGF receptor to try inhibiting CPX + S1P induced angiogenesis in *in vitro* microfluidics. Gefitinib was used at 10 µM based on the previously reported *in vitro* inhibition dose [154]. Surprisingly, I observed no negative effects on capillary sprouting when I introduced Gefitinib together with CPX + S1P as shown in Figure 5-8. The migration of endothelia and the sprouting density in collagen gel were similar between the Gefitinib treated group, vehicle control group and CPX + S1P positive control group. Therefore, I confirmed that Gefitinib was not effective in against CPX + S1P induced angiogenesis in the *in vitro* settings which also suggested that EGF was not a critical protein in regulating CPX + S1P induced angiogenesis.

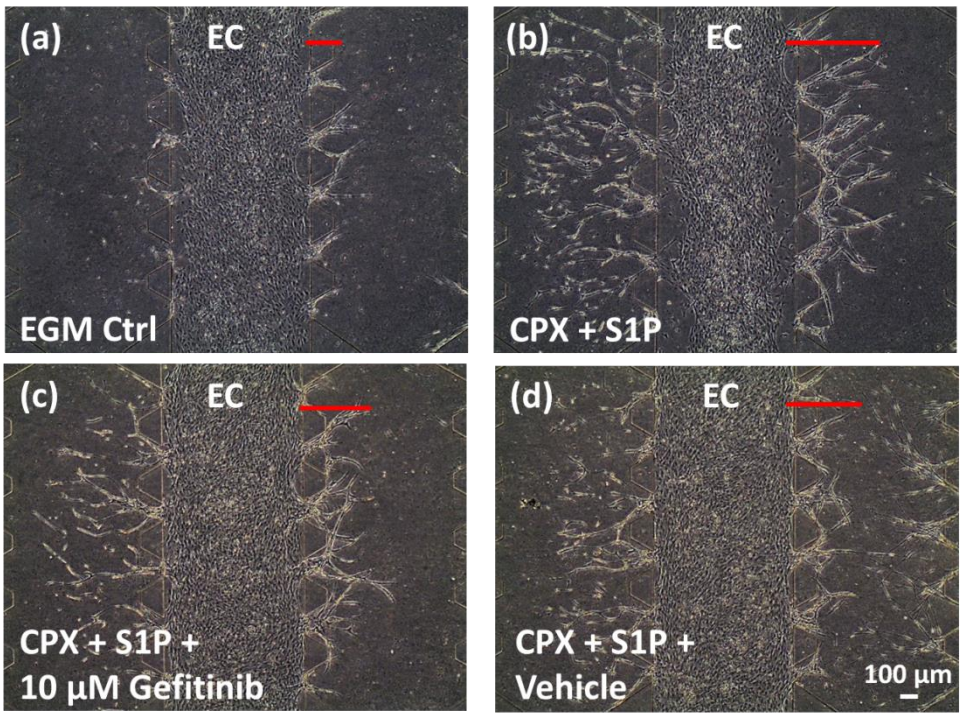

Figure 5-8 EGF receptor inhibitor, Gefitinib does not affect CPX + S1P induced angiogenesis. (a) – (d) 4x phase contrast images of endothelial capillary sprouting in collagen gel in the presence of fibroblasts encapsulated alginate beads under different pharmacological conditions. Gefitinib did not negatively regulate CPX + S1P induced capillary sprouting in collagen gel as compared to vehicle treated group. Red bars denote approximate length of sprouts. Scale bar = 100 µm. Error bars denote standard error. * $p < 0.05$

5.6 S1P increases cell migration in microfluidics

Through proteomic profiling assay and ELISA, I have shown that CPX was responsible for the upregulation of multiple angiogenic proteins from both endothelial and fibroblast cultures. Furthermore, the VEGF ligand inhibition experiment also suggested that CPX induced VEGF was important in CPX + S1P promoted angiogenesis. However, the role of S1P remains unclear especially since no significant reduction of angiogenic events was observed when an EGFR inhibitor was employed even though S1P in combination with CPX further boosted EGF secretion by 45 % in endothelial culture. I then continued the studies to look into direct pro-angiogenic effects of S1P on endothelia instead of possible paracrine or autocrine effects induced by S1P.

Microfluidic serves as an excellent platform for studying 3D cell migration in particular the design that I employed as it presents a collagen gel control on one (control) side (towards empty alginate beads) where endothelia received no inducement to form capillary sprouts due to the absence of fibroblasts. Instead, most of the endothelia that invaded into collagen gel on the control side would initially form immature sprouts but then detached from the endothelial monolayer and converted to individual cell migration on day 4. Based on previous experiments, I observed that whenever S1P was introduced, large numbers of endothelial cells showed migrating behavior in collagen gel on the control side as compared to the treatment groups without S1P (see Figure 5-9 (a-d)). I then quantified the number of migrating cells and migration distance on the control side to confirm if S1P increased endothelial cell migration. The quantification results were in line with qualitative comparison where S1P and CPX + S1P increased the number of migrating cells from 12.3 ± 1.7 in the media control group to 48.5 ± 6.4 and 68.8 ± 11.1, respectively. In the same context, the endothelial migration distance measured from the S1P and CPX + S1P treated groups were increased from 135 ± 21 µm in the media control group to 319 ± 14 and 327 ± 11 µm, respectively. In contrast, CPX did not influence endothelial cell migration as determined by both metrics used. Consequently, the pro-migratory effects of S1P have been confirmed in the *in vitro* microfluidic settings.

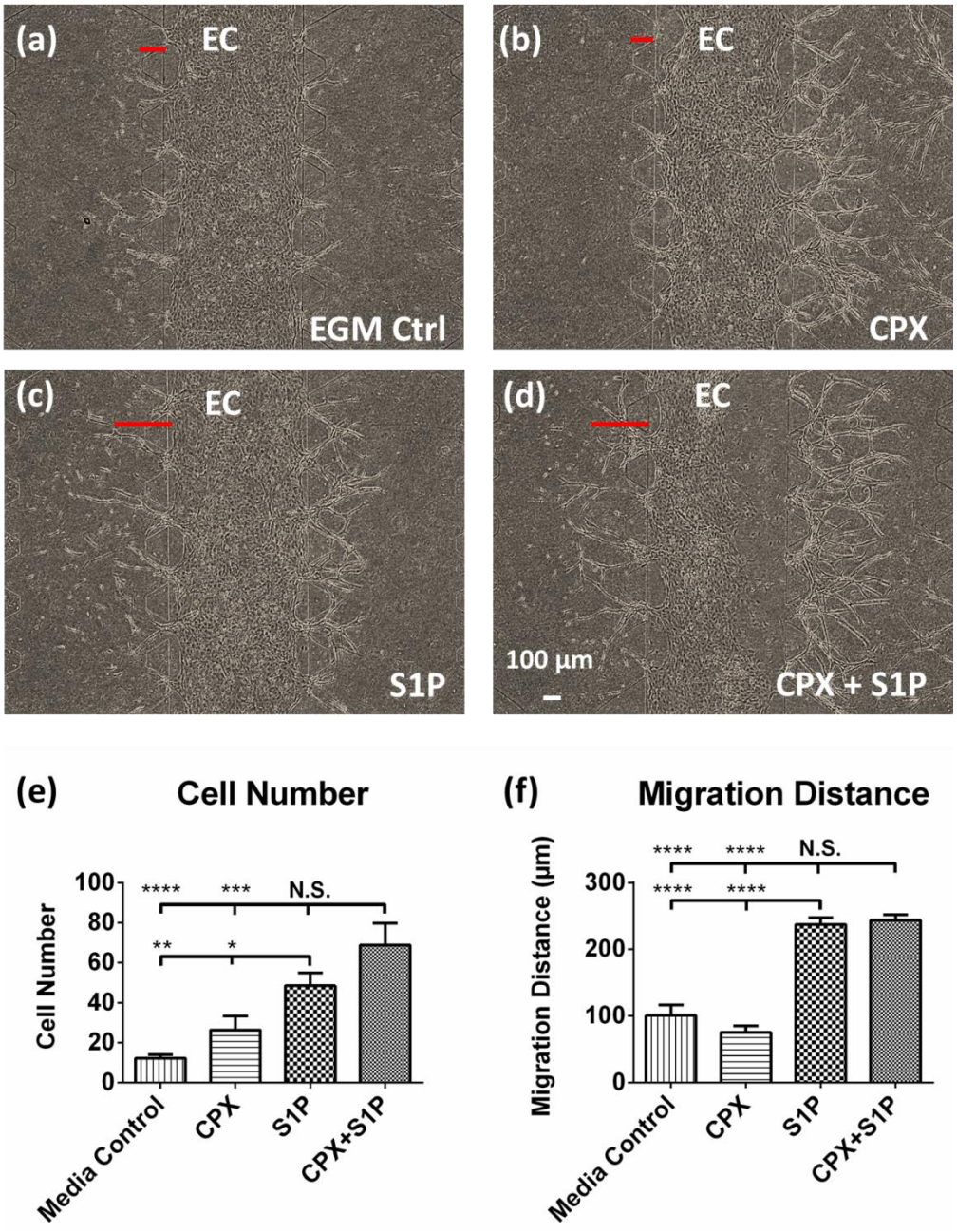

Figure 5-9 S1P promotes endothelial cell migration. (a) – (d) 4x phase contrast images of endothelial cells sprouting and migrating into collagen gels under different pharmacological conditions. Endothelia migrated into collagen gel on the control side (towards empty alginate beads) of the channel. Red bars denote approximate length of migration distance. (e) – (f) Quantifications of cell number and migration distance. S1P promoted endothelia invasion into collagen gel and also increased endothelial migration distance but these effects were not seen in CPX treated groups. Scale bar = 100 µm. Error bars denote standard error. * $p \leq 0.05$, ** $p \leq 0.01$, *** $p \leq 0.001$, **** $p \leq 0.0001$

5.7 Expression of $S1P_1$ on Endothelia

Several reports have indicated that S1P could induce endothelial cell migration through $S1P_1$ activation in *in vitro* transwell assays [97, 155]. It has also been shown that $S1P_1$ expression is dependent on type of endothelial cell [156]. Therefore, I proceeded to determine if $S1P_1$ was expressed on the HUVEC that I used. If it was, I then asked if its expression could be altered by either CPX or S1P. Based on Figure 5-10, I confirmed that $S1P_1$ is indeed present on the endothelia I used and surprisingly, its expression levels were also increased when treated with either CPX alone, S1P alone or CPX + S1P combination as compared to the media control group.

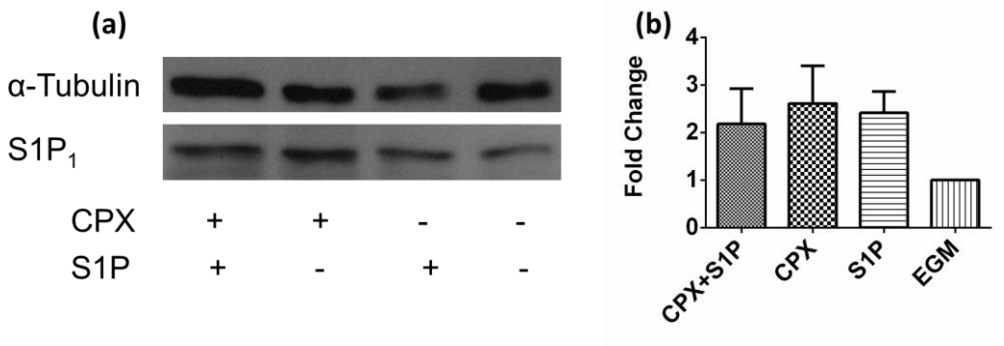

Figure 5-10 Expression of $S1P_1$ on endothelia is affected by S1P and CPX. (a) Immunoblots were stained with antibodies against $S1P_1$ and α-tubulin to detect $S1P_1$ expression in endothelial cell lysate under different pharmacological conditions. α-tubulin was used as loading control. (b) Quantification of fold change of treatment groups as compared to EGM media control group. Error bars denote SE.

5.8 Angiogenic effects of S1P were mediated through $S1P_1$ receptor

S1P exerts its functions on cells through five G-protein coupled receptors, $S1P_1$ to $S1P_5$ [89]. As previously reported, $S1P_1$ is involved in angiogenesis and I have also shown that endothelia expressed higher $S1P_1$ level with CPX or S1P treatment [101]. In order to further investigate its importance in CPX + S1P induced angiogenesis, a $S1P_1$ receptor specific inhibitor, W146 was used

to determine if S1P could enhance angiogenesis through $S1P_1$ in the microfluidic settings. W146 was used at 10 µM based on previously reported concentration that could fully inhibit ligand induced internalization of $S1P_1$ and its downstream events *in vitro* [157]. Treatment with 10 µM of W146 in all channels effectively reduced the sprouting response induced by CPX + S1P to baseline levels. Although I observed the negative effects on angiogenesis caused by equal volume of vehicle (ethanol), the inhibitory effects caused by W146 could still be clearly differentiated from the vehicle control group (Figure 5-11 (a)-(d)). I then quantified the skeletal length, number of cells and maximum length of sprouts to further confirm the inhibitory effects of W146. As demonstrated in Figure 5-11 (e)-(F), the skeletal length of sprouts in the W146 treated group was reduced from 9670 ± 2150 to 2910 ± 899 µm; while number of cells was reduced from 239 ± 38 to 93 ± 19 and maximum sprout length was also reduced from 325 ± 33 to 119 ± 33 µm as compared to the vehicle control. Similar to qualitative comparisons based on phase contrast images, the vehicle control showed slight inhibitory effects as compared to the CPX + S1P positive control group but this did not affect the observation of true inhibition caused by W146. These results not only confirm the importance of $S1P_1$ in CPX + S1P induced angiogenesis but also demonstrate the usefulness of microfluidics in differentiating various degrees of inhibition caused by either W146 or the vehicle control.

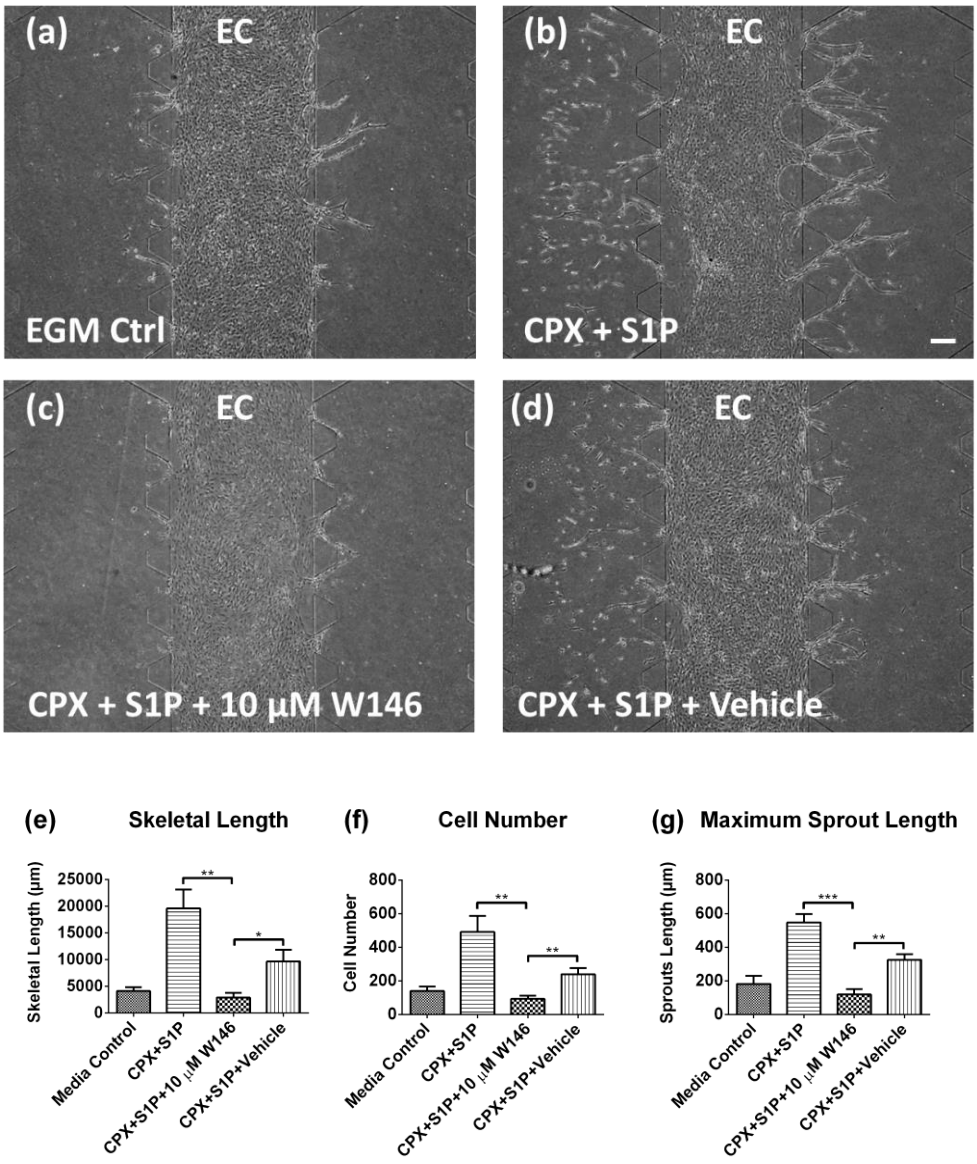

Figure 5-11 $S1P_1$ specific inhibitor, W146 inhibits CPX and S1P induced angiogenesis. (a) - (d) 4X phase contrast images show that the inhibitory effects of W146 were obvious on CPX and S1P induced angiogenesis. (e) - (g) Quantifications of skeletal length, cell number and maximum sprout length. Attenuation effects of W146 on capillary sprouting were clearly seen in terms of shorter skeletal and maximum sprout length and reduced cell number despite of the negative effects caused by the vehicle control. Scale bar = 100 µm. * $p \leq 0.05$, ** $p \leq 0.01$, *** $p \leq 0.001$

As $S1P_1$ also plays roles in regulating cell migration, I then quantified the endothelial migration in collagen gel on control side(towards empty alginate beads). As shown in Figure 5-12, the number of migrating cells and migration distance in W146 treated group were reduced to baseline levels which were

from 31.5 ± 3.2 to 10.0 ± 1.9 cells and 147 ± 8 to 104 ± 15 µm, respectively, as compared to the vehicle control. These results were also in line with the quantifications of skeletal length, cell number in sprouts and maximum sprout length where the vehicle control group showed reduced cell migration but not as significant as W146 treated group.

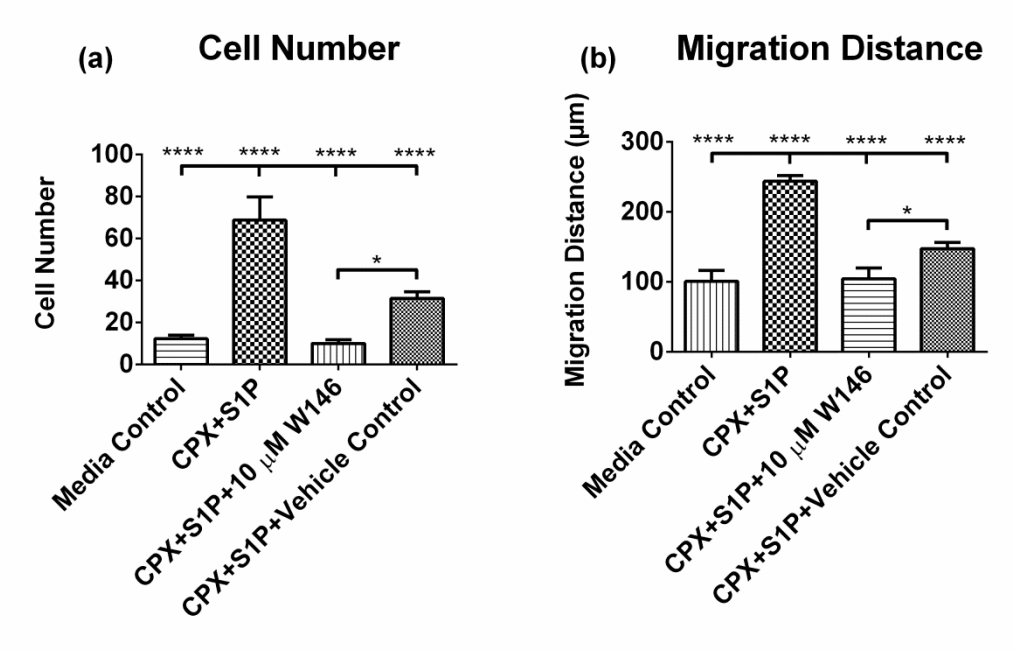

Figure 5-12 Effects of W146 on endothelial migration. (a) and (b) Quantifications of cell number and migration distance. W146 inhibited endothelial cell migration in 3D collagen gel scaffold resulting in fewer migrating cells and shorter migration distance over 4 day. Error bars denote standard error. * $p \leq 0.05$, **** $p \leq 0.0001$

In order to test if lower concentration of W146 could also inhibit angiogenesis in a dose dependent manner, I then reduced the concentration of W146 to 1 µM. However, with lower concentration of W146, I were unable to achieve significant inhibition on angiogenesis based on the skeletal length of capillary sprouts (see Figure 5-13(e)). Nevertheless, I observed changes in morphologies of sprouts which were similar to Avastin inhibition where diameter of capillary sprouts increased. Moreover, the ends of capillary sprouts where tip cells usually extend their filopodia were blunted in most of the cases as compared to the vehicle control group (see Figure 5-13(b) and (d)). These phenomena were more prominent when I reduced the

concentration of W146 from 10 µM to 1 µM as 10 µM of W146 almost abrogated the angiogenic events completely which made the observation of sprouting behavior become more challenging. I then quantified the diameter of capillary sprouts and I showed that with 1 µM of W146, the diameter of sprouts increased by 91 % or increased from 15.5 ± 0.3 to 29.7 ± 2.3 µm as compared to the vehicle control. Nevertheless, the diameters between non-W146 treated groups were similar. With these results, I have demonstrated that W146 not only inhibits angiogenesis but also changes the morphologies of sprouts.

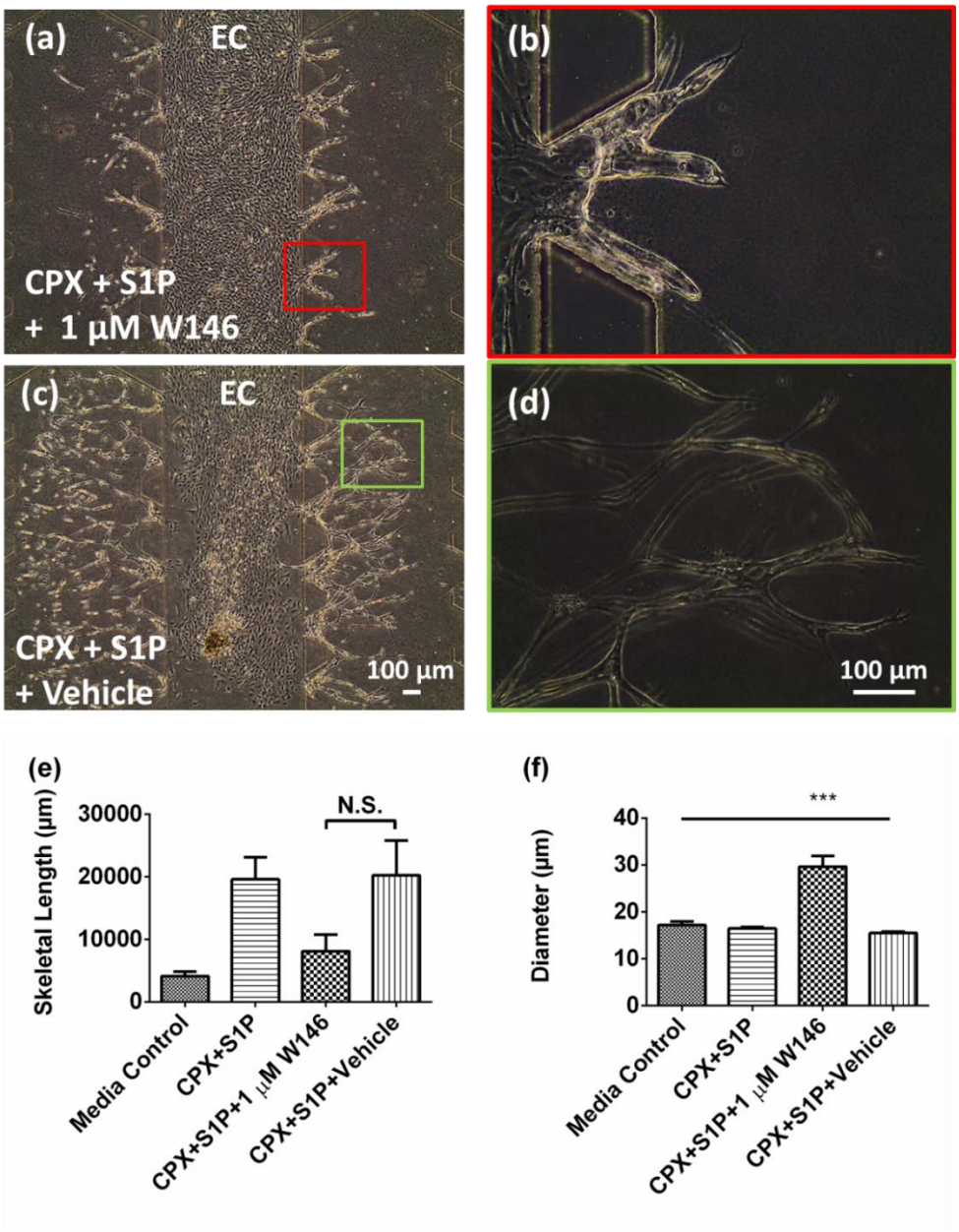

Figure 5-13 W146 increases diameter of sprouts. 4x phase contrast images of CPX + S1P induced capillary sprouting in microfluidics with (a) 1 µM W146 or (c) equal volume of vehicle. (b) and (d) Magnified images of specified areas (marked by red and green rectangles) in (a) and (c) respectively that show the detailed morphologies of sprouts in collagen gel. Some sprouts were out of focus because they were growing across different depths in 3D collagen gel. Quantifications of (e) skeletal length and (f) diameter of sprouts under the effects of CPX + S1P, CPX + S1P + 1 µM W146 and CPX + S1P + vehicle in culture media. W146 at concentration of 1 µM did not cause significant reduction in skeletal length but the diameter of sprouts was increased by 91 % as compared to the vehicle control group. The diameters of sprouts between non-W146 treated groups were not significantly different. Scale bar = 100 µm. Error bars denote standard error. *** $p \leq 0.001$

5.9 Endothelial cell CM increases MCP-1 secretion by IMR90

I have shown the pro-angiogenic effects of CPX and S1P in combination and these improvements to capillary sprouting were more significant if fibroblasts were present. Therefore, I continued the studies to investigate the possible interaction between endothelia and fibroblasts that is important in angiogenesis. To study the influence of endothelial cells on fibroblasts, I cultured IMR90 cells in EC CM with or without the addition of CPX+ S1P and quantified factors secreted by fibroblasts by proteomic profiler and ELISA. Among the 55 angiogenesis related proteins that the proteomic profiler can detect, MCP-1 was the only cytokine derived from fibroblasts that showed significant change when treated with EC CM. Interestingly, MCP-1 has also been reported to play a role in promoting angiogenesis through VEGF pathway [158]. To further validate the results, I did ELISA to measure the concentration of MCP-1 quantitatively. I detected a basal secretion level of 2450 ± 511 pg/ml-Million cell-day in fibroblasts culture. Endothelial cell CM induced the secretion of MCP-1 by fibroblasts by 3-fold in the absence of any CPX + S1P induction, however, the combination of both pharmacological agents increased MCP-1 secretion by a further 39%. As monosubstances, neither S1P nor CPX were able to increase basal MCP-1 secretion. However, MCP-1 secretion by EC was downregulated by CPX + S1P, from 1695 ± 32.8 to 955 ± 62.2 pg/ml-Million cell-day (Figure 5-14).

Previously, endothelin-1 and EGF have been shown to activate fibroblasts to secrete higher level of MCP-1 [159, 160]. Interestingly, CPX + S1P combination was able to upregulate endothelin-1 and EGF expressions by EC but did not show similar effects on fibroblasts culture. Instead, endothelin-1 and EGF level measured from fibroblasts cultured in EC CM showed values lower than the basal levels. These indicated either cellular uptake (taken by fibroblasts in this case) or degradation of the measured proteins.

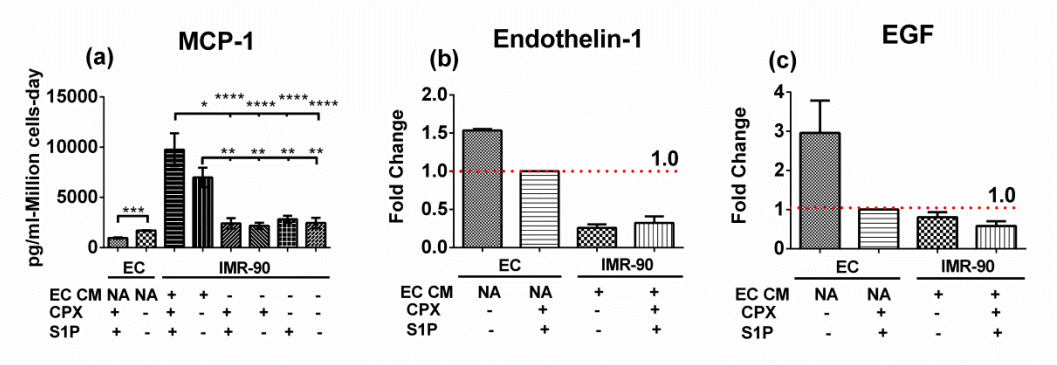

Figure 5-14 Endothelial CM modulates growth factor secretion by fibroblasts. (a) ELISA: fibroblasts secrete 3 times more MCP-1 when cultured in EC CM. No significant difference in MCP-1 secretion is elicited by CPX or S1P in fibroblasts culture. (b) and (c): semi-quantitative proteomic array plots showing clearance of EC secreted endothelin-1 and EGF from culture media in the presence of fibroblasts suggestive of either cellular uptake or degradation of measured target proteins . * $p \leq 0.05$, ** $p \leq 0.01$, *** $p \leq 0.001$, **** $p \leq 0.0001$

5.10 Diffusion profiles of VEGF and PlGF in fibroblast populated devices

The presence of fibroblasts was indispensable in the system as shown earlier although they were kept separated from endothelial cells by collagen gel where soluble factors are able to diffuse through. Therefore, I hypothesized that soluble factors derived from endothelia and fibroblasts play important role in CPX + S1P induced angiogenesis. This hypothesis has been supported by the proteomic profiling data where I detected the upregulations of different sets of angiogenic cytokines from endothelia and fibroblasts when they were treated with CPX. Most importantly, fibroblasts not only responded to the stimulation of CPX but also to the treatment of EC CM. I have shown that the MCP-1 secretion level of fibroblasts was directly influenced by endothelial cell CM and this suggests that EC-fibroblast communication is important in determining the proteomic secretion profiles of each cell type.

Since endothelia and fibroblasts rely on diffusive factors to communicate in microfluidics, I further the studies by employing COMSOL *Multiphysics*

simulation software to study the concentration profiles of secreted protein in microfluidic devices. PlGF secreted by EC and VEGF secreted by fibroblasts were used as representative proteins. The model was built based on a 2D transport of diluted species model. The diffusion coefficients of VEGF and PlGF in cell culture media, collagen gel and alginate beads were estimated based on a 40 kDa inert molecule from Stokes-Einstein equation and also adapted based on previous findings [130, 131]. The secretion and consumption rates of VEGF and PlGF were calculated based on the ELISA results that I obtained previously and normalized against cell number in microfluidics. The initial concentration of VEGF and PlGF was set as 3.198×10^{-8} mol/m^3 and 0 respectively based on the concentration of these two proteins in culture media as determined through ELISA. Modeling showed that the concentration gradients of PlGF and VEGF could be maintained across the collagen gel after 24 h with concentration gradients of -0.206 pg/ml·µm (negative sign denotes the convention of diffusion direction) and 1.07 pg/ml·µm, respectively (Figure 5-15). These simulations demonstrate that soluble growth factors could diffuse through collagen gel and also suggest that communication between EC and fibroblasts is bi-directional.

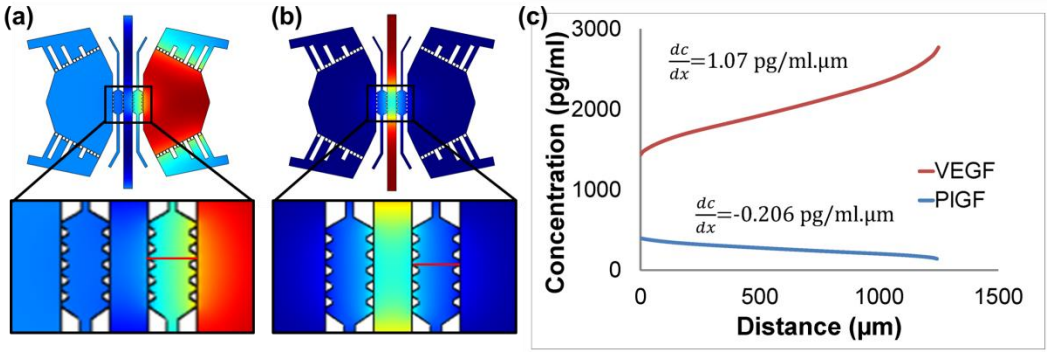

Figure 5-15 COMSOL simulations of growth factor concentration profiles in microfluidic devices. 2D concentration heat maps depict the modeled concentration profiles of (a) VEGF and (b) PlGF at 24 h. Call out pictures: red lines across the collagen gel regions represent the trajectories along which the concentration distributions in (c) are calculated. (a) and (b) Concentration heat maps; high concentration (red) to low concentration (blue). (c) The mean concentration gradient was 1.07 pg/ml.µm for VEGF and -0.206 pg/ml.µm for PlGF at 24 h

5.11 MCP-1 neutralizing antibody inhibits CPX and S1P induced angiogenesis

Fibroblast-derived MCP-1 has been shown to be upregulated by EC CM. To identify its mechanism of action in CPX + S1P induced angiogenesis, the spouting assay was repeated with CPX + S1P but with human MCP-1 neutralizing antibody (anti-MCP-1), AF-279-NA added at 2 μg/ml or with addition of 2 μg/ml of IgG as a control in all channels. The presence of anti-MCP-1 reduced angiogenesis to baseline levels while IgG control showed little or no effect. I then quantified the skeletal length of sprouts, number of cells and maximum sprout length. Anti-MCP-1 reduced the skeletal length of sprouts from 14100 ± 2090 to 6660 ± 963 μm, decreased the cell number from 460 ± 83 to 137 ± 25 and shortened the maximum sprout length from 374 ± 47 to 192 ± 34 μm as compared to the IgG control group. (Figure 5-16(e)-(g)). Consequently, I conclude that MCP-1 plays an important role in CPX + S1P induced angiogenesis in an EC-fibroblasts co-culture *in vitro* model.

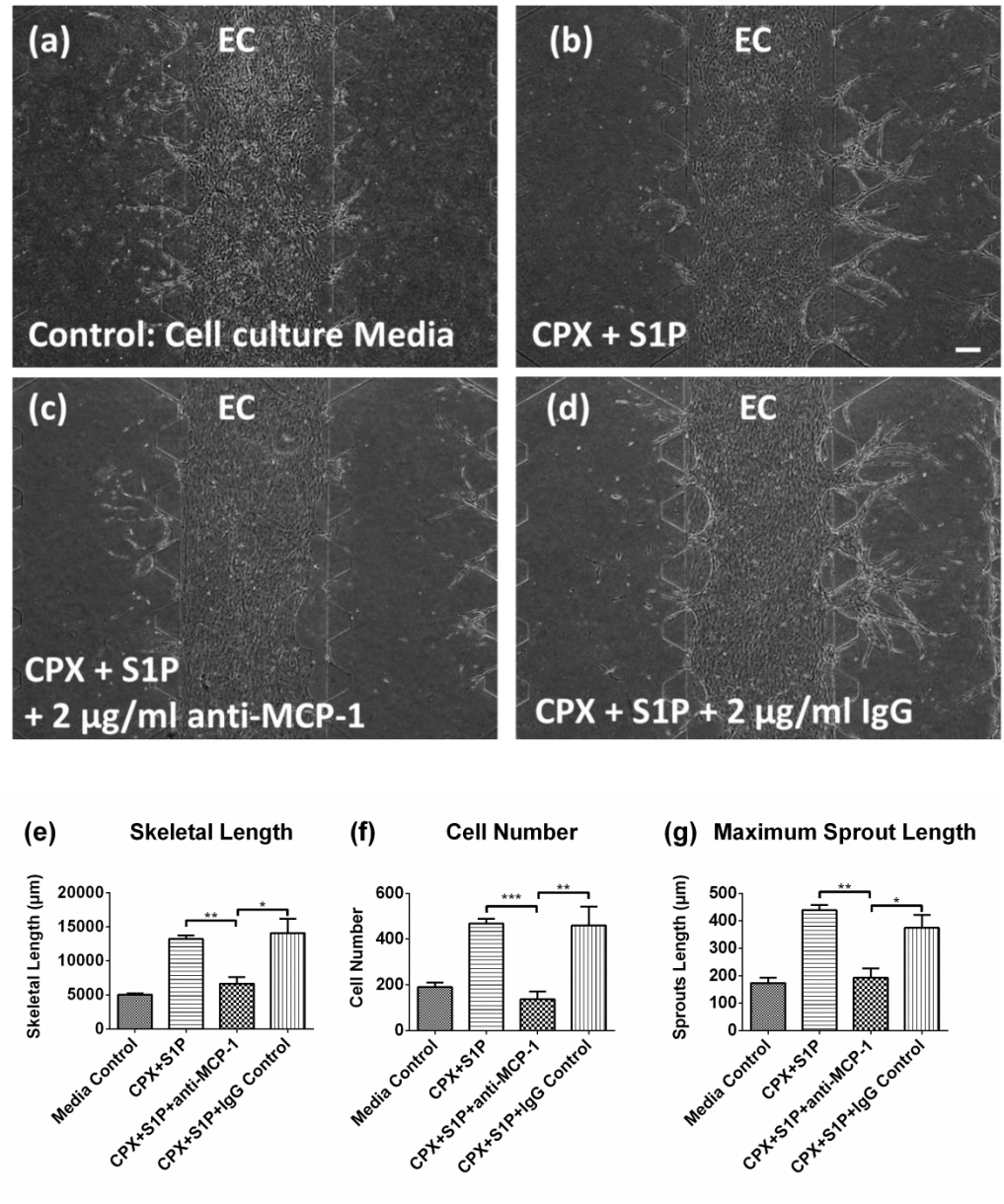

Figure 5-16 MCP-1 neutralizing antibody inhibits CPX and S1P induced angiogenesis. (a) - (d) 4X phase contrast images show the inhibitory effects of MCP-1 neutralizing antibody (anti-MCP-1) on CPX and S1P induced angiogenesis. Sprout formation was inhibited when ECs were treated with 2 µg/ml anti-MCP-1 together with CPX and S1P stimulation. EC treated with 2 µg/ml IgG and CPX + S1P formed extensive sprouts that were similar to the positive control where CPX + S1P was used to stimulate angiogenesis. (e) - (g) Quantifications of skeletal length, cell number and maximum sprout length. Anti-MCP-1 effectively attenuated the angiogenic events that were induced by CPX + S1P as reflected by significantly shorter skeletons, fewer cells, and fewer sprouts. Scale bar = 100 µm. * $p \leq 0.05$, ** $p \leq 0.01$, *** $p \leq 0.001$

5.12 Conditioned medium of IMR-90 induces non-directional sprouting

Based on the results that suggested the soluble factors derived from endothelia would influence the proteomic secretion profiles of fibroblasts, I hypothesized that the interactions between endothelia and fibroblasts were important to CPX + S1P enhanced angiogenesis. In order to confirm this hypothesis, conditioned medium (CM) from fibroblast culture that received no inducement factors from endothelia was collected and then circulated through microfluidic devices that were seeded with endothelial cells. Fibroblast CM was able to induce angiogenesis, but with less intensity. In addition, the sprouts formed under the induction of fibroblast CM were less organized as compared to the sprouts formed in fibroblast-seeded devices. The fibroblast CM-induced sprouts also invaded into the collagen collectively and failed to form a distinct vascular network structure. Furthermore, confocal images also showed that the VE-cadherin staining in CM-induced sprouts was more diffuse in contrast to the crisp and clear VE-cadherin staining in the sprouts formed in fibroblast-seeded devices (Figure 5-17(b)). The high density of CM-induced sprouts made identification of individual sprouts and assessment of skeletal length per unit length difficult. Instead, I measured the fluorescent area (of sprouts) per unit length to compare the morphologies of sprouts under these two conditions. The area per unit length of sprouts in the CM treated group was 135 % larger or increased from 89.9 ± 7.4 to 211.5 ± 11.2 μm as compared to the fibroblast-seeded control group (Figure 5-17(c)).

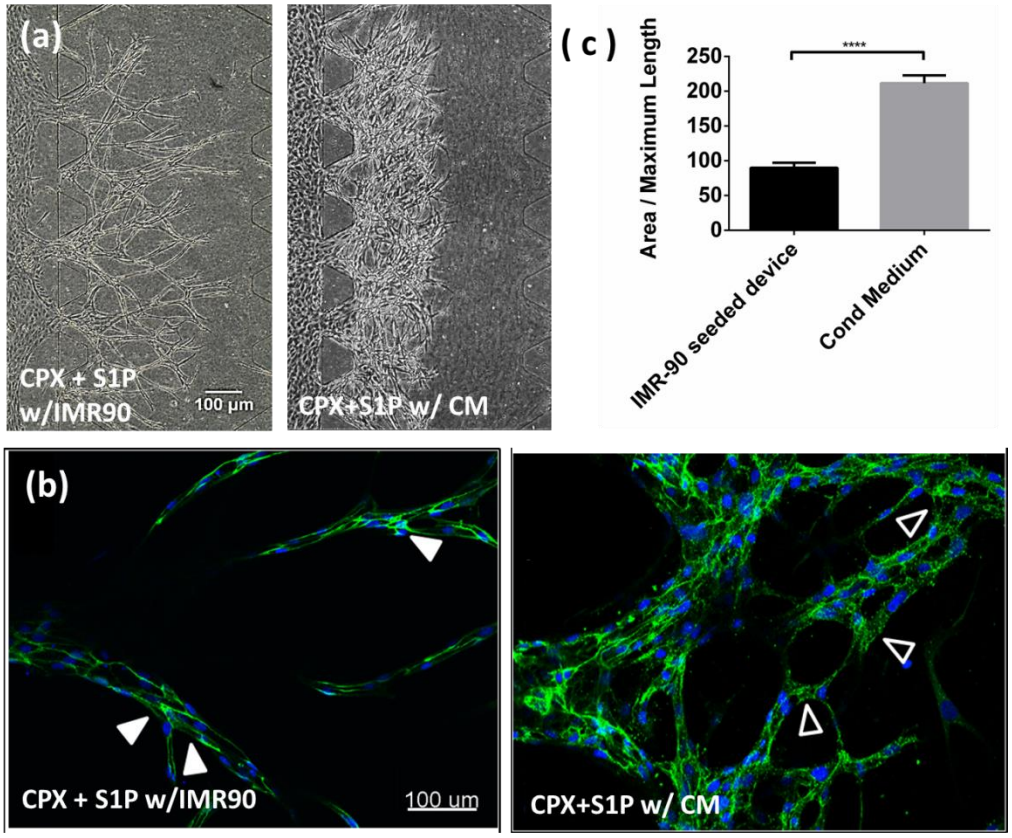

Figure 5-17 Fibroblast conditioned medium induces sprouts that are less organized. (a) 4x phase contrast images: fibroblast CM- induced sprouting (right) differed from those seen in EC-fibroblast co-culture (left) under induction of CPX + S1P. Fibroblast CM did induce sprout formations but they were in a collective migration pattern rather than distinct vascular network formation as seen in fibroblast-seeded devices. (b) 20 X confocal images of Hoechst stained nuclei (blue) and Alexa fluor 488 immunostained VE-cadherin (green): fibroblast CM induced sprouts showed diffuse cytoplasmic VE-cadherin staining pattern in contrast to crisp and clear pericellular VE-cadherin staining in fibroblast-seeded control group (c) quantitative comparison between fibroblast-seeded control group (fibroblasts seeded devices) and fibroblast CM treated group (conditioned medium). Area of sprouts were normalized against maximum sprout length to approximate the complexity and tortuosity of the sprouts formed. Scale bar = 100 µm. **** $p \leq 0.0001$

5.13 Effects of A549 lung carcinoma epithelial cells on endothelial sprouting

As I have shown earlier, fibroblasts are important in mediating CPX + S1P induced angiogenesis. I then asked if these effects were specific to endothelia and fibroblast co-culture. Since A549 lung carcinoma epithelial cells have

been shown to promote angiogenesis through secretion of VEGF and this secretion can also be further boosted by treatment of PHi [161, 162], I used A549 lung carcinoma as mediating cell type to substitute the roles of fibroblasts. Lung carcinomas were encapsulated by alginate beads with identical two-phase microfluidic method and same cell concentration as used in fibroblast encapsulation. As shown in Figure 5-18(b), A549 lung carcinoma epithelial cells can be encapsulated with homogeneous cell distribution due to their less adherent nature as compared to fibroblast. Similar to previous experiments, CPX + S1P combination was applied in all channels to induce angiogenesis. Based on Figure 5-18(c)-(f), I could compare the capillary sprouting between EC-lung carcinoma and EC-fibroblast co-cultures qualitatively where EC-lung carcinoma co-culture resulted in reduced density of sprouts in collagen gel (towards cell encapsulated beads) and the sprouts tended to detach from endothelial monolayer after 4 day as compared to EC-fibroblast co-culture. In addition, sprouts between adjacent posts did not anastomose as readily in EC- co-culture. Therefore, I have shown that not all cell types possess the same potential to induce sprouting, and even in a single cell type, the potential can be regulated by externally-applied factors.

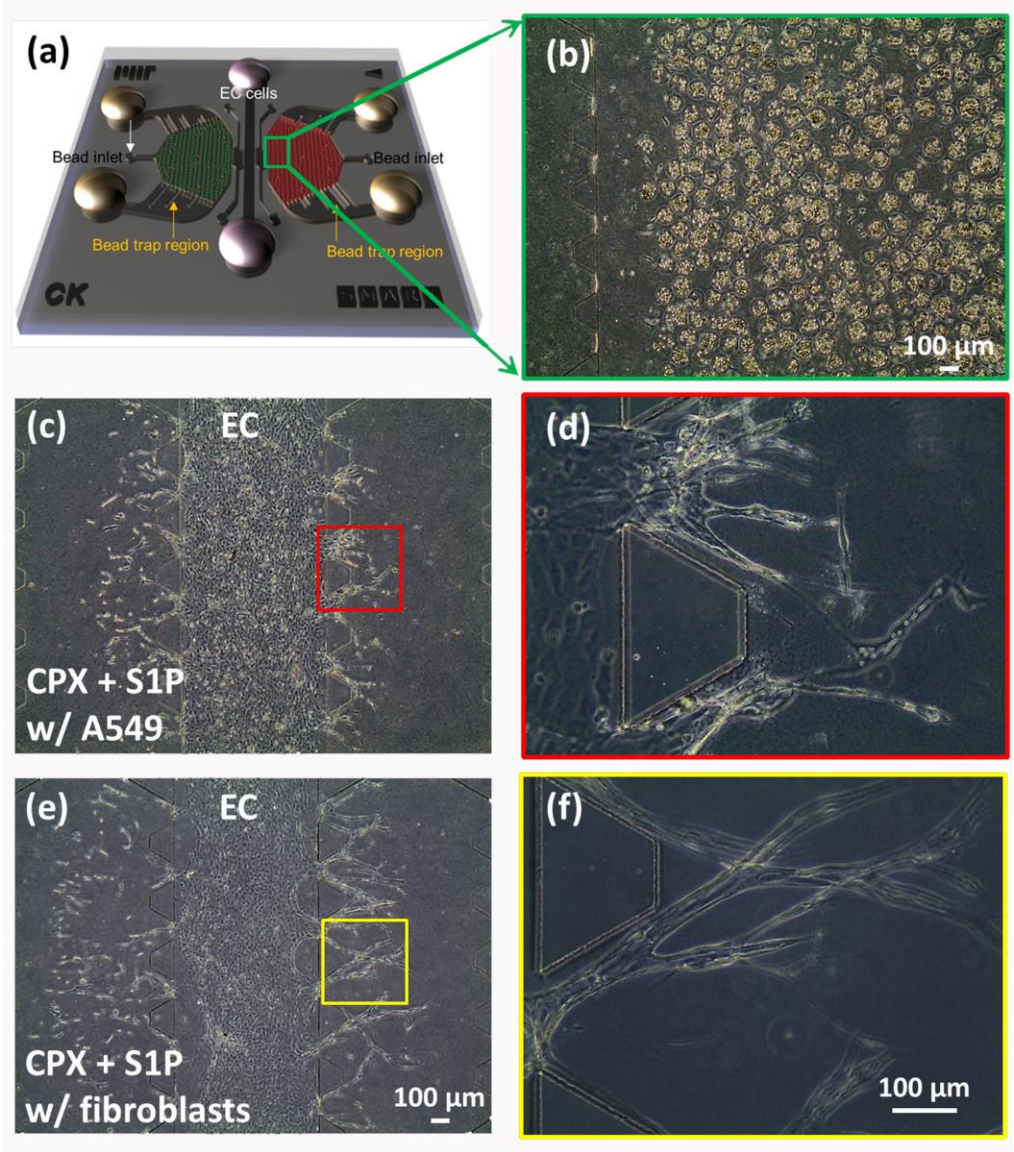

Figure 5-18 Endothelia-lung carcinoma co-culture induces sparser capillary sprouting as compared to the endothelia-fibroblast co-culture under the induction of CPX + S1P. (a) Schematic diagram of the microfluidic device used. (b) 4x phase contrast images of A549 lung carcinoma epithelial cells encapsulated alginate beads in right channel. CPX + S1P induced capillary sprouting in microfluidics with encapsulated (c) A549 lung carcinoma epithelial cells or (e) fibroblasts as mediating cells. (d) and (f) Magnified images of specified areas (marked by red and yellow rectangles) in (c) and (e) respectively that showed the detailed morphologies of sprouts in collagen gel. EC-lung carcinoma co-culture elicited capillary sprouting with different sprouts morphologies as compared to EC-fibroblast co-culture under induction of CPX + S1P. Scale bar = 100 µm.

CHAPTER 6. DISCUSSION

There is strong evidence from the literature that both S1P and HIF-1 are important for angiogenesis, however, it has remained unclear which of the two factors dominates in a regulatory hierarchy [111, 112, 163, 164]. Anelli et al. have shown that hypoxia can upregulate the expression of Sphk1, an enzyme that phosphorylates sphingosine into S1P [111]. In addition, Ader et al. showed that Sphk1 can stabilize HIF-1α through Akt/glycogen synthase kinase-3β pathway [163]. Therefore, it is possible that S1P and hypoxia can form a feed-forward amplification loop to augment the angiogenic effects of both hypoxia and S1P. In addition, VEGF, a growth factor that is upregulated in hypoxia, has been shown to mediate S1P induced angiogenesis [7]. This finding further supports the hypothesis that hypoxia and S1P can together exert greater proangiogenic effects. As both factors have been considered in isolation I set out to study the interplay between S1P and HIF-1 in a co-culture system to predict their utility for neovascularization approaches in regenerative medicine. In order to modulate HIF-1 activity, I employed prolyl hydroxylase inhibitors (PHis) that could prevent the degradation of HIF-1α, a subunit of HIF-1 that would otherwise be degraded rapidly under normoxia [48]. Among the three PHis tested, CPX showed the greatest angiogenic potential while PDCA could only induce little to no sprout formation. The pro-angiogenic performance of HDZ lay between CPX and PDCA. Interestingly, addition of S1P did not increase formation of capillaries in the PDCA treated group but addition of S1P further boosted the angiogenic potentials of both HDZ and CPX in the same context. The different angiogenic effects of PHis might be due to the different regulating mechanisms as PDCA is a 2-oxoglutarate (2-OG) analog while HDZ and CPX are iron chelators [4, 63, 80]. As reported earlier, 2,4-pyridine dicarboxylate (PDCA) and 2,5-pyridine dicarboxylate are both 2-OG anologs with similar structures but they bind differently to the prolyl hydroxylase domains (PHD) 1, PHD2 and PHD3 of

HIF-1α [165]. Therefore, the respective binding affinities and specificities of HDZ and CPX to PHD isoforms can be very different even though they are both iron chelators. As a consequence, their abilities to induce angiogenesis in *in vitro* microfluidics are different. Since CPX showed the greatest potential in inducing angiogenesis in microfluidics, I therefore combined S1P with CPX to maximize the angiogenic effects in the following studies.

I teamed endothelial cells up with fibroblasts, as the latter cell type is abundantly present in almost every tissue, and as it has been shown to produce angiogenic factors to stabilize vessel formations and these effects can be further augmented in the presence of PHis [4, 166, 167]. IMR-90 human lung fibroblasts were chosen for current study as our group has previously shown that IMR-90 respond to PHi stimulations by upregulating VEGF secretion to mediate angiogenesis. As observed, the immature sprouts that formed in collagen gel scaffold can grow into a more developed capillary network only if fibroblasts were present which reflects their importance in a microfluidic setting. In order to focus on the angiogenic effects of fibroblast-secreted growth factors, I kept both cell types physically separate; through alginate beads encapsulation technique, to generate soluble factor gradients while preventing juxtracrine signaling. Kim et al. showed that the viability of fibroblasts was not affected by alginate encapsulation [9]. In addition, Kim et al and Keshaw et al both showed that the encapsulation of fibroblasts with alginate did not impede the VEGF production from fibroblasts and the encapsulated fibroblasts were also shown to be pro-angiogenic [9, 168]. Furthermore, Shoichet et al. also showed that proteins with various sizes can diffuse through alginate gels with a diffusion coefficient close to diffusion in water [169]. While alginate does not affect the viability and angiogenic potential of fibroblasts, alginate itself does not presence in *in vivo*. With alginate encapsulation, fibroblasts cluster within the core of alginate beads and this change of microenvironment might affect the fibroblast-derived secretomes. Kankuri et al. showed that hepatocyte growth factor was upregulated by more than 200 fold in fibroblast clusters as compared to

monolayer culture [170]. I understand that both encapsulated fibroblasts and fibroblasts in monolayer culture are not able to replicate the *in vivo* conditions perfectly but the encapsulation technique allows us to achieve a 4 to 1 ratio of fibroblast to EC that is more physiologically relevant. Besides, it also allows us to study the paracrine effects of fibroblasts in angiogenesis in a controlled way where most of the fibroblasts do not invade into collagen and this prevents the collapse of collagen due to the fibroblast contraction. Nevertheless, the strength of alginate will decrease over time especially if cells are encapsulated as shown by Shoichet et al. [169]. Therefore, some of the encapsulated fibroblasts broke free from the alginate beads after 4 days of culture and a few of those invaded into the collagen gel. Invasion of fibroblasts into collagen gel will lead to collagen gel remodelling which results in matrix contraction [171]. In addition, Velazquez et al. also showed that the presence of fibroblasts in close proximity to endothelial cells promoted the formation of vascular network in an *in vitro* collagen sandwich assay [172]. Consequently, I do not rule out the possibility that fibroblasts might exert pro-angiogenic effects when they are in close contact to endothelial cell. Nonetheless, the number of fibroblasts that successfully invaded into the collagen region was limited and usually less than 10 cells per device (Figure 5-3 and Figure 5-4) as compared to 100 k fibroblasts in the side channel. As a consequence, the paracrine effects exerted by alginate encapsulated fibroblasts are the main effects that I am looking into.

I showed that the presence of fibroblasts in the devices was indispensable in generating a sprouting response, spontaneously and in the presence of the compounds. However, the combination of CPX + S1P yielded a surprisingly extensive formation of a highly complex vascular network with lumina within 4 days that almost completely traversed the 1.25 mm collagen gel region. Hence , this combination held the promise to be used to develop capillaries into fully functional network in a relatively short time and this would be especially beneficial for therapeutic angiogenesis. The angiogenic potential of CPX + S1P can only be shown in an EC and fibroblast co-culture context.

Conventional in vitro assay such as Matrigel assay is usually not suitable for the studies involved co-culture with nonendothelial origin such as fibroblasts that may respond to Matrigel and form cords [135]. While the Transwell assay is suitable for co-culture assay, it can only study the endothelial migration; which is only a step of the complicated angiogenesis processes. In addition, the generation and control of solute concentrations can be done in the microfluidic assay. The importance of VEGF gradient was demonstrated by Gerhardt et al. that directed tip cell migration is dependent on a VEGF gradient in the rat aortic ring and retina development assays [146]. Furthermore, the microfluidic approach also allows us to focus on the paracrine effects between EC and fibroblasts under the induction of CPX + S1P where some other conventional assays may not be able to do so such as Matrigel assay. Nevertheless, I still need to rely on other biochemistry assays such as ELISA and proteomic analysis membrane to determine the specific angiogenic proteins that are relevant in CPX + S1P induced angiogenesis. While I understand that a microfluidic platform is not a single solution for all questions that need to be answered in angiogenesis, the microfluidic platform acts as a functional assay to study closely on how CPX + S1P can affect the formation and morphogenesis of angiogenesis in 3D in the presence of fibroblasts, which is otherwise unobtainable with Matrigel or Transwell assays. With this microfluidic platform, I successfully recapitulated the endothelial migration, proliferation, lumen formation and sprouts anastomosis which are key steps in *in vivo* angiogenesis [173]. Furthermore, I also clearly showed that VE-cadherin that is important in vascular permeability, endothelial survival and lumen formation distributes predominantly at intercellular junctions and this further confirms that the integrity of the sprouts is conserved in *in vitro* mirofludics [174].

6.1 CPX induced differential expressions of angiogenic proteins from both endothelia and fibroblasts

While the combination of S1P and CPX showed a clear morphological advantage over the single use of either compound, CPX seemed to be the key component in augmenting the secretion of various angiogenic factors. In addition, endothelia and fibroblasts obviously responded to CPX with a different repertoire of angiogenic growth factors. This ties in with earlier findings where different mesenchymal cell types were induced to overexpress HIF-1 and different cell types showed the increases of different angiogenic growth factors [51]. In the experimental system, human fetal lung fibroblasts mainly secreted HGF, IGFBP-2, uPA and VEGF under the influence of CPX (Figure 5-5). This is coherent with previous reports showing stabilization or upregulation of these proteins or their mRNA under hypoxic conditions [51, 56, 57, 60]. Since the discovery of VEGF in 1980s, VEGF has quickly been recognized as one of the most potent growth factors with pleiotropic functions in driving angiogenesis [175]. While HGF regulates endothelial cell growth and survival, IGFBP-2 enhances VEGF production and uPA participates in the degradation of ECM which then facilitates the release of matrix-bound growth factors and enhances cell motility [176-180]. Among these, HGF has been shown to be released from fibroblasts in EC-fibroblast co-culture and the inhibition of HGF would greatly reduce angiogenesis [22, 23, 181]. The secretion of these proteins in fibroblasts can be further boosted by CPX which also verifies the importance of fibroblasts as mediating cells in the system.

In contrast, endothelial cells showed an upregulation of PlGF, endothelin-1, EGF and IL-8 (Figure 5-5). This is highly significant, since at least five different synergistic angiogenic effects of PlGF with VEGF have been proposed [182]. There is currently only one report on the effects of PHi using L-mimosine in a model of a thrombosed vena cava on increased PlGF present in the vessel

wall, but the cell source for PlGF was not established [183]. The chemokine IL-8 has been implicated in promoting angiogenesis by enhancing EC proliferation and migration via autocrine signaling [184]. Hypoxia has been reported to increase the secretion of IL-8 chemokine in *in vitro* endothelial cultures through the activation of HIF-1α [58]. Hirata et al. and Sun et al. have shown that downregulation of EGF receptor could effectively block angiogenesis *in vitro* and these findings also confirm the pro-angiogenic role of EGF [185, 186]. As reviewed by Knowles et al., ET-1 enhances angiogenesis through multiple pathways including direct stimulation of HUVEC proliferation, migration and invasion, increase production of VEGF and also activation of fibroblasts that helps matrix remodeling [187].

Apart from those 8 cytokines that were significantly upregulated in endothelial or fibroblast cultures by CPX or CPX + S1P, other angiogenesis related proteins that have been reported to favor or oppose angiogenesis were detected in the proteomic profiling assay too. Amphiregulin, IGFBP3 and PEDF were the three proteins only found in fibroblast culture. Amphiregulin, which is a ligand for EGFR, could help promote angiogenesis through increasing the expressions of MMP-2 and MMP-9 [188]. IGFBP3 could increase the vascular survival and regrowth after oxygen-induced vasoobliteration in mice retina [189]. In contrast, PEDF is a potent angiogenic inhibitor that blocks neo-vessel formation in rat corneal model under normoxia [190]. Several other proteins have also been detected in both endothelial and fibroblast cultures including endostatin, PTX3, PAI-1, TIMP-1 and thrombospondin-1. Among these, PAI-1 is the only protein that has been reported to be pro-angiogenic but the rest of the group are known inhibitors of angiogenesis [191-195]. It is logical that cells, especially endothelia would secrete inhibitors of angiogenesis to maintain the quiescent state of endothelium during non-pathological or normoxic conditions. All of the proteins that were upregulated by CPX as mentioned earlier are indeed pro-angiogenic but the levels of anti-angiogenic proteins remained unchanged

when treated with CPX. This explains the increased angiogenesis as induced by CPX which mimics a hypoxic condition in microfluidics.

To further confirm the increase of pro-angiogenic proteins is indeed the reason for the enhanced angiogenesis, inhibitors that are specific to the secreted proteins or their respective receptors were used. VEGF secreted by fibroblasts and EGF secreted by endothelia were chosen for the inhibitor studies as VEGF is a key angiogenic factor that regulates multiple angiogenesis related activities. In addition, only EGF secretion was further boosted by CPX + S1P as compared to CPX alone (Figure 5-5 (c)).

The VEGF ligand inhibitor, Avastin could inhibit the angiogenesis induced by CPX + S1P and brought it back to baseline levels that were similar to the culture media control (Figure 5-6). Interestingly, the diameter of capillary sprouts also increased significantly in the Avastin treated group as compared to the IgG control group (Figure 5-7). Previous findings have indicated that diameter of sprouts grown *in vitro* is affected by different VEGF isoforms and VEGF concentrations where $VEGF_{189}$ reduces vessel diameter while $VEGF_{165}$ and $VEGF_{121}$ lead to increased vessel diameter in a concentration dependent manner [150, 196]. The ELISA assay primarily detects $VEGF_{165}$ and $VEGF_{165b}$, hence I cannot rule out the possibility that splice variants different from $VEGF_{165}$ are present and exert angiogenic effects in the system. Nonetheless, it is surprising to observe larger sprout diameter in the presence of Avastin as Avastin neutralizes every splice form of human VEGF including $VEGF_{165}$ that increases vessel diameter [197]. However, the previous findings were done based on exogenously added recombinant VEGF in the presence of skin fibroblasts but not with inhibition or interference of VEGF [150]. Hence, the results indicate the possibility of a biphasic behavior of sprout diameter in response to VEGF concentration. Besides, I also showed that the lumen formation in capillary sprouts were not affected by Avastin although VEGF has been suggested to help lumen formation in previous study [198].

EGFR inhibitor, Gefitinib was ineffective in inhibiting angiogenesis in the settings (Figure 5-8). This is an unexpected observation although previous

findings have shown that EGF could induce angiogenesis in mouse corneal model [185, 199]. Nevertheless, researchers from the same group also showed that EGFR inhibitors, Iressa and Gefitinib could only attenuate EGF induced angiogenesis but not VEGF induced angiogenesis. As elevated secretion of VEGF from fibroblasts is expected when CPX + S1P is introduced, this might be the reason why Gefitinib is ineffective in attenuating the angiogenesis induced by CPX + S1P in the presence of fibroblasts. The VEGF and EGFR inhibitor studies demonstrate that the growth factors secreted by fibroblasts in response to CPX + S1P treatment, such as VEGF, definitely play a critical role in angiogenesis but single inhibitor would not be sufficient for total inhibition due to the complex nature of sprout formation and the involvement of multiple chemokines in modulating angiogenesis.

6.2 S1P induced EC migration and angiogenesis is $S1P_1$ dependent

All soluble factors chosen for analysis, some of which showed significant upregulation in the presence of CPX, remained unchanged in the presence of S1P. I therefore asked what could be the role of S1P in a PHi induced angiogenesis model? S1P is known to induce endothelial migration which is also a key process during angiogenesis [90, 155]. The immature sprouts that invaded into collagen gel on control side (towards empty alginate beads) usually converted to single cell migration on day 4 which offered an excellent platform for quantifying the effects of S1P on endothelial migration. The increased cell migration in the S1P and CPX + S1P treated groups were confirmed based on the increased number of migrating cell and migration distance in collagen gel as compared to the CPX treated group and the culture media control (Figure 5-9). This suggests that endothelial migration, which is a key step in angiogenesis, can only be enhanced by S1P but not by CPX in a microfluidic setting.

Among the five G-protein coupled receptors $S1P_1$ to $S1P_5$, $S1P_1$ and $S1P_3$ have been associated with S1P induced cell migration and angiogenesis [16, 98, 99]. I showed that the endothelial cells that I used did express $S1P_1$ under different pharmacological treatments. Surprisingly, I observed increased $S1P_1$ expression in the CPX treated, S1P treated and CPX + S1P treated groups. Since the CPX + S1P combination did not further increase $S1P_1$ expression as compared to the CPX monosubstance or S1P monosubstance treated groups, the combined angiogenic effects induced by CPX + S1P remains unclear at this point. A plausible explanation can be derived from the observation that VEGF increases the amount of $S1P_1$ receptor on endothelial cells in a dose-dependent manner [7]. In a co-culture system therefore the CPX-induced factors such as VEGF from fibroblasts could enhance the sensitivity of endothelial cells to S1P, which, via the Rho family GTPase Rac activation, then would induce cell migration, tube formation and increase the integrity of the endothelial barrier (Figure 6-1) [6, 100].

To further test the importance of $S1P_1$ in CPX + S1P induced angiogenesis, I then probed the culture system with a $S1P_1$ inhibitor, W146, sprouting was brought down to baseline levels (Figure 5-11). Similar findings in a rabbit cornea model have been reported where VEGF-induced angiogenesis is inhibited with a novel specific $S1P_1$ blocker [101]. However, I also observed reduced angiogenic sprouting in the ethanol vehicle control group. The inhibitory effects of ethanol were confirmed in previous findings that acute ethanol exposure would impair angiogenesis in a scald burn wound model in mice [200]. Nonetheless, there was significant difference between the W146 treated group and the vehicle control group as reflected by fewer and shorter capillary sprouts in collagen gel. As discussed earlier, $S1P_1$ involves in S1P induced cell migration and this is once again confirmed in the assay where I show that W146 not only reduced the number of migrating cells but also the migration distance in collagen gel on control side (towards empty alginate beads) as compared to the vehicle control group (Figure 5-12).

Since the use of ethanol as vehicle exerted certain inhibitory effects, I then reduced the concentration of W146 so did volume of ethanol by 10 times to test if a lower concentration of W146 was still effective in inhibiting angiogenesis. At lower concentration, I were unable to obtain statistical significance in the metrics that I used to quantify angiogenesis as compared to the control groups (Figure 5-7). Nonetheless, I observed a 91 % increase of sprout diameter in the W146 treated group. Previous findings show that inhibition of $S1P_3$ alone by a $S1P_3$ specific inhibitor, VPC01091, increases both arteriolar and venular diameters as compared to the scaffold control in a dorsal skinfold window chamber assay on mice [201]. As $S1P_1$ and $S1P_3$ work hand in hand in S1P induced angiogenesis, the increased diameter of sprouts caused by $S1P_1$ inhibition further confirms this observation. The W146 inhibition was similar to Avastin inhibition where diameter of sprouts in both cases increased. However, they were also different from the aspect that W146 almost blunted the capillary sprouts and led to the disappearance of filopodia, which was an indication of the loss of tip cells [202]. Although previous findings have suggested that tip cell formation and migration are related to VEGF gradient, yet I have found that $S1P_1$ inhibition was more effective than VEGF inhibition in reducing tip cell formation [146]. The $S1P_1$ inhibitor studies not only confirm the importance of $S1P_1$ in S1P induced cell migration but also show that $S1P_1$ can modulate the morphologies of capillary sprouts.

6.3 Interactions between EC and fibroblasts are important in CPX+S1P induced angiogenesis

I have thus far shown that CPX and S1P each play a different role in CPX + S1P induced angiogenesis and the presence of fibroblasts is a prerequisite for the angiogenic effects to occur. Previous findings have confirmed that the pro-angiogenic potential of fibroblasts is acted through secretion of cytokines but this study is the first that investigates the fibroblast and EC cytokine profiles

under CPX, S1P or CPX + S1P inductions [21, 22, 166, 203]. In addition, only a few studies focus on the effects of EC derived factors on fibroblasts. EC CM has been shown to induce fibroblast proliferation while EC CM collected post-hypoxia treatment induced the migration of fibroblasts in a ET-1 and PDGF dependent manner [204, 205]. Previous findings also suggest that EC and fibroblast interactions are dependent on ET-1 mediated activation of fibroblasts which then enhance angiogenesis [25]. In addition to ET-1, EGF is another growth factor that has been shown to be capable of activating fibroblasts [206, 207]. Activated fibroblasts are known to secrete more angiogenic growth factors including HGF and FGF but more intriguingly, activated fibroblasts would also secrete MCP-1, a key chemokine in regulating migration, filtration and recruitment of monocytes/macrophages that play important roles in promoting aniogenesis [208-210]. Therefore, the upregulation of ET-1 and EGF in endothelia culture as induced by CPX + S1P suggests that they might have potential roles in mediating endothelia-fibroblast interactions. Moreover, the levels of ET-1 and EGF measured from fibroblasts that were cultured in the EC CM were reduced as compared to the baseline levels which also implied either cellular uptake by fibroblasts or degradation of these two proteins. Interestingly, I also found that MCP-1 secretion by fibroblasts was dramatically increased by EC CM treatment but was only marginally increased by the combination of CPX + S1P (Figure 5-14). Previously, the MCP-1 expression in the skin fibroblasts harvested from diabetic patients has been shown to be increased by exogenously added ET-1 [159]. Similarly, EGF has also been shown to induce expression of MCP-1 in synovial fibroblasts [160]. The finite element simulation coupled with the fluorescent-dextran assay also showed that the secretomes derived from either endothelia or fibroblasts can diffuse through the collagen and reach the other cell type. Therefore, the communications between endothelia and fibroblasts are not impeded in microfluidics. These findings strongly suggest that ET-1 and EGF secreted by endothelia potentially enhanced the MCP-1 secretion in fibroblasts.

MCP-1 has long been associated with inflammatory response, a concomitant, if not indispensable mechanism to spur neoangiogenesis [27]. The active role of endothelial cells in this inflammatory response has been defined in increasing detail recently [29, 211, 212]. MCP-1 has been reported to induce angiogenesis by activating the VEGF-A pathway and recruiting mural cells [158, 213]. To further confirm the angiogenic effects of MCP-1 and to understand its mechanism of action, I employed neutralizing antibody against MCP-1 which brought down the CPX + S1P induced capillary sprouting to baseline levels as compared to the corresponding IgG control (Figure 5-16). Here I show for the first time in microfluidic settings that fibroblast-derived MCP-1 induces sprouting as a consequence of fibroblast activation through endothelial factors.

To confirm the importance of endothelia-fibroblast crosstalk, I tested the efficacy of fibroblast CM in inducing angiogenesis. The CM of fibroblasts induced capillary sprouting events and this demonstrated that secretomes derived from fibroblasts did promote angiogenesis. Nonetheless, the morphologies of sprouts formed as induced by fibroblasts CM were different from sprouts seen in fibroblast populated devices where CM induced sprouts were more irregular with less directional extension. More often, the sprouts invaded into the collagen gel in a collective manner which also rendered the identification of single sprout or capillary network much more difficult. Based on confocal images, I could observe that VE-cadherin that was supposed to localize around intercellular junctions was more diffuse in cytoplasm which suggested that the integrity of the sprouts such as permeability was compromised [214]. The tortuous and unorganized morphologies together with diffuse VE-cadherin showed that the CM induced capillary sprouting events were poorly regulated just like the tumor vasculatures [215].

Another facet to consider is the loss of angiogenic proteins during sample processing. Although the CM collected from the fibroblasts was used immediately for culturing EC to minimize protein denaturation caused by freeze and thaw cycles, some of the proteins or signalling molecules may lose

in the dialysis process. Wang et al. showed that the production of nitric oxide (NO) was not exclusive to EC and immune cells as human dermal fibroblasts can produce NO too [216]. It was very likely that fibroblast derived NO would pass through the membrane and lost in the dialysis process due to its small size. Furthermore, NO has a very short half-life of 20 min in aqueous solution which was shorter than the time required for sample preparation [217]. The possible loss of NO might explain the discrepancy between the results obtained from conditioned media experiments and the microfluidic experiment as nitric oxide is a key player with multi-factorial effects in angiogenesis including increase of EC survival and proliferation and induction of the EC derived bFGF autocrine loop [218]. Unfortunately, the dialysis step was required to concentrate the conditioned medium to the level that was comparable to the concentration in microfluidic assay. The high density cell culture cannot be achieved in a 2D well plate culture as the evaporation of media caused the cell death. With these, I further confirm that the communication between endothelia and fibroblasts is dependent on paracrine signaling and these interactions are important in modulating sprouting behavior and cannot be replaced by fibroblast CM.

The enhanced angiogenesis induced by CPX + S1P relies on interactions between endothelia and fibroblasts and I asked if these angiogenic effects can take place in EC co-culture with another cell type. A549 lung carcinoma epithelial cells have been shown to induce angiogenesis through secretion of VEGF and bFGF in a dorsal mice air sac model [161]. Furthermore, the expression of VEGF in A549 culture is upregulated by hypoxia and PHi treatments [162]. Nonetheless, I did not observe extensive angiogenic response in endothelia-lung carcinoma co-culture model even when the cells were induced by CPX + S1P. The capillaries formed with A549 lung carcinoma epithelial cells as mediating cells were sparser and less developed as compared to those formed in fibroblast populated devices. This might due to the fact that A549 lung carcinoma epithelial cells are of epithelial lineage while fibroblasts are of mesenchymal lineage [219]. Nevertheless, A549 lung

carcinoma epithelial cells remained encapsulated in the alginate capsules but some fibroblasts would break free from the alginate beads after 4 days of culture. Although the diffusion coefficients of proteins in media and in alginate layers are very similar, the closer proximity of some fibroblasts to the endothelial cells might enhance the angiogenic response as compared to encapsulated A549 lung carcinoma epithelial cells [169].

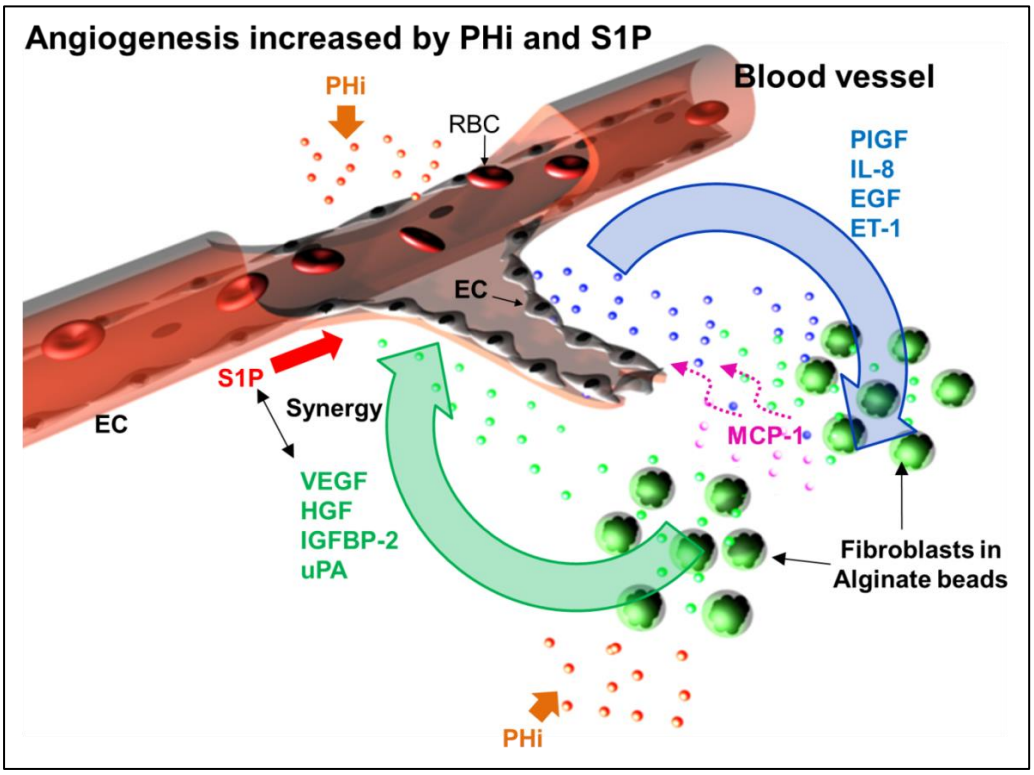

Figure 6-1 Schematic diagram of PHi + S1P-driven capillary sprouting. PHi exerts differential effects on EC and fibroblasts that lead to upregulation of PlGF, IL-8, EGF and ET-1 from EC and upregulation of VEGF, HGF, IGFBP-2 and uPA from fibroblasts. The soluble factors secreted by fibroblasts together with S1P promote angiogenesis. Fibroblasts-derived MCP-1 is induced by endothelial factors and it also supports the growth of capillaries

In conclusion, I have characterized a novel, powerful combination of CPX, a HIF-1α inducer, and S1P, a Rac signalling activator, for therapeutic angiogenesis. The efficacy of this combination is based on the pharmacological induction of a physicological crosstalk of endothelia and

fibroblasts that occurs in angiogenesis and emulates a wound healing response.

6.4 Limitations of current work

Although the sprouting network formed in collagen scaffold grew in 3D, the quantification metrics: skeletal length and maximum sprout length that I used were based on the projected 2D images. Therefore, the length that I measured might underestimate the actual sprouting length as projected 2D images did not consider the vessel length that spanned across different depth in collagen gel. Nevertheless, I showed that the sprouting network preferentially extended towards fibroblast encapsulated beads as opposed to growing vertically up to the PDMS surface or down to the glass substrate (Figure 6-2).

Another limitation of the current work is the lack of systemic approach to optimize the concentrations of CPX and S1P as a combination. Although the concentrations of CPX and S1P were chosen based on previous studies[4, 151], the optimum concentrations for these two angiogenic compounds as a combination have never been tested. Therefore, the current concentrations that I used might be sub-optimal.

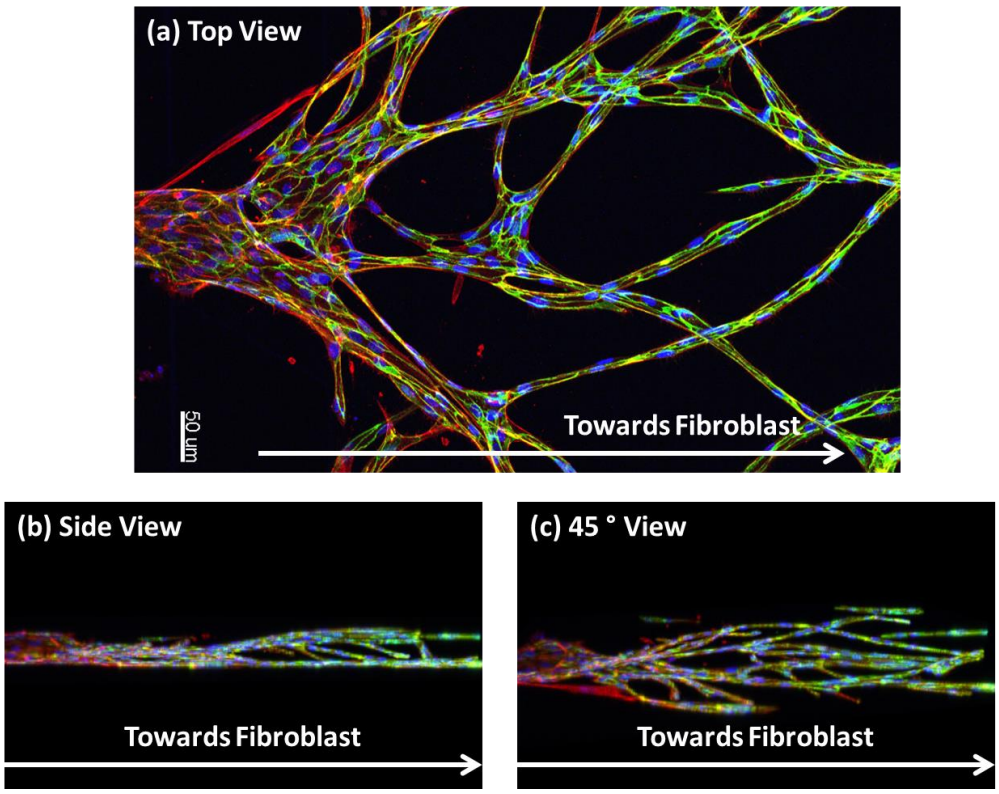

Figure 6-2 Different angle of views of sprouting network. (a) Top view, (b) side view and (c) 45 ° angle view of CPX + S1P induced sprouting network in a microfluidic device. Preferentially, the vessels grew towards fibroblast encapsulated beads instead of extending towards PDMS top or glass bottom. Scale bar = 50 µm.

CHAPTER 7. CONCLUSION AND FUTURE WORK

7.1 Contributions of this work

This thesis has focused on how endothelial sprouting can be pharmacologically enhanced by CPX and S1P, and how this enhancement is orchestrated via endothelial-fibroblast crosstalk in a microfluidic platform. :

- the unexpectedly strong angiogenic effects of CPX and sphingosine 1-phosphate in combination as expressed in morphological development of capillary sprouts

- the differential secretion of complementary angiogenic factors by either cell type when stimulated with CPX while secretion of other anti-angiogenic factors remain unchanged

- the increase of VEGF secretion by fibroblasts as induced by CPX. The introduction of VEGF ligand inhibitor, Avastin also suppressed and affected morphologies of CPX + S1P induced capillary sprouts

- the effects of S1P in increasing cell motility and the critical role of S1P in this system as a downstream effector and amplifier of signals initiated by and associated with HIF-1α stabilization

- the importance of $S1P_1$ in mediating S1P induced endothelial migration in microfluidics. $S1P_1$ also modulates angiogenesis whereby the inhibition of $S1P_1$ not only attenuates capillary sprouting but also increases sprout diameter

- the crucial role of endothelia in eliciting MCP-1 secretion from fibroblast that is independent of pharmacological stimulation while the neutralization of MCP-1 also results in reduction of capillary sprouts

- the pro-angiogenic effects of fibroblasts in microfluidics cannot be replicated through conditioned medium from fibroblasts or by substituting fibroblasts with A549 lung carcinoma epithelial cells

Together, these findings show the possibility of modulating angiogenesis through the combination of CPX and S1P in the presence of fibroblasts as mediating cells. The effectiveness of this newly proposed strategy relies on pharmacological induction of a physiological crosstalk between endothelia and fibroblasts that emulates the wound healing response as seen in angiogenesis. With the ability to effect multiple angiogenic proteins and also the key processes during angiogenesis, this novel vascularization strategy is therefore of particular interest for therapeutic angiogenesis. Furthermore, this angiogenesis assay also opens up new possibilities not only for developing neo-blood vessels in *in vitro* systems but also for understanding the mechanism behind CPX and S1P regulated angiogenesis. The knowledge can then be widely applied in various fields including in anti-vascularization strategies for cancer research. In conclusion, I believe that I have discovered, with the help of a unique microfluidic assay, a therapeutically valuable combination of agents to induce tissue repair and regeneration and also contributed to the growing knowledge of modulating angiogenesis.

7.2 Future directions

This work has provided some insights in CPX + S1P induced angiogenesis but further work is needed to fully understand its mechanism. Firstly, ligand or receptor inhibitions on those proteins that are upregulated by CPX can be

performed in a similar way as I did for VEGF and EGFR inhibitions. These could help to further confirm which proteins are truly necessary in CPX + S1P elicited angiogenesis. Although I have shown that $S1P_1$ is critical in CPX + S1P induced angiogenesis, the functions of the other four S1P receptors remain unknown. Specific receptor inhibitors can be utilized to further dissect their role in angiogenesis, especially for $S1P_2$ and $S1P_3$ that have been suggested to play a role in angiogenesis. Besides, the effects of S1P on fibroblasts in these setups are yet to be discovered whereby previous findings have shown that S1P could affect the collagen deposition and fibroblast chemotaxis in a $S1P_2$ dependent manner [220, 221]. Also, the interplay between endothelia and fibroblasts can be examined more closely by determining if MCP-1 secretion from fibroblasts will be affected by downregulation of ET-1 or EGF.

With the vision to develop a multi-cellular *in vitro* model that mimics certain tissue or organ such as human heart for the better understanding of angiogenesis, other cell types can be introduced in the microfluidics that can accommodate up to 5 different cells in separate entities. For example, cardiac myocytes have been shown to interact with both endothelial cells and fibroblasts and these interactions are crucial in angiogenesis in heart [26, 145, 222, 223]. Consequently, cardiac myocytes can be incorporated into the multi-cellular system via cell encapsulation technique or by seeding them into the 3D collagen matrix. In addition, importance of mural cells has been discussed before and it is clear that pericytes and smooth muscle cells (SMC) play pivotal roles in vascular maturation. Hence, seeding of pericytes/SMC in the same channel as endothelia could help us further understand their functional roles in angiogenesis.

This model can also be used as a screening platform for both pro- and anti-angiogenic compounds. For example, perfusable vasculature growing in or around a cancer spheroid can serve as an excellent model to study the potency of anti-angiogenic compounds in cancer research. As suggested by recent study, the endothelia and cancer cell interactions would greatly alter the IC50 values of anti-cancer compounds [224]. Similarly, other

proangiogenic compounds can be tested in a more physiological relevant model which could bridge the gap between *in vitro* and *in vivo* studies.

APPENDICES

Appendix A: Comparison between simulated and experimental results

A model was built based on a 2D transport of diluted species model by using COMSOL *Multiphysics* simulation software. The diffusion coefficients of 40 kDa Texas-red conjugated dextran in cell culture media and collagen gel were estimated based on a 40 kDa inert molecule from Stokes-Einstein equation and also adapted based on previous findings [130, 132] as summarized in Table 4. The initial concentration of 40 kDa dextran was set as 2x10-3 mol/m3 in the right channel and 0 in every other region based on the concentration of 40 kDa that has been added into the microfluidic. As the diffusion coefficients for dextran in media and dextran in collagen gel were different, the slope of the diffusion profile changed at the two edges of the collagen gel and resulted in a sigmoidal diffusion profile. The simulated diffusion profile across the collagen gel (in between middle channel and right channel) was coherent with the experimental results and confirmed the formation of a solute concentration gradient in the microfluidic device.

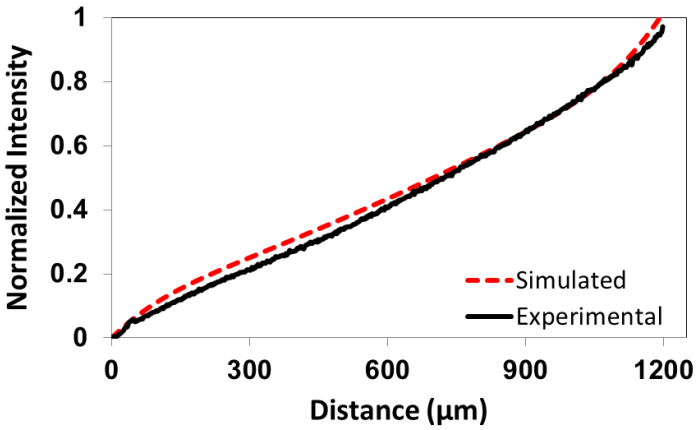

Figure S1 Comparison between simulated and experimental concentration gradients. The dash line represents the simulated concentration gradient obtained from COMSOL Multiphysics and the solid line represents the experimental data in a microfluidic device. Distance 0 denotes the edge between the middle channel and the collagen gel.

Appendix B: List of publication, presentations and patent

Publication

- **Sei Hien Lim**, Choong Kim, Amir R. Aref, Roger D. Kamm, Michael Raghunath. Complementary effects of prolyl hydroxylase inhibitors and sphingosine 1-phosphate on fibroblasts and endothelial cells in driving capillary sprouting. Integrative Biology, 2013. 5(12): p. 1474-1484.

- Young K. Park, Ting-Yuan Tu, **Sei Hien Lim**, Ivan J.M. Clement, Se Y. Yang, Roger D. Kamm. In Vitro Microvessel Growth and Remodeling within a Three-Dimensional Microfluidic Environment. Cellular and Molecular Bioengineering, 2014. 7(1): p. 15-25.

Oral Presentations

- **Sei Hien Lim**, Amir R. Aref, Choong Kim, Michael Raghunath, Roger D. Kamm, "Induction of Angiogenesis in microfluidic devices using prolyl hydroxylase inhibitors and sphingosine-1 phosphase", MicroTAS-2012, Oct., 2012 (CBMS Travel Award)

- **Sei Hien Lim**, Amir R Aref, Michael Raghunath, Roger D Kamm, "Induction of Angiogenesis in Microfluidic Devices using Prolyl Hydroxylase Inhibitors," Tissue Engineering & Regenerative Medicine International Society 2011 Asia Pacific Meeting (Termis 2011), Singapore, August, 2011.

- **Sei Hien Lim**, Amir R. Aref, M. Raghunath, Roger D. Kamm, "Induction of Angiogenesis in Microfluidic Devices using Prolyl Hydroxylase Inhibitors," 2nd Conference on Advances in Microfluidics and Nanofluidics and Asian Pacific International Symposium on Lab on chip (AMN-APLOC), Jan 2011, Singapore

Poster Presentation

- **Sei Hien Lim**, Amir R Aref, Michael Raghunath, Roger D Kamm, "Induction of Angiogenesis in Microfluidic Devices using Prolyl Hydroxylase Inhibitors and Sphingosine-1 Phosphate," Keystone Symposium on Molecular and Cellular Biology, Snowbird, Utah, USA, January, 2012

Patent

- Michael Raghunath, **Sei Hien Lim**, Roger D Kamm, "Compositions And Methods For Neovascularization" US patent: US 20130197038 A1, Published August 1, 2013

REFERENCE LIST

1. Moncada, S., et al., *Principles and Therapeutic Implications of Angiogenesis, Vasculogenesis and Arteriogenesis*, in *The Vascular Endothelium II*2006, Springer Berlin Heidelberg. p. 157-212.
2. Carmeliet, P., *Angiogenesis in life, disease and medicine.* Nature, 2005. **438**(7070): p. 932-936.
3. Lovett, M., et al., *Vascularization strategies for tissue engineering.* Tissue Eng Part B Rev, 2009. **15**(3): p. 353-70.
4. Raghunath, M., et al., *Pharmacologically induced angiogenesis in transgenic zebrafish.* Biochemical and Biophysical Research Communications, 2009. **378**(4): p. 766-771.
5. Manalo, D.J., et al., *Transcriptional regulation of vascular endothelial cell responses to hypoxia by HIF-1.* Blood, 2005. **105**(2): p. 659-669.
6. Takuwa, Y., et al., *Roles of sphingosine-1-phosphate signaling in angiogenesis.* World J Biol Chem, 2010. **1**(10): p. 298-306.
7. Igarashi, J., et al., *VEGF induces S1P1 receptors in endothelial cells: Implications for cross-talk between sphingolipid and growth factor receptors.* Proceedings of the National Academy of Sciences, 2003. **100**(19): p. 10664-10669.
8. Cuvillier, O., et al., *Hypoxia, Therapeutic Resistance, and Sphingosine 1-Phosphate*, in *Role of Sphingolipids in Cancer Development and Therapy*, J.S. Norris, Editor 2013, Elsevier Academic Press Inc: San Diego. p. 117-141.
9. Kim, C., et al., *In vitro angiogenesis assay for the study of cell-encapsulation therapy.* Lab on a Chip, 2012. **12**: p. 2942-2950.
10. Al Sabti, H., *Therapeutic angiogenesis in cardiovascular disease.* Journal of Cardiothoracic Surgery, 2007. **2**: p. 7.
11. Jain, R.K., *Molecular regulation of vessel maturation.* Nature Medicine, 2003. **9**(6): p. 685-693.
12. Stratman, A.N., et al., *Endothelial cell lumen and vascular guidance tunnel formation requires MT1-MMP-dependent proteolysis in 3-dimensional collagen matrices.* Blood, 2009. **114**(2): p. 237-247.
13. Reed, M.J., et al., *Inhibition of TIMP1 enhances angiogenesis in vivo and cell migration in vitro.* Microvascular Research, 2003. **65**(1): p. 9-17.
14. Jakobsson, L., et al., *Endothelial cells dynamically compete for the tip cell position during angiogenic sprouting.* Nature Cell Biology, 2010. **12**(10): p. 943-953.
15. Stratman, A.N., et al., *Pericyte recruitment during vasculogenic tube assembly stimulates endothelial basement membrane matrix formation.* Blood, 2009. **114**(24): p. 5091-5101.
16. Kluk, M.J. and T. Hla, *Role of the sphingosine 1-phosphate receptor EDG-1 in vascular smooth muscle cell proliferation and migration.* Circulation Research, 2001. **89**(6): p. 496-502.
17. Lindahl, P., et al., *Pericyte loss and microaneurysm formation in PDGF-B-deficient mice.* Science, 1997. **277**(5323): p. 242-245.
18. Hellstrom, M., et al., *Lack of pericytes leads to endothelial hyperplasia and abnormal vascular morphogenesis.* Journal of Cell Biology, 2001. **152**(3): p. 543-553.
19. Loughna, S. and T.N. Sato, *Angiopoietin and Tie signaling pathways in vascular development.* Matrix Biology, 2001. **20**(5-6): p. 319-325.

20. Senger, D.R. and G.E. Davis, *Angiogenesis.* Cold Spring Harbor Perspectives in Biology, 2011. **3**(8).
21. Hurley, J.R., S. Balaji, and D.A. Narmoneva, *Complex temporal regulation of capillary morphogenesis by fibroblasts.* American Journal of Physiology - Cell Physiology, 2009. **299**(2): p. C444-C453.
22. Newman, A.C., et al., *Analysis of Stromal Cell Secretomes Reveals a Critical Role for Stromal Cell–Derived Hepatocyte Growth Factor and Fibronectin in Angiogenesis.* Arteriosclerosis, Thrombosis, and Vascular Biology, 2013. **33**(3): p. 513-522.
23. Martin, T.A., K.G. Harding, and W.G. Jiang, *Regulation of angiogenesis and endothelial cell motility by matrix-bound fibroblasts.* Angiogenesis, 1999. **3**(1): p. 69-76.
24. Saito, M., M. Hamasaki, and M. Shibuya, *Induction of tube formation by angiopoietin-1 in endothelial cell/fibroblast co-culture is dependent on endogenous VEGF.* Cancer Science, 2003. **94**(9): p. 782-790.
25. Villaschi, S. and R.F. Nicosia, *Paracrine interactions between fibroblasts and endothelial cells in a serum-free coculture model: Modulation of angiogenesis and collagen gel contraction.* Laboratory Investigation, 1994. **71**(2): p. 291-299.
26. Bowers, S.L.K., T.K. Borg, and T.A. Baudino, *The dynamics of fibroblast–myocyte–capillary interactions in the heart.* Annals of the New York Academy of Sciences, 2010. **1188**(1): p. 143-152.
27. Ribatti, D., E. Crivellato, and A. Vacca, *Inflammation and Antiangiogenesis in Cancer.* Current Medicinal Chemistry, 2012. **19**(7): p. 955-960.
28. Arroyo, A.G. and M.L. Iruela-Arispe, *Extracellular matrix, inflammation, and the angiogenic response.* Cardiovasc Res, 2010. **86**(2): p. 226-35.
29. Mor, F., F.J. Quintana, and I.R. Cohen, *Angiogenesis-Inflammation Cross-Talk: Vascular Endothelial Growth Factor Is Secreted by Activated T Cells and Induces Th1 Polarization.* The Journal of Immunology, 2004. **172**(7): p. 4618-4623.
30. Bhadada, S.V., B.R. Goyal, and M.M. Patel, *Angiogenic targets for potential disorders.* Fundamental & Clinical Pharmacology, 2011. **25**(1): p. 29-47.
31. Post, M.J., et al., *Therapeutic angiogenesis in cardiology using protein formulations.* Cardiovascular Research, 2001. **49**(3): p. 522-531.
32. Henry, T.D., et al., *Vascular endothelial growth factor in ischemia for vascular angiogenesis.* Circulation, 2003. **107**(10): p. 1359-1365.
33. Simons, M., et al., *Pharmacological treatment of coronary artery disease with recombinant fibroblast growth factor-2 - Double-blind, randomized, controlled clinical trial.* Circulation, 2002. **105**(7): p. 788-793.
34. Zachary, I. and R.D. Morgan, *Therapeutic angiogenesis for cardiovascular disease: biological context, challenges, prospects.* Heart, 2011. **97**(3): p. 181-189.
35. Kukula, K., et al., *Intramyocardial plasmid-encoding human vascular endothelial growth factor A165/basic fibroblast growth factor therapy using percutaneous transcatheter approach in patients with refractory coronary artery disease (VIF-CAD).* American Heart Journal, 2003. **161**(3): p. 581-589.
36. Belch, J., et al., *Effect of fibroblast growth factor NV1FGF on amputation and death: a randomised placebo-controlled trial of gene therapy in critical limb ischaemia.* The Lancet, 2011. **377**(9781): p. 1929-1937.
37. Yla-Herttuala, S. and K. Alitalo, *Gene transfer as a tool to induce therapeutic vascular growth.* Nature Medicine, 2003. **9**(6): p. 694-701.

38. Sieveking, D.P. and M.K.C. Ng, *Cell therapies for therapeutic angiogenesis: back to the bench.* Vascular Medicine, 2009. **14**(2): p. 153-166.
39. Menasche, P., *Cellular therapy in thoracic and cardiovascular disease.* The Annals of thoracic surgery, 2007. **84**(1): p. 339-342.
40. Hur, J., et al., *Characterization of two types of endothelial progenitor cells and their different contributions to neovasculogenesis.* Arteriosclerosis Thrombosis and Vascular Biology, 2004. **24**(2): p. 288-293.
41. Yoon, C.H., et al., *Synergistic Neovascularization by mixed transplantation of early endothelial progenitor cells and late outgrowth endothelial cells - The role of angiogenic cytokines and matrix metalloproteinases.* Circulation, 2005. **112**(11): p. 1618-1627.
42. Min, J.H., et al., *Structure of an HIF-1 alpha-pVHL complex: Hydroxyproline recognition in signaling.* Science, 2002. **296**(5574): p. 1886-1889.
43. Fong, G.H., *Mechanisms of adaptive angiogenesis to tissue hypoxia.* Angiogenesis, 2008. **11**(2): p. 121-140.
44. Muchnik, E. and J. Kaplan, *HIF prolyl hydroxylase inhibitors for anemia.* Expert Opinion on Investigational Drugs, 2011. **20**(5): p. 645-656.
45. Hara, S., et al., *Expression and Characterization of Hypoxia-Inducible Factor (HIF)-3α in Human Kidney: Suppression of HIF-Mediated Gene Expression by HIF-3α.* Biochemical and Biophysical Research Communications, 2001. **287**(4): p. 808-813.
46. Ando, H., et al., *A hypoxia-inducible factor (HIF)-3α splicing variant, HIF-3α4 impairs angiogenesis in hypervascular malignant meningiomas with epigenetically silenced HIF-3α4.* Biochemical and Biophysical Research Communications, 2013. **433**(1): p. 139-144.
47. Augstein, A., et al., *Cell-specific and hypoxia-dependent regulation of human HIF-3α: inhibition of the expression of HIF target genes in vascular cells.* Cellular and Molecular Life Sciences, 2011. **68**(15): p. 2627-2642.
48. Semenza, G.L., *Hydroxylation of HIF-1: Oxygen sensing at the molecular level.* Physiology, 2004. **19**(4): p. 176-182.
49. Mole, D.R. and P.J. Ratcliffe, *Cellular oxygen sensing in health and disease.* Pediatric Nephrology, 2008. **23**(5): p. 681-694.
50. Choi, Y.K., et al., *Carbon Monoxide Promotes VEGF Expression by Increasing HIF-1 alpha Protein Level via Two Distinct Mechanisms, Translational Activation and Stabilization of HIF-1 alpha Protein.* Journal of Biological Chemistry, 2010. **285**(42): p. 32116-32125.
51. Kelly, B.D., et al., *Cell type-specific regulation of angiogenic growth factor gene expression and induction of angiogenesis in nonischemic tissue by a constitutively active form of hypoxia-inducible factor 1.* Circulation Research, 2003. **93**(11): p. 1074-1081.
52. Yamakawa, M., et al., *Hypoxia-Inducible Factor-1 Mediates Activation of Cultured Vascular Endothelial Cells by Inducing Multiple Angiogenic Factors.* Circulation Research, 2003. **93**(7): p. 664-673.
53. Calvani, M., et al., *Hypoxic induction of an HIF-1α–dependent bFGF autocrine loop drives angiogenesis in human endothelial cells.* Blood, 2006. **107**(7): p. 2705-2712.
54. Munk, M., et al., *Hypoxia Changes the Expression of the Epidermal Growth Factor (EGF) System in Human Hearts and Cultured Cardiomyocytes.* PLoS ONE, 2012. **7**(7): p. e40243.
55. Okuyama, H., et al., *Expression of Vascular Endothelial Growth Factor Receptor 1 in Bone Marrow-derived Mesenchymal Cells Is Dependent on*

Hypoxia-inducible Factor 1. Journal of Biological Chemistry, 2006. **281**(22): p. 15554-15563.
56. Chu, S.-H., et al., *Stabilization of hepatocyte growth factor mRNA by hypoxia-inducible factor 1.* Molecular Biology Reports, 2009. **36**(7): p. 1967-1975.
57. Averbukh, E., et al., *Gene expression of insulin-like growth factor-I, its receptor and binding proteins in retina under hypoxic conditions.* Metabolism, 1998. **47**(11): p. 1331-1336.
58. Kim, K.S., et al., *A novel role of hypoxia-inducible factor in cobalt chloride- and hypoxia-mediated expression of IL-8 chemokine in human endothelial cells.* Journal of Immunology, 2006. **177**(10): p. 7211-7224.
59. Ceradini, D.J., et al., *Progenitor cell trafficking is regulated by hypoxic gradients through HIF-1 induction of SDF-1.* Nat Med, 2004. **10**(8): p. 858-864.
60. Daniel, R.J. and R.W. Groves, *Increased Migration of Murine Keratinocytes Under Hypoxia Is Mediated by Induction of Urokinase Plasminogen Activator.* 2002. **119**(6): p. 1304-1309.
61. Chen, K.H., M.A. Paz, and P.M. Gallop, *COLLAGEN PROLYL HYDROXYLATION IN WI-38 FIBROBLAST-CULTURES - ACTION OF HYDRALAZINE.* In Vitro-Journal of the Tissue Culture Association, 1977. **13**(1): p. 49-54.
62. Knowles, H.J., et al., *Novel mechanism of action for hydralazine: Induction of hypoxia-inducible factor-1 alpha, vascular endothelial growth factor, and angiogenesis by inhibition of prolyl hydroxylases.* Circulation Research, 2004. **95**(2): p. 162-169.
63. Fraisl, P., J. Aragones, and P. Carmeliet, *Inhibition of oxygen sensors as a therapeutic strategy for ischaemic and inflammatory disease.* Nature Reviews Drug Discovery, 2009. **8**(2): p. 139-152.
64. Milkiewicz, M., C.W. Pugh, and S. Egginton, *Inhibition of endogenous HIF inactivation induces angiogenesis in ischaemic skeletal muscles of mice.* The Journal of Physiology, 2004. **560**(1): p. 21-26.
65. Sridharan, V., et al., *The prolyl hydroxylase oxygen-sensing pathway is cytoprotective and allows maintenance of mitochondrial membrane potential during metabolic inhibition.* American Journal of Physiology - Cell Physiology, 2007. **292**(2): p. C719-C728.
66. Freret, T., et al., *Delayed administration of deferoxamine reduces brain damage and promotes functional recovery after transient focal cerebral ischemia in the rat.* European Journal of Neuroscience, 2006. **23**(7): p. 1757-1765.
67. Dendorfer, A., et al., *Deferoxamine induces prolonged cardiac preconditioning via accumulation of oxygen radicals.* Free Radical Biology and Medicine, 2005. **38**(1): p. 117-124.
68. Warnecke, C., et al., *Activation of the hypoxia-inducible factor pathway and stimulation of angiogenesis by application of prolyl hydroxylase inhibitors.* Faseb Journal, 2003. **17**(6): p. 1186-+.
69. Ju, H., et al., *Antiproliferative and antifibrotic effects of mimosine on adult cardiac fibroblasts.* Biochimica et Biophysica Acta (BBA) - Molecular Cell Research, 1998. **1448**(1): p. 51-60.
70. Agis, H., G. Watzek, and R. Gruber, *Prolyl hydroxylase inhibitors increase the production of vascular endothelial growth factor by periodontal fibroblasts.* Journal of Periodontal Research, 2012. **47**(2): p. 165-173.

71. Ivan, M., et al., *Biochemical purification and pharmacological inhibition of a mammalian prolyl hydroxylase acting on hypoxia-inducible factor.* Proceedings of the National Academy of Sciences, 2002. **99**(21): p. 13459-13464.
72. Rosenberger, C., et al., *Activation of hypoxia-inducible factors ameliorates hypoxic distal tubular injury in the isolated perfused rat kidney.* Nephrology Dialysis Transplantation, 2008. **23**(11): p. 3472-3478.
73. Bao, W.K., et al., *Chronic Inhibition of Hypoxia-inducible Factor Prolyl 4-hydroxylase Improves Ventricular Performance, Remodeling, and Vascularity After Myocardial Infarction in the Rat.* Journal of Cardiovascular Pharmacology, 2010. **56**(2): p. 147-155.
74. Michels, C., et al., *Hypoxic pre-conditioning in a rat renal ischemia model: an evaluation of the use of hydralazine.* World Journal of Urology, 2009. **27**(6): p. 817-823.
75. Nangaku, M., et al., *A novel class of prolyl hydroxylase inhibitors induces angiogenesis and exerts organ protection against ischemia.* Arteriosclerosis Thrombosis and Vascular Biology, 2007. **27**(12): p. 2548-2554.
76. Schlemminger, I., et al., *Analogues of dealanylalahopcin are inhibitors of human HIF prolyl hydroxylases.* Bioorganic & Medicinal Chemistry Letters, 2003. **13**(8): p. 1451-1454.
77. Warshakoon, N.C., et al., *Structure-based design, synthesis, and SAR evaluation of a new series of 8-hydroxyquinolines as HIF-1 alpha prolyl hydroxylase inhibitors.* Bioorganic & Medicinal Chemistry Letters, 2006. **16**(21): p. 5517-5522.
78. Warshakoon, N.C., et al., *Design and synthesis of a series of novel pyrazolopyridines as HIF 1-alpha prolyl hydroxylase inhibitors.* Bioorganic & Medicinal Chemistry Letters, 2006. **16**(21): p. 5687-5690.
79. Katschinski, D.M., *In vivo functions of the prolyl-4-hydroxylase domain oxygen sensors: direct route to the treatment of anaemia and the protection of ischaemic tissues.* Acta Physiologica, 2009. **195**(4): p. 407-414.
80. Shen, X., et al., *Prolyl Hydroxylase Inhibitors Increase Neoangiogenesis and Callus Formation following Femur Fracture in Mice.* Journal of Orthopaedic Research, 2009. **27**(10): p. 1298-1305.
81. Botusan, I.R., et al., *Stabilization of HIF-1 alpha is critical to improve wound healing in diabetic mice.* Proceedings of the National Academy of Sciences of the United States of America, 2008. **105**(49): p. 19426-19431.
82. Nagel, S., et al., *Therapeutic Manipulation of the HIF Hydroxylases.* Antioxidants & Redox Signaling, 2010. **12**(4): p. 481-501.
83. Rose, N.R., et al., *Inhibitor Scaffolds for 2-Oxoglutarate-Dependent Histone Lysine Demethylases.* Journal of Medicinal Chemistry, 2008. **51**(22): p. 7053-7056.
84. Maxwell, P.H., et al., *Assays, methods and means relating to hypoxia inducible factor (HIF) hydroxylase*, 2002, ISIS INNOVATION LTD., Maxwell, Patrick Henry, Pugh, Christopher William, Ratcliffe, Peter John, Schofield, Christopher Joseph
85. Klaus, S.J. and P.J. Ratcliffe, *Inhibitors of 2-oxoglutarate dioxygenase as gamma globin inducers*, 2005, FIBROGEN, INC., ISIS INNOVATION LIMITED, Klaus, Stephen J., Ratcliffe, Peter J.
86. Semenza, G.L., *Stable hypoxia inducible factor-1α and method of use*, 2003, The Johns Hopkins University School of Medicine: United States.

87. Arbeit, J.M., *Use of HIF-1a variants to accelerate wound healing*, 2005, The Regents of the University of California: United States.
88. Maceyka, M., et al., *Sphingosine-1-phosphate signaling and its role in disease.* Trends in Cell Biology, 2012. **22**(1): p. 50-60.
89. Takabe, K., et al., *"Inside-Out" Signaling of Sphingosine-1-Phosphate: Therapeutic Targets.* Pharmacological Reviews, 2008. **60**(2): p. 181-195.
90. English, D., et al., *Sphingosine 1-phosphate released from platelets during clotting accounts for the potent endothelial cell chemotactic activity of blood serum and provides a novel link between hemostasis and angiogenesis.* Faseb Journal, 2000. **14**(14): p. 2255-2265.
91. Spiegel, S. and S. Milstien, *Sphingosine-1-phosphate: An enigmatic signalling lipid.* Nature Reviews Molecular Cell Biology, 2003. **4**(5): p. 397-407.
92. Pham, T.H.M., et al., *S1P1 Receptor Signaling Overrides Retention Mediated by G±i-Coupled Receptors to Promote T Cell Egress.* Immunity, 2008. **28**(1): p. 122-133.
93. Allende, M.L., et al., *Sphingosine-1-phosphate Lyase Deficiency Produces a Pro-inflammatory Response While Impairing Neutrophil Trafficking.* Journal of Biological Chemistry, 2011. **286**(9): p. 7348-7358.
94. Jenne, C.N., et al., *T-bet–dependent S1P5 expression in NK cells promotes egress from lymph nodes and bone marrow.* The Journal of Experimental Medicine, 2009. **206**(11): p. 2469-2481.
95. Kono, M., et al., *The sphingosine-1-phosphate receptors S1P1, S1P2, and S1P3 function coordinately during embryonic angiogenesis.* J Biol Chem, 2004. **279**(28): p. 29367-73.
96. Kimura, T., et al., *Sphingosine 1-phosphate stimulates proliferation and migration of human endothelial cells possibly through the lipid receptors, Edg-1 and Edg-3.* Biochem J, 2000. **348 Pt 1**: p. 71-6.
97. Kimura, T., et al., *High-Density Lipoprotein Stimulates Endothelial Cell Migration and Survival Through Sphingosine 1-Phosphate and Its Receptors.* Arteriosclerosis, Thrombosis, and Vascular Biology, 2003. **23**(7): p. 1283-1288.
98. Paik, J.H., et al., *Sphingosine 1-Phosphate-induced Endothelial Cell Migration Requires the Expression of EDG-1 and EDG-3 Receptors and Rho-dependent Activation of αvβ3- and β1-containing Integrins.* Journal of Biological Chemistry, 2001. **276**(15): p. 11830-11837.
99. Chae, S.-S., et al., *Requirement for sphingosine 1–phosphate receptor-1 in tumor angiogenesis demonstrated by in vivo RNA interference.* The Journal of Clinical Investigation, 2004. **114**(8): p. 1082-1089.
100. Feistritzer, C. and M. Riewald, *Endothelial barrier protection by activated protein C through PAR1-dependent sphingosine 1–phosphate receptor-1 crossactivation.* Blood, 2005. **105**(8): p. 3178-3184.
101. Yonesu, K., et al., *Involvement of sphingosine-1-phosphate and S1P1 in angiogenesis: Analyses using a new S1P1 antagonist of non-sphingosine-1-phosphate analog.* Biochemical Pharmacology, 2009. **77**(6): p. 1011-1020.
102. Skoura, A. and T. Hla, *Regulation of vascular physiology and pathology by the S1P2 receptor subtype.* Cardiovascular Research, 2009. **82**(2): p. 221-228.
103. Inoki, I., et al., *Negative regulation of endothelial morphogenesis and angiogenesis by S1P2 receptor.* Biochemical and Biophysical Research Communications, 2006. **346**(1): p. 293-300.

104. Nofer, J.-R., et al., *HDL induces NO-dependent vasorelaxation via the lysophospholipid receptor S1P3.* The Journal of Clinical Investigation, 2004. **113**(4): p. 569-581.
105. Hait, N.C., et al., *Regulation of Histone Acetylation in the Nucleus by Sphingosine-1-Phosphate.* Science, 2009. **325**(5945): p. 1254-1257.
106. Brinkmann, V., et al., *Fingolimod (FTY720): discovery and development of an oral drug to treat multiple sclerosis.* Nat Rev Drug Discov, 2010. **9**(11): p. 883-897.
107. Astafieva, I., T. Glauser, and S.F.A. Hossainy, *Coatings for implantable medical devices containing attractants for endothelial cells*, 2007: United States.
108. Trollsas, M.O., et al., *Implantable device having a slow dissolving polymer*, 2009: United States.
109. Elbert, D., et al., *Biomaterials having nanoscale layers and coatings*, 2009, Washington University in St. Louis (St. Louis, MO, US): United States.
110. Shults, M., et al., *Biointerface membranes incorporating bioactive agents*, 2006: United States.
111. Anelli, V., et al., *Sphingosine kinase 1 is up-regulated during hypoxia in U87MG glioma cells.* Journal of Biological Chemistry, 2008. **283**(6): p. 3365-3375.
112. Ader, I., B. Malavaud, and O. Cuvillier, *When the sphingosine kinase 1/sphingosine 1-phosphate pathway meets hypoxia signaling: New targets for cancer therapy.* Cancer Research, 2009. **69**(9): p. 3723-3726.
113. LaMontagne, K., et al., *Antagonism of Sphingosine-1-Phosphate Receptors by FTY720 Inhibits Angiogenesis and Tumor Vascularization.* Cancer Research, 2006. **66**(1): p. 221-231.
114. Vickerman, V., et al., *Design, fabrication and implementation of a novel multi-parameter control microfluidic platform for three-dimensional cell culture and real-time imaging.* Lab on a Chip, 2008. **8**(9): p. 1468-1477.
115. Chung, S., et al., *Cell migration into scaffolds under co-culture conditions in a microfluidic platform.* Lab on a Chip, 2009. **9**(2): p. 269-275.
116. Chung, S., et al., *Surface-Treatment-Induced Three-Dimensional Capillary Morphogenesis in a Microfluidic Platform.* Advanced Materials, 2009. **21**(47): p. 4863-+.
117. Sudo, R., et al., *Transport-mediated angiogenesis in 3D epithelial coculture.* Faseb Journal, 2009. **23**(7): p. 2155-2164.
118. Shin, Y., et al., *In vitro 3D collective sprouting angiogenesis under orchestrated ANG-1 and VEGF gradients.* Lab on a Chip, 2011. **11**(13): p. 2175-2181.
119. Nehls, V., et al., *Contact-dependent inhibition of angiogenesis by cardiac fibroblasts in three-dimensional fibrin gels in vitro: Implications for microvascular network remodeling and coronary collateral formation.* Cell and Tissue Research, 1998. **293**(3): p. 479-488.
120. Shamloo, A. and S.C. Heilshorn, *Matrix density mediates polarization and lumen formation of endothelial sprouts in VEGF gradients.* Lab on a Chip, 2010. **10**(22): p. 3061-3068.
121. Shamloo, A., H. Xu, and S. Heilshorn, *Mechanisms of vascular endothelial growth factor-induced pathfinding by endothelial sprouts in biomaterials.* Tissue Eng Part A, 2012. **18**(3-4): p. 320-30.

122. Nguyen, D.-H.T., et al., *Biomimetic model to reconstitute angiogenic sprouting morphogenesis in vitro.* Proceedings of the National Academy of Sciences, 2013.
123. Kim, S., et al., *Engineering of functional, perfusable 3D microvascular networks on a chip.* Lab on a Chip, 2013. **13**(8): p. 1489-1500.
124. Yeon, J.H., et al., *In vitro formation and characterization of a perfusable three-dimensional tubular capillary network in microfluidic devices.* Lab on a Chip, 2012.
125. Zheng, Y., et al., *In vitro microvessels for the study of angiogenesis and thrombosis.* Proceedings of the National Academy of Sciences, 2012.
126. Barkefors, I., et al., *Endothelial cell migration in stable gradients of vascular endothelial growth factor a and fibroblast growth factor 2 - Effects on chemotaxis and chemokinesis.* Journal of Biological Chemistry, 2008. **283**(20): p. 13905-13912.
127. Hirota, K. and G.L. Semenza, *Regulation of angiogenesis by hypoxia-inducible factor 1.* Critical Reviews in Oncology/Hematology, 2006. **59**(1): p. 15-26.
128. Kim, C., et al., *Rapid exchange of oil-phase in microencapsulation chip to enhance cell viability.* Lab on a Chip - Miniaturisation for Chemistry and Biology, 2009. **9**(9): p. 1294-1297.
129. Arganda-Carreras, I., et al., *3D reconstruction of histological sections: Application to mammary gland tissue.* Microscopy Research and Technique, 2010. **73**(11): p. 1019-1029.
130. Zervantonakis, I., et al., *Concentration gradients in microfluidic 3D matrix cell culture systems.* International Journal of Micro-Nano Scale Transport, 2010. **1**(1): p. 27-36.
131. Laca, A., et al., *Protein diffusion in alginate beads monitored by confocal microscopy. The application of wavelets for data reconstruction and analysis.* Journal of Industrial Microbiology & Biotechnology, 1999. **23**(3): p. 155-165.
132. Braga, J., J.M. Desterro, and M. Carmo-Fonseca, *Intracellular macromolecular mobility measured by fluorescence recovery after photobleaching with confocal laser scanning microscopes.* Mol Biol Cell, 2004. **15**(10): p. 4749-60.
133. DiSalvo, J., et al., *Purification and Characterization of a Naturally Occurring Vascular Endothelial Growth Factor · Placenta Growth Factor Heterodimer.* Journal of Biological Chemistry, 1995. **270**(13): p. 7717-7723.
134. Athanassiades, A. and P.K. Lala, *Role of placenta growth factor (PIGF) in human extravillous trophoblast proliferation, migration and invasiveness.* Placenta, 1998. **19**(7): p. 465-73.
135. Auerbach, R., et al., *Angiogenesis Assays: A Critical Overview.* Clinical Chemistry, 2003. **49**(1): p. 32-40.
136. Leng, S.X., et al., *ELISA and multiplex technologies for cytokine measurement in inflammation and aging research.* J Gerontol A Biol Sci Med Sci, 2008. **63**(8): p. 879-84.
137. Song, J.W. and L.L. Munn, *Fluid forces control endothelial sprouting.* Proceedings of the National Academy of Sciences, 2011.
138. Song, J.W., et al., *RhoA mediates flow-induced endothelial sprouting in a 3-D tissue analogue of angiogenesis.* Lab on a Chip, 2012. **12**(23): p. 5000-5006.
139. Heldin, C.H., et al., *High interstitial fluid pressure - an obstacle in cancer therapy.* Nat Rev Cancer, 2004. **4**(10): p. 806-13.

140. Barreto-Ortiz, S.F., et al., *A Novel <italic>In Vitro</italic> Model for Microvasculature Reveals Regulation of Circumferential ECM Organization by Curvature.* PLoS ONE, 2013. **8**(11): p. e81061.
141. Eble, J.A. and S. Niland, *The Extracellular Matrix of Blood Vessels.* Current Pharmaceutical Design, 2009. **15**(12): p. 1385-1400.
142. Mammoto, A., et al., *A mechanosensitive transcriptional mechanism that controls angiogenesis.* Nature, 2009. **457**(7233): p. 1103-1108.
143. Lopez-Garcia, M.D., D.J. Beebe, and W.C. Crone, *Young's modulus of collagen at slow displacement rates.* Biomed Mater Eng, 2010. **20**(6): p. 361-9.
144. Banerjee, I., et al., *Determination of cell types and numbers during cardiac development in the neonatal and adult rat and mouse.* American Journal of Physiology - Heart and Circulatory Physiology, 2007. **293**(3): p. H1883-H1891.
145. Baudino, T.A., et al., *Cardiac fibroblasts: Friend or foe?* American Journal of Physiology - Heart and Circulatory Physiology, 2006. **291**(3): p. H1015-H1026.
146. Gerhardt, H., et al., *VEGF guides angiogenic sprouting utilizing endothelial tip cell filopodia.* The Journal of Cell Biology, 2003. **161**(6): p. 1163-1177.
147. Horowitz, A. and M. Simons, *Branching Morphogenesis.* Circulation Research, 2008. **103**(8): p. 784-795.
148. Goodwin, A.M., *In vitro assays of angiogenesis for assessment of angiogenic and anti-angiogenic agents.* Microvasc Res, 2007. **74**(2-3): p. 172-83.
149. Kubota, Y., et al., *Role of laminin and basement membrane in the morphological differentiation of human endothelial cells into capillary-like structures.* J Cell Biol, 1988. **107**(4): p. 1589-98.
150. Nakatsu, M.N., et al., *VEGF(121) and VEGF(165) regulate blood vessel diameter through vascular endothelial growth factor receptor 2 in an in vitro angiogenesis model.* Lab Invest, 2003. **83**(12): p. 1873-85.
151. Farahat, W.A., et al., *Ensemble Analysis of Angiogenic Growth in Three-Dimensional Microfluidic Cell Cultures.* PLoS ONE, 2012. **7**(5): p. e37333.
152. Folkman, J., *How Is Blood Vessel Growth Regulated in Normal and Neoplastic Tissue?—G. H. A. Clowes Memorial Award Lecture.* Cancer Research, 1986. **46**(2): p. 467-473.
153. Han, Y.S., et al., *Inhibitory effects of bevacizumab on angiogenesis and corneal neovascularization.* Graefes Arch Clin Exp Ophthalmol, 2009. **247**(4): p. 541-8.
154. Guillamo, J.-S., et al., *Molecular Mechanisms Underlying Effects of Epidermal Growth Factor Receptor Inhibition on Invasion, Proliferation, and Angiogenesis in Experimental Glioma.* Clinical Cancer Research, 2009. **15**(11): p. 3697-3704.
155. Panetti, T.S., J. Nowlen, and D.F. Mosher, *Sphingosine-1-Phosphate and Lysophosphatidic Acid Stimulate Endothelial Cell Migration.* Arteriosclerosis, Thrombosis, and Vascular Biology, 2000. **20**(4): p. 1013-1019.
156. Mascall, K.S., et al., *Sphingosine-1-phosphate-induced release of TIMP-2 from vascular smooth muscle cells inhibits angiogenesis.* Journal of Cell Science, 2012. **125**(9): p. 2267-2275.
157. Sanna, M.G., et al., *Enhancement of capillary leakage and restoration of lymphocyte egress by a chiral S1P1 antagonist in vivo.* Nat Chem Biol, 2006. **2**(8): p. 434-441.
158. Hong, K.H., J. Ryu, and K.H. Han, *Monocyte chemoattractant protein-1–induced angiogenesis is mediated by vascular endothelial growth factor-A.* Blood, 2005. **105**(4): p. 1405-1407.

159. Solini, A., et al., *Effects of endothelin-1 on fibroblasts from type 2 diabetic patients: Possible role in wound healing and tissue repair.* Growth Factors, 2007. **25**(6): p. 392-399.
160. Swanson, C.D., et al., *Inhibition of Epidermal Growth Factor Receptor Tyrosine Kinase Ameliorates Collagen-Induced Arthritis.* The Journal of Immunology, 2012. **188**(7): p. 3513-3521.
161. Aonuma, M., et al., *Tumorigenicity depends on angiogenic potential of tumor cells: dominant role of vascular endothelial growth factor and/or fibroblast growth factors produced by tumor cells.* Angiogenesis, 1998. **2**(1): p. 57-66.
162. Asikainen, T.M., et al., *Stimulation of HIF-1 alpha, HIF-2 alpha, and VEGF by prolyl 4-hydroxylase inhibition in human lung endothelial and epithelial cells.* Free Radical Biology and Medicine, 2005. **38**(8): p. 1002-1013.
163. Ader, I., et al., *Sphingosine kinase 1: A new modulator of hypoxia inducible factor 1alpha during hypoxia in human cancer cells.* Cancer Research, 2008. **68**(20): p. 8635-8642.
164. Michaud, M.D., et al., *Sphingosine-1-phosphate: a novel nonhypoxic activator of hypoxia-inducible factor-1 in vascular cells.* Arterioscler Thromb Vasc Biol, 2009. **29**(6): p. 902-8.
165. Myllyharju, J., *HIF Prolyl 4-Hydroxylases and their Potential as Drug Targets.* Current Pharmaceutical Design, 2009. **15**(33): p. 3878-3885.
166. Montesano, R., M.S. Pepper, and L. Orci, *Paracrine induction of angiogenesis in vitro by Swiss 3T3 fibroblasts.* Journal of Cell Science, 1993. **105**(4): p. 1013-1024.
167. Mansbridge, J.N., et al., *Growth factors secreted by fibroblasts: role in healing diabetic foot ulcers.* Diabetes, Obesity and Metabolism, 1999. **1**(5): p. 265-279.
168. Keshaw, H., A. Forbes, and R.M. Day, *Release of angiogenic growth factors from cells encapsulated in alginate beads with bioactive glass.* Biomaterials, 2005. **26**(19): p. 4171-4179.
169. Shoichet, M.S., et al., *Stability of hydrogels used in cell encapsulation: An in vitro comparison of alginate and agarose.* Biotechnol Bioeng, 1996. **50**(4): p. 374-81.
170. Kankuri, E., et al., *Induction of Hepatocyte Growth Factor/Scatter Factor by Fibroblast Clustering Directly Promotes Tumor Cell Invasiveness.* Cancer Research, 2005. **65**(21): p. 9914-9922.
171. Tamariz, E. and F. Grinnell, *Modulation of fibroblast morphology and adhesion during collagen matrix remodeling.* Mol Biol Cell, 2002. **13**(11): p. 3915-29.
172. VELAZQUEZ, O.C., et al., *Fibroblast-dependent differentiation of human microvascular endothelial cells into capillary-like 3-dimensional networks.* The FASEB Journal, 2002. **16**(10): p. 1316-1318.
173. Cliff, W.J., *Kinetics of Wound Healing in Rabbit Ear Chambers, a Time Lapse Cinemicroscopic Study.* Experimental Physiology, 1965. **50**(1): p. 79-89.
174. Wallez, Y., I. Vilgrain, and P. Huber, *Angiogenesis: The VE-Cadherin Switch.* Trends in Cardiovascular Medicine, 2006. **16**(2): p. 55-59.
175. Ferrara, N., *Vascular Endothelial Growth Factor.* Arteriosclerosis, Thrombosis, and Vascular Biology, 2009. **29**(6): p. 789-791.
176. Taniyama, Y., et al., *Therapeutic angiogenesis induced by human hepatocyte growth factor gene in rat and rabbit hindlimb ischemia models: preclinical*

study for treatment of peripheral arterial disease. Gene Ther, 2001. **8**(3): p. 181-9.
177. Azar, W.J., et al., *IGFBP-2 Enhances VEGF Gene Promoter Activity and Consequent Promotion of Angiogenesis by Neuroblastoma Cells.* Endocrinology, 2011. **152**(9): p. 3332-3342.
178. Ribatti, D., et al., *In vivo angiogenic activity of urokinase: role of endogenous fibroblast growth factor-2.* Journal of Cell Science, 1999. **112**(23): p. 4213-4221.
179. Oh, C.W., J. Hoover-Plow, and E.F. Plow, *The role of plasminogen in angiogenesis in vivo.* Journal of Thrombosis and Haemostasis, 2003. **1**(8): p. 1683-1687.
180. Raghu, H., et al., *uPA and uPAR shRNA inhibit angiogenesis via enhanced secretion of SVEGFR1 independent of GM-CSF but dependent on TIMP-1 in endothelial and glioblastoma cells.* Molecular oncology, 2012. **6**(1): p. 33-47.
181. Jiang, W.G. and K.G. Harding, *Enhancement of wound tissue expansion and angiogenesis by matrix-embedded fibroblast (dermagraft), a role of hepatocyte growth factor/scatter factor.* Int J Mol Med, 1998. **2**(2): p. 203-210.
182. Luttun, A., et al., *Genetic dissection of tumor angiogenesis: are PlGF and VEGFR-1 novel anti-cancer targets?* Biochimica et Biophysica Acta (BBA) - Reviews on Cancer, 2004. **1654**(1): p. 79-94.
183. Evans, C.E., et al., *Upregulation of hypoxia-inducible factor 1 alpha in local vein wall is associated with enhanced venous thrombus resolution.* Thrombosis Research, 2011. **128**(4): p. 346-351.
184. Li, A., et al., *Autocrine Role of Interleukin-8 in Induction of Endothelial Cell Proliferation, Survival, Migration and MMP-2 Production and Angiogenesis.* Angiogenesis, 2005. **8**(1): p. 63-71.
185. Hirata, A., et al., *Direct inhibition of EGF receptor activation in vascular endothelial cells by gefitinib ('Iressa', ZD1839).* Cancer Science, 2004. **95**(7): p. 614-618.
186. Sun, Q.M., et al., *BB, a new EGFR inhibitor, exhibits prominent anti-angiogenesis and antitumor activities.* Cancer Biology & Therapy, 2009. **8**(17): p. 1647-1654.
187. Knowles, J., M. Loizidou, and I. Taylor, *Endothelin-1 and angiogenesis in cancer.* Current Vascular Pharmacology, 2005. **3**(4): p. 309-314.
188. Menashi, S., et al., *Regulation of Extracellular Matrix Metalloproteinase Inducer and Matrix Metalloproteinase Expression by Amphiregulin in Transformed Human Breast Epithelial Cells.* Cancer Research, 2003. **63**(22): p. 7575-7580.
189. Lofqvist, C., et al., *IGFBP3 suppresses retinopathy through suppression of oxygen-induced vessel loss and promotion of vascular regrowth.* Proceedings of the National Academy of Sciences, 2007. **104**(25): p. 10589-10594.
190. Dawson, D.W., et al., *Pigment Epithelium-Derived Factor: A Potent Inhibitor of Angiogenesis.* Science, 1999. **285**(5425): p. 245-248.
191. Marneros, A.G. and B.R. Olsen, *Physiological role of collagen XVIII and endostatin.* The FASEB Journal, 2005. **19**(7): p. 716-728.
192. Rusnati, M., et al., *Selective recognition of fibroblast growth factor-2 by the long pentraxin PTX3 inhibits angiogenesis.* Blood, 2004. **104**(1): p. 92-99.
193. Isogai, C., et al., *Plasminogen Activator Inhibitor-1 Promotes Angiogenesis by Stimulating Endothelial Cell Migration toward Fibronectin.* Cancer Research, 2001. **61**(14): p. 5587-5594.

194. Ikenaka, Y., et al., *Tissue inhibitor of metalloproteinases-1 (TIMP-1) inhibits tumor growth and angiogenesis in the TIMP-1 transgenic mouse model.* International Journal of Cancer, 2003. **105**(3): p. 340-346.
195. Iruela-Arispe, M.L., et al., *Inhibition of Angiogenesis by Thrombospondin-1 Is Mediated by 2 Independent Regions Within the Type 1 Repeats.* Circulation, 1999. **100**(13): p. 1423-1431.
196. Carmeliet, P., *Mechanisms of angiogenesis and arteriogenesis.* Nat Med, 2000. **6**(4): p. 389-395.
197. Hilmi, C., M. Guyot, and G. Pagès, *VEGF Spliced Variants: Possible Role of Anti-Angiogenesis Therapy.* Journal of Nucleic Acids, 2012. **2012**.
198. Hoeben, A., et al., *Vascular Endothelial Growth Factor and Angiogenesis.* Pharmacological Reviews, 2004. **56**(4): p. 549-580.
199. Hirata, A., et al., *ZD1839 (Iressa) induces antiangiogenic effects through inhibition of epidermal growth factor receptor tyrosine kinase.* Cancer Res, 2002. **62**(9): p. 2554-60.
200. Radek, K.A., et al., *Acute ethanol exposure impairs angiogenesis and the proliferative phase of wound healing.* American Journal of Physiology - Heart and Circulatory Physiology, 2005. **289**(3): p. H1084-H1090.
201. Sefcik, L.S., et al., *Selective activation of sphingosine 1-phosphate receptors 1 and 3 promotes local microvascular network growth.* Tissue Eng Part A, 2011. **17**(5-6): p. 617-29.
202. Herbert, Shane P., Julia Y.M. Cheung, and Didier Y.R. Stainier, *Determination of Endothelial Stalk versus Tip Cell Potential during Angiogenesis by H2.0-like Homeobox-1.* Current biology : CB, 2012. **22**(19): p. 1789-1794.
203. Newman, A.C., et al., *The requirement for fibroblasts in angiogenesis: fibroblast-derived matrix proteins are essential for endothelial cell lumen formation.* Molecular Biology of the Cell, 2011. **22**(20): p. 3791-3800.
204. Scarrà, G.B., et al., *Effect of endothelial cell conditioned medium on the growth of human bone marrow fibroblasts.* Journal of Cellular Physiology, 1985. **123**(3): p. 343-346.
205. Dawes, K.E., et al., *Characterization of fibroblast mitogens and chemoattractants produced by endothelial cells exposed to hypoxia.* American Journal of Respiratory Cell and Molecular Biology, 1994. **10**(5): p. 552-559.
206. Shi-Wen, X., et al., *Endothelin-1 Promotes Myofibroblast Induction through the ETA Receptor via a rac/Phosphoinositide 3-Kinase/Akt-dependent Pathway and Is Essential for the Enhanced Contractile Phenotype of Fibrotic Fibroblasts.* Molecular Biology of the Cell, 2004. **15**(6): p. 2707-2719.
207. Iwabu, A., et al., *Epidermal Growth Factor Induces Fibroblast Contractility and Motility via a Protein Kinase C δ-dependent Pathway.* Journal of Biological Chemistry, 2004. **279**(15): p. 14551-14560.
208. Kalluri, R. and M. Zeisberg, *Fibroblasts in cancer.* Nat Rev Cancer, 2006. **6**(5): p. 392-401.
209. Strieter, R.M., et al., *Monocyte chemotactic protein gene expression by cytokine-treated human fibroblasts and endothelial cells.* Biochem Biophys Res Commun, 1989. **162**(2): p. 694-700.
210. Niu, J., et al., *Monocyte chemotactic protein (MCP)-1 promotes angiogenesis via a novel transcription factor, MCP-1-induced protein (MCPIP).* J Biol Chem, 2008. **283**(21): p. 14542-51.
211. Pober, J.S. and W.C. Sessa, *Evolving functions of endothelial cells in inflammation.* Nat Rev Immunol, 2007. **7**(10): p. 803-815.

212. Rao, R.M., et al., *Endothelial-Dependent Mechanisms of Leukocyte Recruitment to the Vascular Wall.* Circulation Research, 2007. **101**(3): p. 234-247.
213. Aplin, A., E. Fogel, and R. Nicosia, *MCP-1 promotes mural cell recruitment during angiogenesis in the aortic ring model.* Angiogenesis, 2010. **13**(3): p. 219-226.
214. Hordijk, P.L., et al., *Vascular-endothelial-cadherin modulates endothelial monolayer permeability.* J Cell Sci, 1999. **112 (Pt 12)**: p. 1915-23.
215. Goel, S., et al., *Normalization of the Vasculature for Treatment of Cancer and Other Diseases.* Physiological Reviews, 2011. **91**(3): p. 1071-1121.
216. Wang, R., et al., *Human Dermal Fibroblasts Produce Nitric Oxide and Express Both Constitutive and Inducible Nitric Oxide Synthase Isoforms.* J Investig Dermatol, 1996. **106**(3): p. 419-427.
217. Hakim, T.S., et al., *Half-life of nitric oxide in aqueous solutions with and without haemoglobin.* Physiol Meas, 1996. **17**(4): p. 267-77.
218. Ziche, M. and L. Morbidelli, *Nitric oxide and angiogenesis.* J Neurooncol, 2000. **50**(1-2): p. 139-48.
219. Kalluri, R., *EMT: When epithelial cells decide to become mesenchymal-like cells.* The Journal of Clinical Investigation, 2009. **119**(6): p. 1417-1419.
220. Gellings Lowe, N., et al., *Sphingosine-1-phosphate and sphingosine kinase are critical for transforming growth factor-β-stimulated collagen production by cardiac fibroblasts.* Cardiovascular Research, 2009. **82**(2): p. 303-312.
221. Hashimoto, M., et al., *Sphingosine 1-phosphate potentiates human lung fibroblast chemotaxis through the S1P2 receptor.* American Journal of Respiratory Cell and Molecular Biology, 2008. **39**(3): p. 356-363.
222. Ottaviano, F.G. and K.O. Yee, *Communication Signals Between Cardiac Fibroblasts and Cardiac Myocytes.* Journal of Cardiovascular Pharmacology, 2011. **57**(5): p. 513-521 10.1097/FJC.0b013e31821209ee.
223. Zhao, L. and M. Eghbali-Webb, *Release of pro- and anti-angiogenic factors by human cardiac fibroblasts: effects on DNA synthesis and protection under hypoxia in human endothelial cells.* Biochimica et Biophysica Acta (BBA) - Molecular Cell Research, 2001. **1538**(2-3): p. 273-282.
224. Aref, A.R., et al., *Screening therapeutic EMT blocking agents in a three-dimensional microenvironment.* Integrative Biology, 2013. **5**(2): p. 381-389.